QUATERNARY AMMONIUM DISINFECTANTS CATALYZE TRANSPOSITION ON PROMISCUOUS CONJUGATIVE PLASMIDS IN *Pseudomonas spp.*

by

Zeynep Şahin

B.Ed. in Molecular Biology and Genetics, Istanbul Technical University, 2020

Submitted to the Institute of Environmental Sciences in partial fulfillment of

the requirements for the degree of

Master of Science

in

Environmental Sciences

Boğaziçi University

2024

QUATERNARY AMMONIUM DISINFECTANTS CATALYZE TRANSPOSITION ON PROMISCUOUS CONJUGATIVE PLASMIDS IN *Pseudomonas spp.*

APPROVED BY:

Assoc. Prof. Dr. Ulaş Tezel . . . . . .
Thesis advisor

Prof. Dr. Raşit Bilgin . . . . . .

Assoc. Prof. Dr. Timuçin Avşar . . . . . .

DATE OF APPROVAL: 28/08/2024

ACKNOWLEDGEMENTS

I would like to express my sincere gratitude to the people who make this thesis possible

I am profoundly grateful to my thesis advisor, Assoc. Prof. Dr. Ulaş Tezel, who deserves my deepest appreciation for his support, patience, and constant encouragement throughout this academic journey. His guidance has been invaluable, shaping not only the outcome of this thesis but also my growth as a researcher. I am grateful for the inspiration he provided by sharing his passion for science with me. The lessons he has taught me will always stay with me.

I extend my heartfelt gratitude to the members of ArGO, Dr. Fahri Koray Sakarya and Recep Can Altınbağ for their friendship and great support to my thesis. Your encouragement has meant more to me than words can express. I am deeply grateful to the members of BIOMIG Lab, Tuna Sürmeli, Rüya Üçel and Dr. Havva Ateş for their unwavering emotional support and companionship. Your presence has been a source of immense strength and inspiration. I am also grateful to colleagues from neighboring labs, Kübra Doymuş, Gökçin Gül, and Suat Vardar for their friendship and collaborative spirit.

Special thanks to my twenty undergraduate interns, especially Muharrem Yıldız and Büşra Toktaş for helping me various parts of my experiments. Through teaching them, I discovered the profound and meaningful journey of teaching, which has touched me deeply.

A heartfelt thank you to my friends from my master's adventure, Irmak Akoğlu, Hira Yousuf, Osman Hakan Can, Manal Yousuf, Berrah Abdul Haleem, and Frances Varty Bayar for their endless support, love, and friendship. You have made my master's journey vibrant and joyful. Your contributions to my life are truly priceless.

I'm grateful to my beloved friends, Aycan Kayrav, Hanife Çelik, Berna Dede, Esma Gül Aydeniz, and Efay İzel Tan for their constant presence in my life since İTÜ, offering infinite support, love, and understanding. Your friendship has been a source of great comfort and joy. I am deeply thankful to Alparslan Köksal for introducing me to mountaineering and being a patient teacher during my bouldering sessions. Bouldering kept me motivated during my intense master's studies. The things you taught me about bouldering and your friendship are priceless.

There are no words sufficient to express my appreciation for my precious family—my mother, father, three brothers, sister, and nephew. Their unconditional love and support have been the foundation of my strength. Their encouragement gives me the courage to pursue my dreams and keep moving forward.

I would like to acknowledge The Scientific and Technological Research Council of Türkiye (TUBİTAK) for supporting me for my study under the grant number 122Z913.

ABSTRACT

QUATERNARY AMMONIUM DISINFECTANTS CATALYZE TRANSPOSITION ON PROMISCUOUS CONJUGATIVE PLASMIDS IN *Pseudomonas spp.*

Transposable elements (TEs) are mobile genetic units crucial to bacterial genome evolution, often mobilizing genes related to antimicrobial resistance and xenobiotic degradation. Beyond their genomic movement, interaction of TEs with other mobile genetic elements, such as conjugative plasmids, raises concerns about the dissemination of resistance genes. The main objective of this study is to evaluate the interaction of TEs with conjugative plasmids when bacteria is exposed to quaternary ammonium disinfectants (QACs). In this study, we used two bacterial strains, *Pseudomonas sessilinigenes* BIOMIG1 (transformed with pRK24) and *Pseudomonas saponiphil*a DSM 9751 (harboring native plasmid p9751), which can degrade QACs and contain numerous TEs in their genome. Strains were incubated in minimal salt medium containing 200 μg/mL benzalkonium chlorides (BACs) with or without 500 μg/mL acetate. As the controls, cultures were incubated in only 1000 μg/mL acetate. After 48-hr incubation when BACs and acetate were fully utilized, plasmids were extracted and sequenced. Plasmid sequences from the transposition experiments were compared with the original sequences of the plasmids revealed two BAC-induced transposition events on p9751 in DSM 9751, IS1474 excision and ISPa33 insertion. pRK24 was under heavy attack of TnPsp::merPTR transposon that translocate itself to three different locations on pRK24 in BIOMIG1 resulting in excision of T4SS region of the plasmid. In conclusion, this study showed that conjugative plasmids native to *Pseudomonas spp.* serve as targets to TEs under the influence of QAC disinfectants. Such transposition events may not only result in horizontal transfer of genes but also genetic diversification of conjugative plasmids.

ÖZET

DÖRDÜNCÜL AMONYUM DEZENFEKTANLAR *Pseudomonas spp.*'DEKİ KONAKÇI SEÇMEYEN KONJUGATİF PLAZMİDLERE TRANSPOZİSYONU KATALİZE EDER

Transpozonlar (TE'ler), otonom hareketlilikleri sayesinde bakteriyel genom evriminde önemli bir rol oynayan genetik araçlardır. TE'ler, özellikle antimikrobiyal direnç ve ksenobiyotik bozunum genlerini mobilize edebilme yetenekleri nedeniyle önemlidir. Genom içindeki hareketlerinin ötesinde, TE'lerin konjugatif plazmidler gibi diğer mobil genetik unsurlarla etkileşimi, direnç genlerinin yayılma potansiyeli hakkında endişeleri artırmaktadır. Bu çalışmanın temel amacı, bakterilerin dördüncül amonyum bileşiklerin (DAB'lar) maruz kaldığında TE'lerin konjugatif plazmidlerle etkileşimini değerlendirmektir. Bu çalışmada, DAB'ları parçalayabilen ve kromozomlarında önemli sayıda TE bulunan iki bakteriyel suş, *Pseudomonas sessilinigenes* BIOMIG1 ve *Pseudomonas saponiphila* DSM 9751 kullanıldı. DSM 9751, doğal bir konjugatif plazmid taşırken, BIOMIG1 pRK24 ile transformasyona uğratılmıştır. Her iki suş da 200 µg/mL benzalkonyum klorür (BAK) içeren minimal tuzlu ortamda, 500 µg/mL asetat ile birlikte ya da asetat olmadan inkübe edilmiştir. Kontrol olarak, kültürler sadece 1000 µg/mL asetat içeren ortamda inkübe edilmiştir. 48 saatlik inkübasyon sonunda BAK ve asetat tamamen tüketildiğinde, plazmidler çıkarılmış ve dizilenmiştir. Transpozisyon deneyleri sırasında elde edilen plazmid dizileri, plazmidlerin orijinal dizileri ile karşılaştırılmış ve transpozisyon olayları tanımlanmıştır. DSM 9751'deki p9751 üzerinde BAK'ler tarafından katalize edilen iki büyük transpozisyon olayı tanımlanmıştır. Birincisi IS21 ailesi IS1474'ün plazmitten kopması, diğeri ise IS1380 ailesi ISPa33'ün plasmide atlamasıdır. pRK24, *merPTR* operonunu taşıyan Tn3 ailesi birim transpozonunun ağır saldırısı altındadır. Bu transpozon, BIOMIG1'deki pRK24 üzerinde üç farklı yere atlayarak plazmidin T4SS transfer bölgesinin kopmasına neden olmuştur. Sonuç olarak, bu çalışma *Pseudomonas* spp.'ye özgü konjugatif plazmidlerin DAB dezenfektanlarının etkisi altında TE'lere hedef olduğunu göstermiştir. Bu tür transpozisyon olaylarının sadece genlerin yatay transferine değil, aynı zamanda konjugatif plazmidlerin genetik çeşitlenmesine de yol açabileceği gösterilmiştir.

TABLE OF CONTENTS

ACKNOWLEDGEMENTS iii
ABSTRACT v
ÖZET vi
LIST OF FIGURES viii
LIST OF TABLES xi
LIST OF SYMBOLS/ABBREVIATIONS xii
1. INTRODUCTION 1
2. LITERATURE BACKGROUND 4
2.1. Conjugative Plasmids: The Engines of Horizontal Gene Transfer 4
2.2. Transposable Elements as Vehicles for Intracellular Gene Translocation 9
2.2.1. Pandemic's Aftermath: The Hidden Role of Quaternary Ammonium Compounds in Accelerating Horizontal Gene Transfer 16
2.3. The Species That Can Degrade QACs Carry Many TEs 17
3. MATERIALS AND METHODS 21
3.1. Bacterial strains and plasmids 21
3.2. Transposition Experiments 21
3.3. Plasmid Isolation 22
3.4. Decontamination, Linearization and Purification of the Plasmid Extracts 23
3.5. Nanopore Sequencing 23
3.6. Bioinformatic Analysis 24
4. RESULTS AND DISCUSSION 27
4.1. Classification of p9751 and pRK24 27
4.2. TEs on *P. saponiphila* DSM 9751 and *P. sessilinigenes* BIOMIG1 Genome 34
4.3. Transposition Events Targeting Conjugative Plasmids During BAC Biodegradation 39
4.4. Structural Modifications on pRK24 due to Transposition of TnPsp::merPTR 58
5. CONCLUSIONS 62
REFERENCES 64
APPENDIX A: *P. saponiphila* DSM 9751 AND *P. sessilinigenes* BIOMIG1 ISs AND TNs DETAILS 82

LIST OF FIGURES

Figure 2.1. The conjugation from a donor cell to a recipient cell 5

Figure 2.2. The commonly found transposable elements in bacteria in their simplified forms 9

Figure 2.3. The transposition mechanisms of DDE transposases 11

Figure 4.1. Plasmid map of the native plasmid of *P. saponiphila* DSM 9751, p9751, and its T4SS gene cluster members 31

Figure 4.2. Plasmid map of the commercial conjugative plasmid, pRK24, and its T4SS gene cluster members 33

Figure 4.3. Images of spots inoculated with *P. saponiphila* DSM 9751 growing in 1000 mg/L acetate, 500 mg/L acetate + 200 mg/L BACs and only 200 mg/L BACs on LB or M63B1*BAC* agar during 48 hours of incubation.....40

Figure 4.4. Profiles of (A) acetate utilization and (B) cell growth in the flasks inoculated with *P. saponiphila* DSM 9751 in Control (1000 mg/L acetate) condition in the course of 48 hours (n=3) 41

Figure 4.5. Profiles of (A) BACs utilization and (B) cell growth in the flasks inoculated with *P. saponiphila* DSM 9751 in BACs (200 mg/L BACs) condition in the course of 48 hours (n= 3) 42

Figure 4.6. Profiles of (A) acetate utilization, (B) BACs utilization, and (C) cell growth in the flasks inoculated with *P. saponiphila* DSM 9751 in Acetate + BACs (500 mg/L acetate and 200 mg/L BACs) condition in the course of 48 hours (n= 3).....42

Figure 4.7. Images of spots inoculated with *P. sessilinigenes* BIOMIG1+pRK24 growing in 1000 mg/L acetate, 500 mg/L acetate + 200 mg/L BACs and only 200 mg/L BACs on LB or M63B1*BAC* agar during 48 hours of incubation.....43

Figure 4.8. Profiles of (A) acetate utilization and (B) cell growth in the flasks inoculated with *P. sessilinigenes* BIOMIG1+pRK24 in Control (1000 mg/L acetate) condition in the course of 48 hours (n= 3) 43

Figure 4.9. Profiles of (A) BACs utilization and (B) cell growth in the flasks inoculated with *P. sessilinigenes* BIOMIG1+pRK24 in BACs (200 mg/L BACs) condition in the course of 48 hours (n= 3).....44

Figure 4.10. Profiles of (A) acetate utilization, (B) BACs utilization, and (C) cell growth in the flasks inoculated with *P. sessilinigenes* BIOMIG1+pRK24 in Acetate + BACs (500 mg/L acetate and 200 mg/L BACs) condition in the course of 48 hours (n= 3).....44

Figure 4.11. Plasmid isolation results of (A) p9751 from *P. saponiphila* DSM 9751 and (B) pRK24 from *P. sesslinigenes* BIOMIG1+pRK24 46

Figure 4.12. HpaI enzyme restriction sites maps of p9751 and pRK24.....48

Figure 4.13. Linear and pure (A) p9751 and (B) pRK24 agarose gel electrophoresis results after PlasmidSafe application, HpaI digestion and magnetic bead purification.....49

Figure 4.14. The quality and length analysis graphs of all sequence reads are done by NanoPlot...50

Figure 4.15. The alignment of pooled p9751 sequence reads to p9751 reference sequence (top graph) and the genomic DNA of *P. saponiphila* DSM 9751 (bottom graph) is presented.....51

Figure 4.16. The alignment of pooled pRK24 sequence reads with both the pRK24 reference sequence (top graph) and the genomic DNA of *P. sessilinigenes* BIOMIG1 (bottom graph) is presented 55

Figure 4.17. The comparison of the annotated reference pRK24 plasmid with two sequence reads that surrounds the excised T4SS gene cluster and harbors the TnPsp::merPTR insertions 59

Figure 4.18. Proposed mechanism of pRK24's structural modification by TnPsp::merPTR transposition 60

Figure 4.19. Proposed maps of circular extrachromosomal DNA fragments generated after TnPsp::merPTR insertions 61

LIST OF TABLES

Table 4.1. MOB-suite plasmid classification analysis results.....29

Table 4.2. The IS/Tn list of *P. saponiphila* DSM 9751 and their properties 36

Table 4.3. The IS/Tn list of *P. sessilinigenes* BIOMIG1 and their properties 37

Table 4.4. The list of inserted gene arrays to p9751 53

Table A.1. The sequences of inverted repeats (IRs) and direct repeats (DRs) of *P. saponiphila* DSM 9751's ISs and Tns. 82

Table A.2. The sequences of inverted repeats (IRs) and direct repeats (DRs) of *P. sessilinigenes* BIOMIG1's ISs and Tns. 83

LIST OF SYMBOLS/ABBREVIATIONS

Abbreviation	Explanation
A	Adenine
AHL	N-acyl homoserine lactone
AMR	Antimicrobial resistance
BAC	Benzalkonium chloride
C	Cytosine
DNA	Deoxyribonucleic acid
DR	Direct repeat
dsDNA	double-stranded DNA
F	Fertility
G	Guanine
HPLC	High performance liquid chromatography
IR	Inverted repeat
IS	Insertion sequence
OD	Optical density
ORI	Origin of replication
oriT	Origin of transfer
QAC	Quaternary ammonium compound
ssDNA	single-stranded DNA
T	Thymine
TE	Transposable element
Tet	Tetracycline
Tn	Transposon
Tpase	Transposase
WWTP	Wastewater treatment plant

1. INTRODUCTION

Plasmids, which are small, circular, extrachromosomal DNA molecules capable of autonomous replication, play a crucial role in bacterial ecosystem. Their diverse gene complements confer non-essential but advantageous traits, such as antimicrobial resistance, biofilm formation, virulence, and heavy metal tolerance, providing competitive and adaptive advantages to their hosts (Virolle et al., 2020). The autonomous replication of plasmids enables their high-copy-number proliferation, further influenced by structural and genetic factors (Snyder et al., 2013).

Conjugative plasmids, distinguished by their larger size and higher GC content, are critical agents of horizontal gene transfer among bacteria (Che et al., 2021). Despite their lower abundance compared to other plasmid types, their ability to mediate intercellular DNA transfer has attracted significant research interest for decades (Che et al., 2021; Virolle et al., 2020). Since its initial characterization in 1946, the unidirectional transfer of genetic material between cells, termed conjugation, has been intrinsically linked to conjugative plasmids, exemplified by the F factor (Lederberg et al., 1952; Virolle et al., 2020). Conjugation empowers bacteria to acquire critical survival genes enabling them to withstand diverse stress factors such as antibiotics, heavy metals, extreme temperatures, and toxic compounds (Cecchetelli et al., 2023). Conjugative plasmids harbor distinct regions. These regions include the origin of transfer (oriT), which is recognized by the relaxase enzyme to initiate the DNA transfer process, and the transfer (*tra*) genes, which encode the components necessary for the formation of the mating pair and the transfer of DNA between cells. The replication region, containing the origin of replication (oriV), ensures the plasmid is duplicated and maintained within the host cell after transfer. Additionally, the plasmid includes stability and maintenance genes, such as partitioning systems, toxin-antitoxin systems, and post-segregational killing mechanisms, which help secure its persistence within bacterial populations (Virolle et al., 2020).

Conjugative plasmids often carry antibiotic resistance, biodegradation or virulence genes that provide a selective advantage to the host bacterium, and these genes are usually located in mobile genetic elements like transposable elements (TEs) or integrons. (Snyder et al., 2013). (Martinez et al., 2001). The synergy between TEs and conjugative plasmids enhances the transfer efficiency of resistance and biodegradation genes. Notably, a majority (63.2%) of recently transferred antimicrobial resistance genes from chromosomal to plasmid DNA are associated with TEs that prefer conjugative plasmids (Che et al., 2021).

Transposable elements (TEs) are mobile genetic elements that significantly impact bacterial evolution through their ability to relocate within the genome (Casacuberta & González, 2013). Over the past two decades, their importance in genome evolution and function has become increasingly evident (Biémont & Vieira, 2006). In bacteria, common TEs include transposons (Tn) and insertion sequences (IS) (Fan et al., 2019). They differ in their complexity and function. IS's are the simplest form of transposable elements, typically consisting of a single gene that encodes the transposase enzyme (Tpase), which is responsible for the element's translocation within the genome (Lipszyc et al., 2022). These elements are flanked by short, inverted repeat sequences (IRs) that are recognized by the Tpase (Siguier et al., 2015). In contrast, Tn's are more complex and often contain additional genes, such as those conferring antibiotic resistance, in addition to the Tpase gene (Siguier et al., 2015). Tn's can be categorized into two main types: simple transposons, which have only one set of inverted repeats and typically move via a "cut-and-paste" or "copy-and-paste mechanism, and composite transposons, which are formed by two ISs flanking additional genes and can facilitate the transfer of these genes between different genomic locations or even between different DNA molecules (Casacuberta & González, 2013; Nojiri et al., 2004). While insertion sequences primarily serve to mobilize themselves, transposons play a broader role in facilitating genetic variation and the spread of beneficial traits within and between bacterial populations (Nojiri et al., 2004).

The complex relationship between transposable elements and conjugative plasmids facilitates the spread of antibiotic resistance genes (ARGs) and other advantageous genetic traits across bacterial populations. The research by Che et al. (Che et al., 2021) sheds light on the critical role of TEs in the acquisition and dissemination of ARGs. The study identified a vast network of ARG transfer between conjugative plasmids and bacterial chromosomes, mediated by ISs like IS26. This mobile element was found to be instrumental in the transfer of crucial resistance genes, including those encoding extended-spectrum β-lactamases (ESBLs) and New Delhi metallo-β-lactamase (NDM-1), highlighting the potential of TEs to mobilize ARGs onto conjugative plasmids, which can then be readily transferred across different bacterial species.

The impact of environmental stressors, such as disinfectants, on this process is investigated by Yang et al. (2023). The study revealed that exposure to benzalkonium chloride disinfectants led to a significant increase in the abundance of both ARGs and mobile genetic elements (MGEs), including integrons and transposons, in sewage sludge microbiomes. The research suggested that disinfectants could co-select for antibiotic resistance by promoting the horizontal transfer of ARGs through MGEs. The increased abundance of MGEs, coupled with the observed rise in ARG diversity and abundance,

suggests that disinfectants may inadvertently create an environment conducive to the spread of antibiotic resistance.

The findings of Hu et al. (2024) further support the fact that environmental stressors can enhance the horizontal transfer of ARGs. The study demonstrated that quaternary ammonium biocides could promote the conjugative transfer of ARGs, potentially by increasing cell membrane permeability and altering bacterial energy metabolism. The research also highlighted the role of recipient bacteria in the transfer process, suggesting that certain pathogens, like *Shigella sonnei*, may be more adept at acquiring and expressing ARGs from environmental bacteria in the presence of biocides.

In conclusion, the interplay between transposable elements and conjugative plasmids, intensified by the presence of disinfectants and antibiotics, represents a significant driver of ARG dissemination. Transposable elements facilitate the mobilization of ARGs onto conjugative plasmids, while environmental stressors like disinfectants can further promote the transfer of these plasmids across bacterial populations. This complex interplay points the urgent need to address the role of disinfectants and other environmental contaminants in the spread of antibiotic resistance and highlights the importance of developing strategies to mitigate their impact on the resistome.

As a result, the objective of this thesis is to explore the interactions between transposable elements and conjugative plasmids in disinfectant-degrading *Pseudomonas* species, specifically *Pseudomonas sessilinigenes* BIOMIG1 and *Pseudomonas saponiphila* DSM 9751. The study aims to investigate how these bacteria, known for their high genomic plasticity and ability to degrade quaternary ammonium compounds (QACs), facilitate the transposition of mobile genetic elements under stress conditions induced by disinfectants like benzalkonium chloride (BAC). By analyzing the transposition events and mapping the plasmids involved, the research seeks to uncover the potential of these plasmids to act as vectors for gene transfer, thereby contributing to the dissemination of resistance and degradation capabilities in bacterial communities. The findings are expected to enhance the understanding of the role of mobile genetic elements in bacterial adaptation and the spread of environmental resistance genes, with implications for addressing pollution and resistance issues in wastewater treatment plants and other environments receiving QAC disinfectants.

2. LITERATURE BACKGROUND

2.1. Conjugative Plasmids: The Engines of Horizontal Gene Transfer

Plasmids are small, circular, extrachromosomal DNA molecules that play a critical role in bacterial adaptation and evolution. They replicate independently and carry a range of non-essential but beneficial genes including those associated with antimicrobial resistance, biodegradation, biofilm formation, virulence, and heavy metal tolerance. These gene provide their bacterial hosts with selective advantages within their ecosystem (Virolle et al., 2020). Plasmids typically have shorter sequence lengths ranging from 1-100 kb, lower GC content, and a unique origin of replication compared to chromosomal DNA (Snyder et al., 2013). Their autonomous replication ability enables them to exist in high copy which is influenced by their structure and genetic content (Snyder et al., 2013) Every plasmid contains an origin of replication (ori), which determines its copy number, and accessory genes that enhance their persistence in microbial communities. Moreover, they include promoters, operators and other sequences that control the expression of genes carried by the plasmids (Cecchetelli et al., 2023).

Plasmids are categorized into three groups based on their transferability: conjugative, mobilizable, and non-mobilizable (Che et al., 2021). Conjugative plasmids are larger (averaging 150 kb) and have a higher GC content (averaging 50.7%) compared to the other two groups. (Che et al., 2021). Despite being the less abundant, they are crucial for the horizontal transfer of genes among bacteria since these plasmids can transfer themselves from one cell to another (Che et al., 2021; Virolle et al., 2020). Therefore, the conjugation process and conjugative plasmids have been a major issue in environmental sciences due to their role in the determining the fate of antibiotic resistance and toxic chemicals, which are priority pollutants, in the environment.

Conjugation is a unidirectional process of genetic material exchange between cells which plays a critical role in evolution by enabling the spread of adaptive traits. Conjugation events occur across diverse environments, including water, sewage, biofilms, soil, plant surfaces, and bacterial communities associated with the host (Virolle et al., 2020). The transfer of genetic material through conjugation allows bacteria to gain advantages in the face of various stresses, such as antibiotics, heavy metals, temperature extremes, and toxic compounds (Cecchetelli et al., 2023). Notably, some conjugative plasmids possess a broad host range, even spanning different genera and kingdoms

(Dionisio et al., 2005). This raise concerns about the potential spread of these plasmids, especially within dense bacterial communities like wastewaters, to pathogenic species (Dionisio et al., 2005).

Bacterial conjugation is mediated by specialized protein apparatuses. Conjugative plasmids encode all the necessary genes to equip their host cell for efficient plasmid dissemination. The F plasmid, the first discovered and well-characterized conjugative plasmid, serves as a model for conjugation in gram-negative bacteria. Understanding its transfer mechanism provides insights into the conjugation process of F-like conjugative plasmids prevalent in these bacteria. The conjugation from the donor cell to the recipient cell is shown in Figure 2.1 in detail.

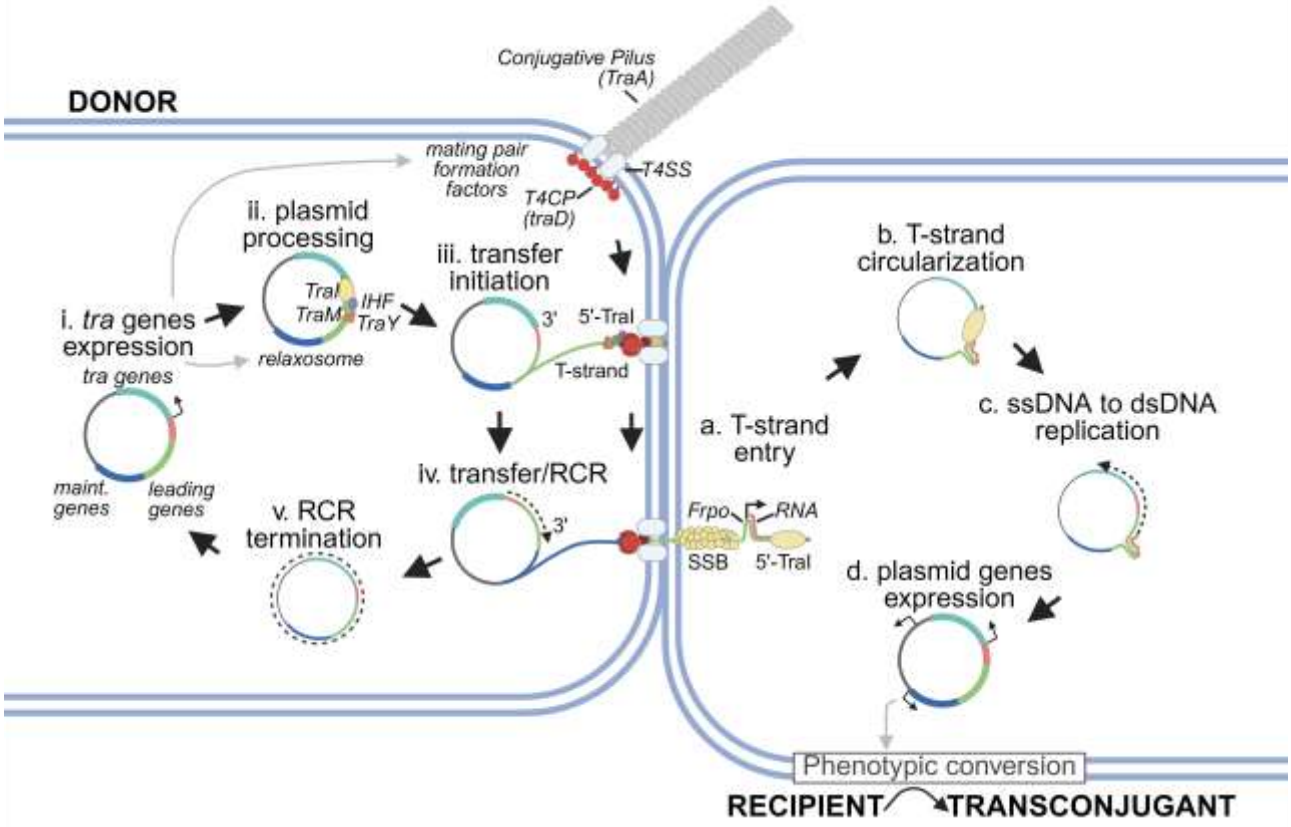

Figure 2.1. The conjugation from a donor cell to a recipient cell. The processes take place in the donor cell are: i. tra genes expression, ii. plasmid processing, iii. transfer initiation, iv. transfer/RCR (rolling circle replication), and v. RCR termination. The processes take place in the recipient cell are: a. T-strand entry, b. T-strand circularization, c. ssDNA to dsDNA replication, and d. plasmid genes expression. After the step d, recipient cell becomes a transconjugant that shows phenotypic properties of the plasmid (Adapted from Virolle et al., 2020).

Conjugation involves multiple steps controlled by plasmid-borne genes and assisted by donor and recipient cell enzymes, transcription, translation, and signaling systems (Virolle et al., 2020). Basically, an F plasmid has *tra* regions (encoding all transfer genes), the oriT region (origin of transfer

region), the leading region (the first region that enters into the recipient cell), and the maintenance region (for plasmid replication and partition) (Virolle et al., 2020).

Conjugation initiation in bacteria depends on the expression of *tra* genes (Figure 2.1 (i)), which encode regulatory and essential proteins for the conjugation machinery (Virolle et al., 2020). These genes are held in the conserved backbone of the plasmid and contribute significantly to its overall size (Partridge et al., 2018). Conjugation is a contact-dependent mechanism, that utilizes a specialized machinery encoded by the *tra* genes (Virolle et al., 2020). The relaxosome complex, produced by *tra* genes, is comprising *traY*, *traI*, and *traM*, which prepares the plasmid for the conjugation process (Figure 2.1 (ii)) (Virolle et al., 2020). The proteins encoded by these genes, TraI, TraY, and TraM, work together to unwind and prepare the plasmid DNA for transfer by nicking one strand at a designated origin of transfer (oriT) site (Virolle et al., 2020).

The *tra* genes also encode conjugative pilus coupled with a type IV secretion system (T4SS) responsible for pair-mating between the cells. The proteins involved in this machinery, such as TraA, TraQ, and TraX, can vary depending on the plasmid and are constructing the pilus (Virolle et al., 2020). Once the pilus and T4SS are formed, the pilus interacts with a compatible receptor on the recipient cell, initiating mating pair formation (Mpf), which is necessary for the successful transfer of the single-stranded plasmid DNA (T-strand) (Figure 2.1 (iii)) (Virolle et al., 2020). The type IV coupling protein (T4CP), encoded by specific *tra* genes, connects relaxosome with the T4SS, ensuring the efficient transfer of T-strand from donor to recipient cell (Figure 2.1 (iv)) (Virolle et al., 2020). The specific proteins that form the T4CP can vary depending on the plasmid, such as TraD and TraG (Virolle et al., 2020). Despite these variations, the role of the T4CP in conjugation keeps its critical and consistent role across different plasmids (Virolle et al., 2020).

The expression of *tra* genes is tightly regulated and influenced by various factors that modulate the frequency of conjugative plasmid spread. These factors include proteins encoded by the plasmid and the host, the physiological state of the host, environmental pressures, and interactions with other bacteria in the population (Virolle et al., 2020). Together, these elements determine whether the plasmid activates its *tra* genes.

Tra proteins directly involved in the conjugation process, a specific regulatory protein, TraJ, is required to activate the expression of other *tra* genes. The promoter for the *traJ* gene (P_J) is distinct from the promoter for the other *tra* genes (P_Y), allowing for a more nuanced control of gene expression (Virolle et al., 2020). Also, host chromosomal proteins, such as the histone-like nucleoid

structuring protein (H-NS), and plasmid-encoded proteins primarily target the P_J promoter to regulate both conjugation and plasmid replication (Virolle et al., 2020). The concentration of H-NS, which varies with the growth phase of the cell—peaking during the exponential phase and decreasing in the stationary phase—plays a critical role in this regulatory process (Brambilla & Sclavi, 2015). The tight regulation of *tra* genes allows the plasmid to fine-tune its transfer efficiency throughout its life cycle. This precise control helps mitigate the fitness cost to the host organism that would result from continuous gene expression.

In F-like systems, two distinct modes of plasmid transfer can occur: distant or tight transfer (Fraikin et al., 2024). In distant transfer, the pilus remains extended, allowing for direct DNA transfer without pulling the cells together (Fraikin et al., 2024). Alternatively, in tight transfer, pilus retraction can facilitate close cell-to-cell contact stabilized by specific protein interactions (such as TraN-OmpA) (Fraikin et al., 2024). The F plasmid-encoded pili can effectively explore a substantial volume, approximately 137.4 μm^3, surrounding the donor cell —a zone that significantly exceeds the average size of a bacterial cell, around 2 μm (Fraikin et al., 2024). The probing efficiency of these pili likely varies considerably across different plasmids, driven primarily by variations in the number and average length of pili, which exhibit significant heterogeneity even among closely related plasmids (Fraikin et al., 2024).

The types of pili found in conjugation systems vary, with two main categories: F-like pili and P-like pil (Schröder & Lanka, 2005) i. F-like pili are generated by plasmids such as IncF, IncH, IncT, and IncJ. These pili are long and flexible, ranging from 2 to 20 μm in length. In contrast, P-like pili are produced by IncP, IncN, IncW, and IncI systems. P-like pili are shorter, measuring between 0.2 to 1 μm, and are rigid, making them more prone to breaking off from the cells that produce them. Generally, the production of sex pili in bacteria is low; for instance, bacteria with the F plasmid typically produce between 1 and 4 pili per cell, and similar quantities are seen in other conjugation systems.

On the recipient side of conjugation, successful integration requires several essential steps: circularization of the transferred single-stranded DNA (ssDNA) plasmid (Figure 2.1 (b)) to evade recipient defense mechanisms, conversion to double-stranded DNA (dsDNA) (Figure 2.1 (c)), establishment of plasmid maintenance for stable replication, and finally, phenotypic conversion of the recipient cell (and terming it as a transconjugant) (Figure 2.1 (d)) (Virolle et al., 2020). While the F plasmid, with its limited host range, struggles to replicate in non-native bacteria like *Pseudomonas aeruginosa* and *P. putida* due to incompatibility with their replication machinery (Fraikin et al.,

2024), *P. aeruginosa* actively defends against conjugation from other species. It achieves this through a communication system called quorum sensing (QS), which involves a molecule called N-acyl homoserine lactone (AHL) (Virolle et al., 2020). Interestingly, AHL can bind to a specific protein in *E. coli*, a typical donor bacteria, and this binding prevents the expression of genes (*traI*) required for conjugation, effectively stopping the spread of plasmids like the broad-host-range RP4 integrated into the *E. coli* chromosome (Virolle et al., 2020). Even though the successful transfer of conjugative plasmids themself can be limited by host range, they still play a significant role in disseminating crucial survival genes within compatible bacterial populations.

Conjugation is naturally influenced by bacterial physiology and environmental factors but is also affected by various chemical stressors in the environment (Amirfard et al., 2024). For instance, low concentrations of certain antibiotics can increase conjugation efficiency (Zhou et al., 2024). This increase is linked to the bacterial SOS response, a stress response triggered by DNA damage. The SOS response activates genes involved in DNA repair and recombination, which can unintentionally promote plasmid transfer and the spread of antibiotic resistance genes. Heavy metal contamination is another environmental factor that changes the dynamics of conjugation (Palm et al., 2022). Exposure to metals like mercury and copper has been shown to raise the frequency of plasmid transfer. This effect is thought to result from the induction of oxidative stress and DNA damage, which also trigger the SOS response. Similarly, exposure to pesticides and industrial effluents can impact conjugation processes by disrupting cell membranes or interfering with gene expression. While the specific mechanisms vary depending on the type and concentration of the chemical, the consistent role of the SOS response in these interactions highlights its importance in how chemical exposure influences conjugation (Matsui & Endo, 2018).

Relatively recently, the study by Hu et al. (2024) showed how quaternary ammonium biocides (QACs) influence the conjugative transfer of antibiotic resistance genes (ARGs) in a structure- and species-dependent manner. The researchers explored the effects of six different QACs on the transfer of ARGs using two conjugation models: one within the same genus (E. coli to E. coli) and another between different genera (*E. coli* to the pathogenic *S. sonnei*). The key findings reveal that QACs significantly promote both intra- and inter-genus conjugative transfers, with the extent of promotion depending on the specific QAC structure and the recipient species. For instance, didecyl dimethyl ammonium chloride (DDAC) was found to enhance conjugative transfer frequencies the most, while benzathine chloride (BEC) had the least impact. The study highlights that the increased cell membrane permeability, reactive oxygen species (ROS) production, and proton motive force (PMF)-induced enhancement of flagellar motility in E. coli are likely responsible for the increased intragenus

transfer. In contrast, S. sonnei exhibited increased membrane permeability and biofilm formation, coupled with reduced flagellar motility, which facilitated inter-genus conjugation (Hu et al., 2024).

2.2. Transposable Elements as Vehicles for Intracellular Gene Translocation

When resistance and catabolic plasmids are investigated, the selective genes, i.e. resistance genes and xenobiotic degradation genes, in those plasmids are mainly on transposable elements.

Transposable elements (TEs) are the nucleic acid sequences that can relocate within the bacterial genome independently (Casacuberta & González, 2013). They used to be called junk DNA because their functions were unknown. However, in the recent two decades, it has been discovered that they have a crucial role in shaping the genome evolution and function (Biémont & Vieira, 2006). The TEs commonly found in bacteria are transposons (Tns) and insertion sequences (ISs) which are simply shown in Figure 2.2 (Shi et al., 2021).

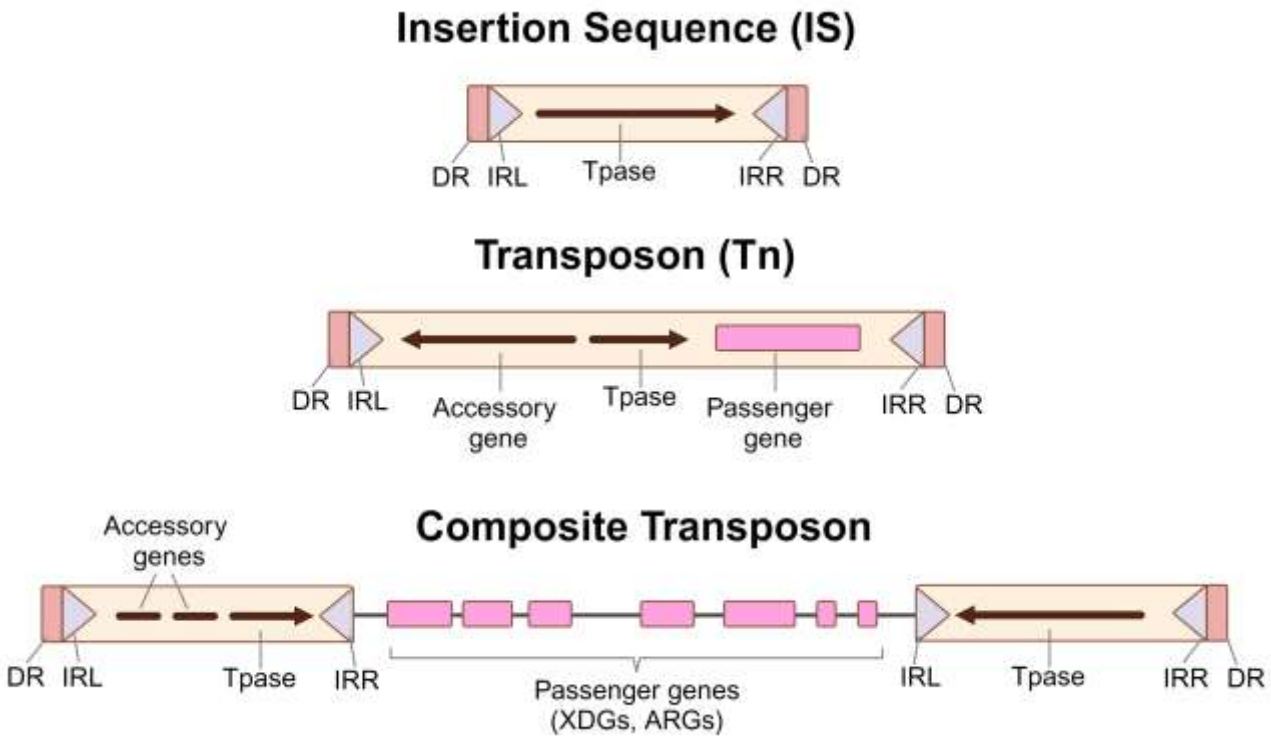

Figure 2.2. The commonly found transposable elements in bacteria in their simplified forms respectively as insertion sequence (IS), transposon (Tn), and a composite transposon. Their directed repeats (DRs), inverted repeats as left and right (IRL and IRR), transposase enzyme (Tpase), and passenger genes are shown (Adapted from Siguier et al., 2015).

Tns are relatively complex structures that can vary widely in size and composition. They typically contain several key components: coding sequences for transposase (TPase) enzymes, which mediate their movement; regulatory sequences that control the expression of genes; and often, additional genes that confer selective advantages, such as antibiotic resistance (Figure 2.2). The transposase gene is central to the function of the transposon, as it encodes an enzyme that recognizes specific sequences at the ends of the transposon, known as terminal inverted repeats (TIRs). These TIRs are crucial for the transposase to cut and paste the transposon into new locations within the genome. Transposons may also include sequences that help in regulating the expression of both the transposase and other genes they carry, contributing to their ability to influence the host genome's function and evolution (Siguier et al., 2015).

ISs, on the other hand, represent the simplest form of transposable elements. They are generally much smaller than transposons, typically ranging from 0.7 to 2.5 kilobases, and contain only the genetic information necessary for their own transposition. This includes one or two open reading frames (ORFs) that encode the transposase enzyme and TIRs that are recognized by the transposase (Figure 2.2). Unlike transposons, ISs do not carry additional genes beyond those involved in their movement, which limits their impact on the host genome to their ability to insert into new locations. However, this insertion can disrupt genes, create mutations, or alter gene expression, contributing to genetic variability. When an IS inserts into the genome, it often leaves behind a short direct repeat (DR) at the insertion site, which is a hallmark of its transposition event (Lipszyc et al., 2022; Siguier et al., 2006). From a genetic perspective, both Tns and ISs are powerful tools for genome evolution. Tns, with their more complex structures, can transfer not only themselves but also other genetic material, such as antibiotic resistance genes, between different genomic locations or even between different organisms. ISs, despite their simplicity, are abundant and can generate significant genetic diversity through their frequent and often random insertion into new sites within the genome. The presence of thousands of different ISs across various species highlights their pervasive role in shaping genomes throughout evolutionary history (Siguier et al., 2015).

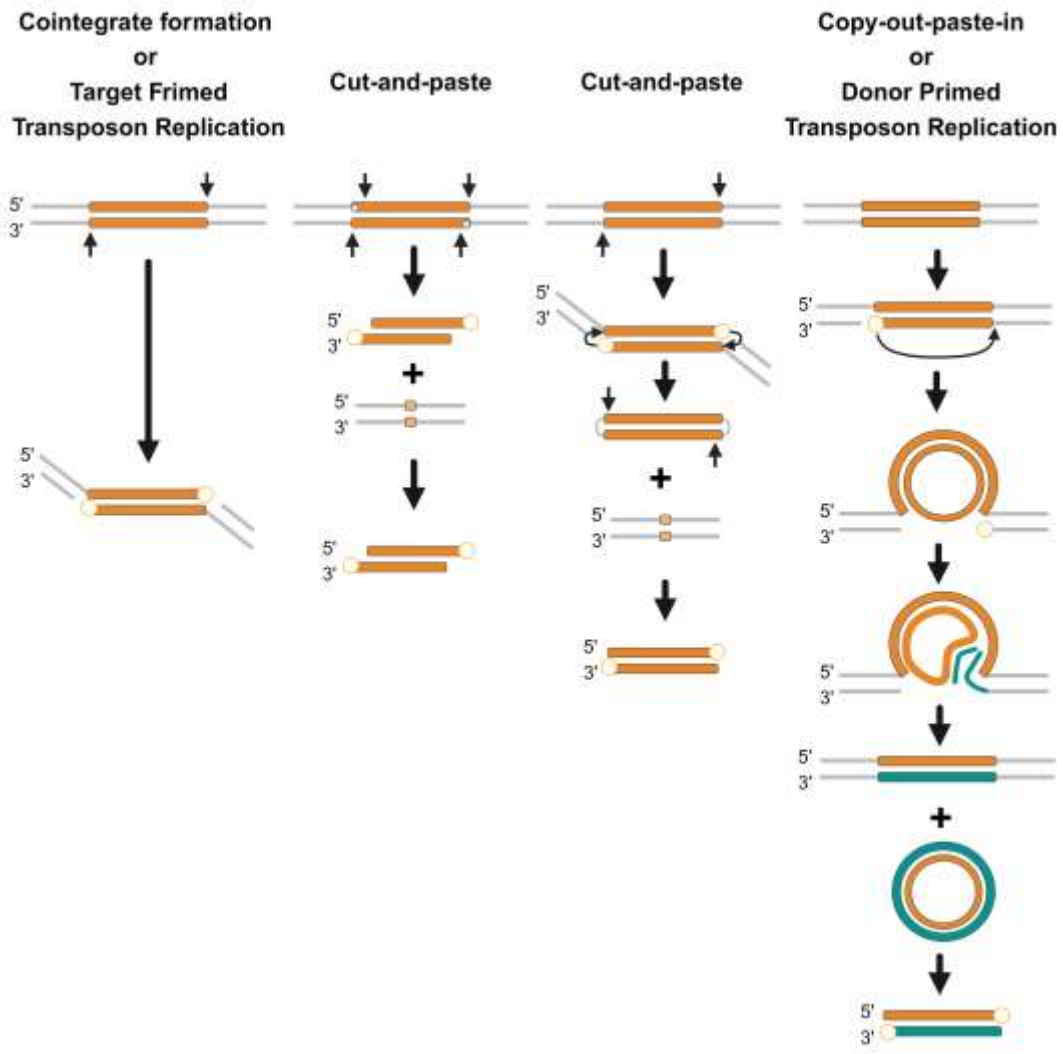

Figure 2.3. The transposition mechanisms of DDE transposases. ISs shown in orange and the flanking DNA in grey. 3’ OH residues are shown in yellow circles. The first column shows how initial cleavages create a 3′OH on the transferred strand, which then attacks to the target DNA (not shown), forming a forked molecule. This process, used by TEs from the Tn3 and IS6 families, is called target-primed transposon replication. The second column describes the IS630 family pathway, where the nontransferred strand is cleaved two bases within the TE before the transferred strand, creating a 3′ OH. This results in a 2-bp scar on the donor molecule, and the process involves cut-and-paste without TE replication. The third column shows transposition via a hairpin intermediate, where the transferred strand is cleaved, and the 3′ OH attacks the opposite strand to form a hairpin at the TE ends. This process releases the TE from the donor DNA and results in a final transposition intermediate. This method is cut-and-paste without TE replication. The fourth column describes a "copy out-paste" mechanism, where one IS end is cleaved, and the 3′ OH attacks the opposite end. The TE replicates using the donor DNA's 3′ OH, a process known as donor-primed transposon replication. This forms a double-strand DNA circle, regenerates the donor molecule, and the circle is then cleaved and inserted (Adapted from Siguier et al., 2015).

Analysis of public databases reveals that ISs relying on DDE transposases are the most common type (Siguier et al., 2015). DDE transposases are named after their characteristic sequence of three amino acids: two aspartic acids (D) and one glutamic acid (E). Although DDE TEs share the same basic chemical process, they show remarkable versatility in how they prepare DNA for integration into the genome. The key difference lies in how they handle the second, "non-transferred" DNA strand after the first strand is cleaved (Siguier et al., 2015). There are two common types of bacterial transposition mechanisms: “cut-and-paste” and “copy-and-paste (or replicative”. During “cut-and-paste transposition”, the transposable element is excised from its original location and inserted into a new site within the genome (Figure 2.3). This process is typically mediated by a transposase enzyme, which recognizes TIRs, at the ends of the transposable element. The transposase cuts the DNA at these sites, removes the element, and then inserts it at a new location, where it reintegrates into the DNA strand. An example of this mechanism is seen in Tn5, a well-known composite transposon in bacteria. Tn5 carries antibiotic resistance genes and is flanked by IS50s, which provide the transposase enzyme required for its movement. The transposase cuts the transposon out of its original location and inserts it into a new target site, often leaving behind a small DR at the insertion site (Kleckner, 1990).

In replicative transposition, the transposable element is copied, and the new copy is inserted into a different location while the original element remains in place. This results in an increase in the number of copies of the transposable element within the genome. This mechanism involves the formation of a complex structure called a cointegrate, where the donor and target sites are temporarily fused. The transposase mediates the cutting and joining of DNA strands, leading to the formation of this intermediate structure. The host's replication machinery then resolves the cointegrate, leaving one copy of the transposon at each site. An example of this mechanism is seen in Tn3, a classic transposon that carries an ampicillin resistance gene. During Tn3 transposition, the transposon is duplicated, and the new copy is inserted into a target site, resulting in two copies of the transposon within the genome.

Another related mechanism, though not as common, is site-specific recombination, which involves the integration of a transposable element into a specific site within the genome. This mechanism is exemplified by bacteriophage λ integration, where the phage integrates into the E. coli genome at a specific site, facilitated by the λ integrase enzyme. While this is not transposition in the traditional sense, it illustrates another method by which genetic elements can move within bacterial genomes.

Tns can have coding, regulatory, and non-coding sequences (Siguier et al., 2015). Their more complex structure contains flanking sequences at each end called inverted repeats (IRs or TIRs (terminal inverted repeats)), a transposase (TPase) coding sequence, and a foreign DNA, which can be a regulatory or resistance gene varies depending on the Tn type (Lipszyc et al., 2022). Meanwhile, ISs are much smaller than Tn and only contain a few base pairs of DNA, which may be non-coding or regulatory sequences (Siguier et al., 2015). Additionally, they can contain promoters and other regulatory sequences that enable the expression of genes (Siguier et al., 2015). Typically, ISs contain one or two open reading frames (ORFs) encoding the TPase, an enzyme facilitating IS movement by cleaving DNA strands and mediating their transfer (Lipszyc et al., 2022; Siguier et al., 2006). Also, it flanks by short (10–40 bp) and imperfect terminal inverted repeat sequences (designated as left IR - IRL and right IR - IRR) that serve as the TPase's binding sites for initiating transposition (Lipszyc et al., 2022; Siguier et al., 2006). ISs constitute the most straightforward class of transposable elements (TEs). They are distinguished by compact size, typically 0.7 to 2.5 kilobases, and harbor genes solely dedicated to transposition and regulation (Siguier et al., 2006). As generally seen in most DNA transposons, when an IS jumps around the bacterial genome and inserts itself into a new location, it often leaves a short, duplicated "scar" at the insertion site that is called a direct repeat (DR) (Siguier et al., 2015).

TEs frequently interact with plasmids and facilitate the horizontal transfer of antibiotic resistance genes and xenobiotic degradation genes within bacterial populations. The review by Partridge et al. (2018) highlights the critical role of resistance transposable elements, such as transposons (Tns) and insertion sequences (ISs), and their interaction with plasmids in the dissemination of antimicrobial resistance genes across bacterial populations. Transposons like those from the Tn3 family, including Tn1, Tn2, and Tn3, are key players in this process; these elements can move resistance genes, such as blaTEM (which encodes beta-lactamase), from one location in a genome to another or between different DNA molecules, including plasmids. These transposons are capable of replicative transposition, creating cointegrates that carry the resistance genes into new genetic contexts, thereby promoting the spread of resistance. Similarly, ISs, such as IS26, are crucial for the mobilization of resistance genes within and between plasmids. IS26, for instance, frequently facilitates the movement of ARGs by creating translocatable units that can integrate into plasmids, contributing to the assembly of complex multi-drug resistance regions. The review discusses how these ISs and transposons often target plasmids, particularly conjugative plasmids like those from the IncF group, which are known for their ability to transfer between bacterial cells through conjugation. This interaction between ISs, transposons, and plasmids enables the rapid and widespread dissemination of resistance genes, including critical genes like blaCTX-M (an ESBL gene) and mcr-1 (a colistin resistance gene). The

combination of these mobile genetic elements with plasmids creates a potent mechanism for the horizontal gene transfer of antimicrobial resistance, allowing bacteria to quickly adapt to antibiotic pressures in various environments. For example, the review discusses how ISs like ISApl1 are involved in the mobilization of the mcr-1 gene, which confers resistance to colistin, a last-resort antibiotic. ISApl1 can capture and mobilize mcr-1 as part of a transposon, which then integrates into plasmids, enabling its spread across different bacterial species (Partridge et al., 2018).

A more comprehensive study by Che et al. (2021) revealed how ISs significantly influence the horizontal transfer of ARGs through their interactions with conjugative plasmids, which are crucial vehicles for gene mobility across bacterial populations. The researchers developed a computational tool named "Plascad" and analyzed a large dataset comprising 14,029 complete plasmid sequences and 12,059 complete bacterial genomes obtained from the NCBI database. The study showed that ARG, such as blaNDM and blaCTX-M, are predominantly enriched in conjugative plasmids. They discovered a large-scale IS-associated network of ARG transfer, involving 245 combinations of 59 AMR gene subtypes and 53 ISs. This network demonstrated how ISs facilitate the movement of AMR genes across diverse bacterial species and plasmid types, contributing to the rapid spread of resistance. For instance, IS26 was found to be particularly successful in mediating the transfer of AMR genes like mcr-1 as mentioned above. Moreover, the authors experimentally validated their bioinformatic predictions by reconstructing the transfer pathways of the gentamicin resistance gene (accC1) in controlled laboratory settings. The experiments showed that IS26-associated ARG genes could integrate into both plasmid and chromosomal DNA, within complex microbial communities. in wastewater treatment plants (Che et al., 2021).

TEs also facilitate the active movement of xenobiotic degradation genes (XDGs) within bacterial genome. XDGs mobilize when they are in transposons (Tn) or flanked with insertion sequences (IS). Such transposable elements (TEs) containing catabolic genes, called catabolic composite transposable elements, are frequently detected in the environment, and they facilitate adaptation and subsistence of bacteria to the environments contaminated with toxic chemicals (Nojiri et al., 2004). A TE that is frequently associated with catabolic genes is IS1071. IS1071 is a Tn3-family transposase that plays a role in mobilizing the catabolic genes in the atrazine (Changey et al., 2011; Martinez et al., 2001) and chlorobenzoate (Campbell Wyndham & NG, 1993; Fulthorpe & Campbell Wyndham, 1992; Ogawa & Miyashita, 1999) degradation pathway. Recently, many other genes related to the biodegradation of various toxic chemicals were detected in the IS1071 TEs (Dunon et al., 2018). The majority of those genes were related to Rieske oxygenases, taurine/a-ketoglutarate dioxygenases, amidohydrolases/amidases, nitrile hydratases, nitrilases, and the enzymes involved in the chlorine

removal (Dunon et al., 2018). In addition to IS1071, ISPpu12 and IS6100, which are responsible for the mobilization of chlorate and methyl parathion biodegradation genes, respectively, are other catabolic TEs reported in the literature to date (Clark et al., 2013; Wei et al., 2009). All those catabolic composite TEs have been detected in promiscuous plasmids of the IncP-1 group (Dunon et al., 2018; Król et al., 2012; Nojiri et al., 2004). This evidence suggests that TEs play a significant role in disseminating catabolic genes among bacteria and adapting microbial communities to toxic synthetic chemicals by facilitating their biodegradation.

Exposure to toxic chemical substances facilitate transposition as they increase conjugation rate. In a recent study by Yao et al. (2022), the transposition dynamics of antibiotic resistance genes (ARGs) between chromosomal and plasmid DNA within bacterial populations under varying antibiotic pressures. The study utilized both synthetic and natural transposons to analyze their behavior in Escherichia coli strains under different antibiotic conditions. The key experimental approach involved creating bacterial strains where a resistance gene, such as *tetA* (tetracycline resistance), was inserted into a miniTn5 transposon integrated into the chromosome. The host bacteria also contained high-copy plasmids that could potentially receive the transposon. the bacteria were exposed to different concentrations of antibiotics, including tetracycline, and the distribution of the transposon between the chromosome and plasmid was measured the growth rates of the bacterial populations were also assessed under these conditions to determine the fitness costs and benefits associated with carrying the resistance genes on plasmids versus chromosomes. The study found that stronger antibiotic selection pressures led to a higher frequency of transposition of the *tetA* resistance gene from the chromosome to plasmids. This was because plasmid-based resistance genes, due to the higher copy number of plasmids, resulted in greater gene expression and, consequently, higher cell survival under antibiotic stress. The experiments demonstrated that this transposition dynamic was not limited to a specific resistance gene or antibiotic. The researchers tested various combinations of promoters, resistance genes (including *ampR*, *kanR*, *cmR*, and *smR*), and plasmid origins, all of which showed similar trends where increased antibiotic concentrations promoted the transposition of resistance genes to plasmids. The study also explored how these transposition events could lead to interpopulation gene transfer. In mixed cultures of bacterial strains, the presence of antibiotics led to the rapid spread of plasmid-borne resistance genes through conjugation, particularly at higher antibiotic doses (Yao et al., 2022).

In another study, Yang et al. (2023) explores the impact of benzalkonium chlorides (BACs), a common disinfectant, on the development of antibiotic resistance in sewage sludge microbiomes. The researchers conducted microcosm experiments where sewage sludge samples were exposed to

varying concentrations of BACs. The effects of this exposure were then analyzed using high-throughput quantitative PCR (HT-qPCR) and Illumina sequencing to assess changes in antibiotic resistance genes (ARGs) and microbial community structure. The diversity and absolute abundance of ARGs increased significantly in the sludge samples exposed to BACs, even at environmentally relevant concentrations. The most enriched ARGs were those conferring resistance to multidrug, aminoglycosides, and sulfonamides. The increase in ARG abundance ranged from 2.15-fold to 3.63-fold compared to the control samples not exposed to BACs. In addition, the study found that the increase in ARGs was primarily driven by the horizontal gene transfer of ARGs facilitated by mobile genetic elements (MGEs) under BACs stress. The abundance of MGEs, such as integrons, transposons, and plasmids, also increased significantly after BACs exposure. The researchers suggest that BACs exposure might induce the overproduction of reactive oxygen species (ROS), which could further facilitate the horizontal transfer of MGEs carrying ARGs (Yao et al., 2022).

Recent studies described above clearly illustrate that certain environmental pollutants including antibiotics and disinfectants promote horizontal gene transfer. Among them, QACs are in particular interest due to their extensive use during the COVID-19 pandemic. While crucial for infection control, the increased environmental release of QACs raises concerns about their long-term ecological and human health impacts. Therefore, studying QACs in the post-pandemic context is crucial.

2.2.1. Pandemic's Aftermath: The Hidden Role of Quaternary Ammonium Compounds in Accelerating Horizontal Gene Transfer

QACs are organic compounds that have been on the market for more than 90 years(Ertekin et al., 2016) and have the highest demand among all disinfectants due to their cationic, nonvolatile, and stable nature (Dewey et al., 2022; Tezel & Pavlostathis, 2011). The QAC disinfectant usage has reached such a level that we can encounter them anywhere, even in breast milk (Zheng et al., 2022). This group of organic compounds is one of the most essential ingredients of more than 200 products (Hora et al., 2020). After the COVID-19 pandemic, they have been used mainly for disinfection almost everywhere, including hospitals, homes, schools, and food processing facilities (Hora et al., 2020). Also, they are present in handwashing soaps (Hora et al., 2020), personal care products, pharmaceuticals, and so on (Zheng et al., 2022). Before the pandemic, since the 1940s, they have been increasingly used, especially in the U.S., as disinfectants in the military, public eateries, the dairy industry, and hospitals (against drug-resistant bacteria strains) (Hora et al., 2020). However, the unrestricted usage of QAC disinfectants has caused a dramatic increase in their concentration in the environment as a chemical contaminant, causing environmental and human life concerns (Dewey et

al., 2022). The increased QAC concentration has many problematic environmental effects, such as inhibiting aerobic wastewater treatment and selecting QAC-degrading and antibiotic-resistant bacteria, which can lead to the emergence of multidrug-resistant strains (Hora et al., 2020). Additionally, QACs contribute to the formation of N-nitrosamines through reactions with chloramines, a known carcinogen, and increase toxicity to aquatic organisms (Hora et al., 2020). The stress caused by the most widely used QAC group, BACs, with alkyl chains eight to 18 carbon atoms long, can cause clinically significant antibiotic resistance (Kim et al., 2018). At this high level of usage of QAC-containing disinfectants, bacteria can be exposed to QACs anywhere, which makes it a significant stress factor that pushes bacteria to adapt in order to survive. QAC resistance in *Pseudomonas* has been attributed to various mechanisms, including changes in membrane lipid composition, the production of lipids, increased phospholipids and fatty/neutral lipids, modifications to cell surface charge, and enhanced efflux systems (Arnold et al., 2023). In some instances, increased tolerance to BACs has been associated with cross-resistance to other QACs and clinically relevant antibiotics (Arnold et al., 2023). Furthermore, the presence of other organisms in the environment may enhance the survival of *Pseudomonas species* under disinfectant stress, highlighting the complex interplay between microbial communities and antimicrobial resistance (Arnold et al., 2023). The tolerance of *Pseudomonas species* to QACs is not the only notable trait related to these compounds. Certain members of this genus have demonstrated the capacity to utilize QACs as an energy source to support their growth and proliferation.

2.3. The Species That Can Degrade QACs Carry Many TEs

Pseudomonas is one of the most diverse and well-studied bacterial groups, with a rich history dating back to its initial description in 1894 by Walter Emil Friedrich August Migula (Peix et al., 2009). *Pseudomonas species* are typically non-spore-forming, aerobic, gram-negative rods that can exist in biofilms or as free-floating planktonic cells (Özen & Ussery, 2012). They can utilize diverse carbon compounds as energy sources and have minimal nutritional requirements (Rumbaugh, 2014). While these bacteria grow under aerobic conditions, they also possess the capacity for anaerobic respiration, utilizing nitrogen as an alternative electron acceptor when oxygen is limited (Rumbaugh, 2014).

The *Pseudomonas* genus is one of the most intricate and diverse groups of bacteria with medical and biotechnological relevance, with a continuously growing number of recognized species. Currently, it represents the Gram-negative bacterial genus with the highest number of validated species (Gomila et al., 2015). According to the NCBI Taxonomy DB, the *Pseudomonas* genus

contains more than 300 species, which harbor remarkably many strains (Schoch et al., 2020). The size of the *Pseudomonas* genus has been steadily expanding, with new species being added to the classification each year, reflecting the diversity of these microorganisms. The ubiquity and adaptability of the *Pseudomonas species* highlight their unique ability to thrive in wide-ranging ecological niches worldwide. They have been found in different environments, including water, soil, seas, and even deserts, ranging from the extreme colds of the Antarctic to the tropical regions (Peix et al., 2009). This broad distribution is enabled by their remarkable metabolic versatility, allowing them to thrive in various environments. They are significant in medical and scientific areas but also crucial in various ecological processes. Many *Pseudomonas* strains are known for their ability to degrade a wide range of organic compounds, including xenobiotics and environmental pollutants (Rumbaugh, 2014). This metabolic diversity makes them valuable in bioremediation efforts, which can be helpful for breaking down and removing contaminants from soil and water (Rumbaugh, 2014). It is underpinned by the genus' large and flexible genomes, which often contain abundant transposable elements (Rajabal et al., 2021). Genomic flexibility, driven by the acquisition and loss of genes, plays a crucial role in the microorganism's ability to adapt to changing environmental pressures. This adaptability is particularly evident in antibiotic-resistance genes often located on mobile genetic structures such as plasmids, transposons, and bacteriophages (Didelot et al., 2016). These mobile elements facilitate the rapid spread of resistance genes among different microbial populations, enabling them to quickly adapt to selective forces (such as antibiotic resistance, xenobiotic resistance, and so on) (Didelot et al., 2016). These mobile genetic elements contribute to the remarkable genomic plasticity of *Pseudomonas*, enabling rapid adaptation to changing environmental conditions.

Pseudomonas genus of bacteria is also responsible for degradation of QACs, besides many other hazardous pollutants, in the environment. QAC degrader strains of Pseudomonas species include *Pseudomonas sessilinigenes* BIOMIG1 (Altinbag et al., 2020; Ertekin et al., 2016) and *Pseudomonas saponiphila* DSM 9751 (Lang et al., 2010). *P. sessilinigenes* BIOMIG1 is a strain belonging to the *Pseudomonas* genus capable of completely mineralizing various homologs of BAC disinfectants (Ertekin et al., 2016). It was isolated from a sample taken from the influent of the Pasakoy urban wastewater treatment plant in Istanbul, Türkiye (Altinbag et al., 2020). The strain's complete genome sequence comprises a single circular chromosome of 7,675,262 base pairs, a relatively large genome size for a *Pseudomonas* species (Altinbag et al., 2020). This microorganism can convert BACs into ammonium through a series of dealkylation, debenzylation, and demethylation reactions, making it the first fully characterized BAC degrader metabolically and genetically (Altinbag et al., 2020) Additionally, *P. sessilinigenes* BIOMIG1 tolerates cationic disinfectants and broad-spectrum antibiotic resistance, primarily through multidrug efflux pumps (Altinbag et al., 2020). The complete

genome contains 104 ISs and 43 integrases, indicating a large and flexible genome that may harbor other novel catabolic functions awaiting discovery (Altinbag et al., 2020). Also, *P. sessilinigenes* BIOMIG1 does not contain a native plasmid.

Pseudomonas saponiphila DSM 9751 is a new *Pseudomonas* strain, exhibiting the typical features of the *Pseudomonas* genus being a gram-negative, aerobic, and motile bacterium (Lang et al., 2010). It was isolated by W.F. Guerin, Michigan State University, due to its ability to utilize cetyltrimethylammonium chloride (CTAC, hexadecyltrimethylammonium chloride), a QAC, as its sole carbon and energy source (Lang et al., 2010). Cetyltrimethylammonium chloride is a QAC commonly incorporated in surface disinfectants (Zhang et al., 2015). The specific source of isolation for this strain remains unknown; however, it has been found commonly in reclaimed water (Wu et al., 2016). *P. saponiphila* DSM 9751 was found to be non-fluorescent, non-denitrifying, and capable of hydrolyzing starch. Interestingly, diverging from many of its closely related strains, this strain displayed oxidase activity, which makes it able to use cetyltrimethylammonium chloride as the sole carbon source, and this property gives this species' name saponiphila meaning soap (detergent)-loving (Lang et al., 2010).

Analysis of the *P. saponiphila* DSM 9751 genome revealed a size of 7.38 Mbp, suggesting a relatively large and versatile genetic repertoire (Hesse et al., 2018). Since its large genome and the remarkable ability to degrade xenobiotics, it is possible that its genome contains various transposable elements. Although the specific details about the *P. saponiphila* DSM 9751 *qxyA* gene cluster and its BAC degradation ability are not provided in the database, according to the study of our group, *P. saponiphila* DSM 9751 can degrade BAC and harbors *qxyA* gene cluster carries in a composite transposon. The *qxyA* gene cluster is flanked with a Tn3 family transposable elements from both ends in *P. sessilinigenes* BIOMIG1. Unlike BIOMIG1, the *qxyA* gene cluster is flanked with IS1380 family TE for *P. saponiphila* DSM 9751. Overall, *P. saponiphila* DSM 9751 represents a novel *Pseudomonas species* capable of degrading xenobiotic compounds with potential applications in bioremediation. Moreover, according to the study of Lang et al. (2010), there was no evidence of an existing plasmid in *P. saponiphila* DSM 9751.

These two strains are remarkable with their high transposition rates, too. According to the results of transposition experiments done by our group, BIOMIG1's two composite transposons and an IS were obtained. The composite transposons and IS are TnPsp::merPTR, TnPses::Qxy, and ISPsP8. TnPsp::merPTR is a composite transposon containing the mercury resistance gene that accounts for the majority of transposition events, and TnPses::Qxy is a composite transposon containing the *qxyA*

gene. These transposition events were detected by extracting and sequencing pMAT1 plasmid from transformed BIOMIG1 cells with the pMAT1. BIOMIG1's transposition rate was calculated as $1.09x10^{-2}$, which is relatively higher than the average transposition rates of bacteria, 10^{-5} and 10^{-6} (Sousa et al., 2013). The same protocol was used for DSM 9751, and its transposition rate was calculated as $1.51x10^{-2}$. The high transposition rates observed in these strains are a significant indicator of highly active Tn/ISs and genomes with high plasticity.

Transposition can be triggered by environmental stress and changes (Vigil-Stenman et al., 2017). QACs are an increasing environmental stress factor (Sakarya et al., 2021). According to Sakarya et al., WWTPs have been used to eliminate QACs; however, despite this effort, there is still a persistent flow into the environment (2021). Particularly after the COVID-19 pandemic (Hora et al., 2020), which may lead to operational challenges and increased antibiotic resistance within the microbial community (Kim et al., 2018). This stress-rich environment could result in the proliferation of resistant microbes, posing significant health risks (Rizzo et al., 2013). Therefore, it is essential to study the mobile genetic elements responsible for these adaptations and causing resistant bacteria. The current database of complete plasmids and genomes is biased towards easily cultured and pathogenic bacteria, suggesting that additional potentially conjugative plasmids remain to be identified and characterized (Che et al., 2021). The potential of adaptation in polluted environments attracts attention to the mechanisms underlying the transfer of AMR (Che et al., 2021) and catabolic genes. It highlights the essential relationships between genetic interactions that drive the dissemination of these genes. Therefore, it is crucial to investigate the potential effects of QACs on highly adaptive bacteria.

3. MATERIALS AND METHODS

3.1. Bacterial strains and plasmids

In this study, experiments were performed on both *Pseudomonas sessilinigenes* BIOMIG1, which was isolated in 2013 in our laboratory (Ertekin et al., 2016)and *Pseudomonas saponiphila* DSM 9751, which was purchased from The Leibniz Institute German Collection of Microorganisms and Cell Cultures GmbH (Leibniz Institute DSMZ). Both strains are able to grow in M63B1 minimal medium composed of 7.4 g/L K_2HPO_4, 3.0 g/L KH_2PO_4, 2g/L $(NH_4)_2SO_4$, 0.1 g/L $MgSO_4.7H_2O$, 0.5 mg/L $FeSO_4.7H_2O$ ve 1 mg/L thiamine hydrochloride (vitamin B1) and 200 mg/L benzalkonium chlorides (BACs, Tekkim, TR) as the sole carbon and energy source.

DSM 9751 has its own plasmid, i.e. p9751 whereas BIOMIG1 was transformed with pRK24 via pair-mating using *E. coli* ECNR2+pRK24 strain obtained from Addgene Inc. Transformation was performed as follows: The donor strain ECNR2+pRK24 was cultured in a 10 mL LB medium containing 36 mg/L tetracycline overnight at 28°C with shaking at 150 rpm while *P. sessilinigenes* BIOMIG1 was cultured in 50 mL M63B1 medium containing 200 mg/L BACs for two days at 28°C with shaking at 110 rpm. When cultures reached to the late log phase, they were centrifuged for 10 minutes at 4500 rpm. They were washed with LB three times and finally centrifuged at 11,300 *xg* for 2 minutes. The pellets were resuspended in 100 µL LB, and the cell density was normalized to 0.2 $OD_{@600nm}$. About 80 µL of ECNR2+pRK24 and 20 µL BIOMIG1 culture solutions were mixed gently by pipetting in a microcentrifuge tube and six 10 µL culture mixture was spotted on an agar plate composed of M63B1 and %1.5 agar. The plate was incubated for three hours at 28ºC. After incubation, spots on the agar surface were collected in 1500 µL LB broth and 50-µL sample was spread on M63B1 agar containing 1000 mg/L BACs and 36 mg/L tetracycline (M63B1*BACTet*) after appropriate dilutions. As controls, 10^{-1} and 10^{-3} dilutions were plated on both LB and M63B1*BAC* agar plates. The colonies grown on the M63B1*BACTet* agar were selected and the transformation was confirmed after plasmid extraction and gel electrophoresis.

3.2. Transposition Experiments

The objective of this experiment was to identify the transposition events on pRK24 and p9751 while the host bacteria of those plasmids were growing on BACs. The experiment was performed in 250-mL Erlenmeyer flasks. Each flask was received 50 mL M63B1 medium that contains 200 mg/L

BACs. A series of flasks containing 200 mg/L and 500 mg/L acetate, and only 1000 mg/L acetate were also prepared. Each flask received 100 µL cell culture previously grown in 1000 mg/L acetate to sustain c.a. 10^6 CFU/mL initial cell concentration in the flasks. Flasks inoculated with BIOMIG1+pRK24 also contained 36 mg/L tetracycline to help BIOMIG1 to keep the plasmid during the incubation period. Controls of each set without cultures were also prepared. Each flask was prepared in triplicates. The flasks were incubated for 48 hours at 28ºC with constant agitation at 110 rpm. Samples were taken at 0^{th}, 24^{th} and 48^{th} hours of incubation.

Total cell density and number of BAC degraders in the culture were measured by spotting a series of 10 µL sample diluted in a range from 10^0 to 10^6 on LB and M63B1*BAC* agar, respectively. Agar plates were incubated at 28ºC for at most 48 hrs. Colonies in the spots were counted and cell density was reported as CFU/mL.

BAC concentration in the samples were measured using a high-performance liquid chromatography (Shimadzu Corporation, Kyoto, Japan) equipped with a Zorbax Eclipse XDB-C18 column (Agilent Technologies, California, USA) (Tezel & Pavlostathis, 2009). A 700 µL sample was first mixed with a 700 µL 3:1 Acetonitrile:50mM phosphate buffer (pH 2.5), vortexed for 20 seconds, and centrifuged for 5 minutes at 10,000 rpm. 50 µL supernatant was injected and BACs were separated on the column receiving 3:1 Acetonitrile:50mM phosphate buffer (pH 2.5) at 1.0 mL/min and maintained at 40ºC. Detection was achieved with a UV-Vis detector at a wavelength of 210 nm.

Acetate concentration in the samples was measured with an Agilent 1100 Series HPLC (Agilent Technologies, Palo Alto, CA, USA) unit equipped with a Hi-Plex H ion exclusion column (300 × 7.8 mm) (Agilent Inc., USA) and UV/visible diode array detector. A 0.01 N H_2SO_4 solution was used as the mobile phase with a flow rate of 0.6 mL/min and the column was maintained at 65ºC. The samples were centrifuged, and the supernatant was acidified with 0.01 N H_2SO_4 in a 1:1 ratio. Acetate was detected by the UV detector at 210 nm wavelength.

3.3. Plasmid Isolation

At the end of the incubation period, the whole content in the flasks remaining after sampling was used for plasmid isolation. The liquid content in the flasks were centrifuged for 10 mins at 4500 rpm, and the pellets were processed using ThermoScientific GeneJET Plasmid Miniprep Kit (Vilnius, Lithuania) according to the manufacturer's instructions to isolate plasmids. The extracts were mixed with 6X TriTrack DNA loading dye (Thermo Scientific) and run on 0.7% agarose gel for 55 minutes

at 70 V against GeneRuler 1 kb DNA Ladder (Thermo Scientific). The gel was visualized using the Gel Doc XR+ Gel Documentation System (BIO-RAD, California, USA) after staining with 1X RedSafe Nucleic acid staining solution (Intron Biotechnology).

3.4. Decontamination, Linearization and Purification of the Plasmid Extracts

In order to prepare plasmid extracts for nanopore sequencing, three significant steps have to be followed: removal of contaminating chromosomal DNA, linearization, and purification and concentration.

Chromosomal DNA contamination in the plasmid extracts was removed the Plasmid-Safe™ ATP-Dependent DNase (Epicentre, Illumina, Madison, WI, USA) kit. In summary, 50 µL extract (<100ng/µL) was incubated with 10U exonuclease for 1 hour at 37 °C, and the enzyme was inactivated for 30 minutes at 70°C. Decontaminated plasmid extracts were linearized with HpaI (NEB, Massachusetts, USA) endonuclease. Both plasmids have two HpaI recognition sites, locations of which are so close to each other. That's why, the integrity of the plasmids does not change after HpaI digestion. After endonuclease digestion, the linearized plasmids were purified to eliminate all the residues from previous enzymatic reactions using MagBead DNA purification kit (MobiomX; Massive Bioinformatics, İstanbul, Türkiye) The purified linear plasmids were controlled by running 0.7% agarose gel electrophoresis for 55 minutes and 70 V, and their imaging was done by Gel Doc XR+ Gel Documentation System (BIO-RAD, California, USA). They were stored at -20°C for further processes.

3.5. Nanopore Sequencing

Ligation sequencing gDNA - Native barcoding kit (SQK-NBD114.24; Oxford Nanopore Technologies, Oxford, United Kingdom) was used to prepare plasmid sequencing libraries. At the end of the library preparation, the samples were pooled into a single sample. Since each plasmid was chemically tagged with a specific predefined barcode provided by the kit, they were safely separated during sequencing. After library preparation was done, the barcoded plasmids were loaded into a Flongle Flow Cell (FLO-FLG114; Oxford Nanopore Technologies, Oxford, United Kingdom). The sequencing was performed on 87 active pores for 24 hours.

3.6. Bioinformatic Analysis

The bioinformatic analysis was done for three purposes: (1) plasmid classification and map generation of p9751 and pRK24 plasmids, (2) IS/Tn analysis of *P. sessilinigenes* BIOMIG1 and *P. saponiphila* DSM 9751, and (3) the analysis of the transposition experiment.

For the plasmid classification and map generation, the plasmid DNA FASTA file of p9751 was obtained from the NCBI database. Since *P. saponiphila* DSM 9751's genome is at the contig level, the NCBI Assembly database (Sayers et al., 2022) was used, and the FASTA file of the plasmid was obtained through WGS project number FNTJ01000004.1 as the fourth contig. The plasmid DNA FASTA file of pRK24 (Addgene plasmid # 51950) was obtained from the Addgene Repository's NGS result (Ma et al., 2014). MOB-suite was used to classify these two plasmids. MOB-suite is a bioinformatics tool designed to classify and characterize mobile genetic elements, particularly plasmids (Robertson & Nash, 2018). This software consists of three interconnected modules: MOB-cluster, MOB-recon, and MOB-typer (Robertson & Nash, 2018). Combining these modules significantly enhances the identification of plasmid sequences, even from whole genome sequencing (WGS) assemblies (Robertson & Nash, 2018). The effectiveness of the MOB-suite relies on an extensive plasmid database, ensuring highly accurate results (Robertson & Nash, 2018). Together, these modules provide insights into various aspects of plasmids, including their replicon, relaxase, mate-pair formation system (Mpf), oriT, mobility predictions, potential host range, and plasmid similarity (Robertson & Nash, 2018).

After classification analysis, the plasmid maps were generated by annotation with PGAP (Tatusova et al., 2013) and oriTfinder (H. Li, 2018). Since these maps were more focused on conjugative and vital properties of plasmids, other genes were not included, and the maps were kept simple. The genes that are closely located and work for a common purpose were shown under a gene cluster array, such as the T4SS gene cluster. The annotated plasmids were screened, and the maps were generated using SnapGene Viewer (v7.2.1) (GSL Biotech, San Diego, CA) software.

For the IS/Tn analysis of *P. sessilinigenes* BIOMIG1 and *P. saponiphila* DSM 9751, the genomic DNA FASTA files were obtained from the NCBI database. *P. sessilinigenes* BIOMIG1's genome was obtained by the NCBI Taxonomy database (Schoch et al., 2020) with GenBank ID CP049045. Since *P. saponiphila* DSM 9751's genome is at the contig level, the NCBI Assembly database (Sayers et al., 2022) was used, and the FASTA file of the genome was obtained through Whole Genome Shotgun (WGS) project number FNTJ01 as four contigs. IS and Tn profiling were done by ISEScan

(v1.7.2.3) (Xie & Tang, 2017), and further analysis to determine the properties of the transposable elements was done by ISfinder database (Siguier et al., 2015). Frequency and ratio graphs of both strains' IS/Tn families were generated using Python toolkits Pandas (v2.2.2) (McKinney, 2010) and Matplotlib (v3.9.1) (Hunter, 2007).

The last of the bioinformatic analysis was processing transposition experiment sequence data. After sequencing of the plasmids obtained from the transposition experiment, the high-quality sequences were taken by doing base-calling and trimming using the ONT's software MinKNOW. At the end of the 24-hour run, 436.42 k reads were generated, which corresponds to 9.56 Gb nucleotide data with an average 3.63 Kb read length by the MinION platform (Lu et al., 2016). The FAST5 formatted raw signal output file was converted into FASTQ format, and the sequence was trimmed from sequencing adapters by Guppy (v3.4.4) base caller software (Wick et al., 2019). The configuration option was selected as "dna_r9.4.1_450bps_fast.cfg" since it is compatible with the flow cell used in the protocol. The FASTQ files were investigated using NanoPlot (v1.42.0) (De Coster & Rademakers, 2023) to understand their read quality and length. For this purpose, all FASTQ files of each plasmid were pooled into a single FASTQ file. After deciding the filters as quality is 8, and length is 1000 to keep the majority of the high-quality data, filtering was done for each barcode separately. Chopper (v0.8.0) (De Coster & Rademakers, 2023) was used to filter the low quality (<Q8) and short length (<1000bp) reads. Then, before further analysis, the pooled sequence files of p9751 and pRK24 were blasted against their host strain's genomic DNA and the plasmids' sequences. For this purpose, Blast+ command line (v2.15.0) (Camacho et al., 2009) was used for alignment, and the Python toolkit Matplotlib (v3.9.1) (Hunter, 2007) was used for plotting.

In order to further analyze the transposition results, the annotation of the sequences was done. Before annotation, several pre-processes were applied. Each barcode file was mapped to its reference plasmid by Minimap2 (v2.28) (H. Li, 2018) to find the parts of the sequences that correspond to the reference, and the FASTQ files were converted to FASTA files after this process. The mapped sequences were blasted by Blast+ (v2.15.0) (Camacho et al., 2009) to create a database from the sequence reads of each barcode. The produced database and the sequence reads were aligned to find the unaligned regions. The unaligned regions are likely to be a transposition event. During this process, some reads were found without unaligned regions, and they were left empty sequences in the FASTA files. So, they had to be cleaned by SeqKit (v2.8.2) (W. Shen et al., 2024) for further processes. The processes were done for each barcode. However, in sequencing data, some reads couldn't be classified. Since the unclassified files were quite large (357 MB, three times larger than other barcodes' file size), they were also processed for analysis. All of the processes were the same

until mapping. For the mapping process, the unclassified file was mapped to p9751 and pRK24 separately to select the sequences from these plasmids. So, the processes for unclassified files were continued with respect to the mapped plasmid. Moreover, all unaligned sequence files were filtered with SeqKit (v2.8.2) (W. Shen et al., 2024) with a minimum 200 bp length since further annotation step has this minimum limit to work.

After all these pre-processes, the unaligned region sequences were annotated by PGAP (v6.7) (Tatusova et al., 2013). PGAP is a straightforward NCBI program that works with a single line code (Tatusova et al., 2013). The annotation reference genomes were limited to *P. saponiphila* DSM 9751 for p9751 and *P. sessilinigenes* BIOMIG1 for pRK24 since the transpositions were expected to be from these strains' genomes. The annotation results were investigated using Geneious Prime (v2024.0.2) (Massachusetts, USA).

4. RESULTS AND DISCUSSION

4.1. Classification of p9751 and pRK24

First, in this study, the plasmid maps were created. According to the study of Lang et al., there was no evidence of an existing plasmid in *P. saponiphila* DSM 9751 (2010). However, we have found a native conjugative plasmid in the contig sequence data obtained from the whole genome shotgun (WGS) sequencing project, which we accessed through NCBI Nucleotide Database (Sayers et al., 2022) with WGS project ID FNTJ01 and the FASTA file of the plasmid was obtained through WGS project number FNTJ01000004.1 as the fourth contig. The plasmid DNA FASTA file of pRK24 (Addgene plasmid # 51950) was obtained from the Addgene Repository's (Ma et al., 2014) NGS sequence. MOB-suite was used to classify these two plasmids. MOB-suite is a bioinformatics tool designed to classify and characterize mobile genetic elements, particularly plasmids (Robertson & Nash, 2018). The detailed classification report obtained by the MOB-suite is given in Table 4.1. The analysis of the plasmids p9751 and pRK24 reveals several important characteristics regarding their structure, function, and potential ecological roles. Both plasmids have a single contig, indicating continuous sequences without interruptions. The size of p9751 is 50534 base pairs, while pRK24 is larger at 65630 base pairs. Both plasmids exhibit high GC content, with p9751 at 59.98% and pRK24 at 60.86%, often associated with increased stability and functionality in plasmid behavior (Chen et al., 2017).

Regarding replicon types, p9751 belongs to the IncQ group, whereas pRK24 is classified as IncP. This classification indicate the incompatibility groups of the plasmids, which affect their ability to coexist within the same bacterial host (Wang et al., 2019). The relaxase types differ as well; p9751 has the MOB_F type, while pRK24 features the MOB_P type. The MOB_F family relaxases have related to rolling-circle transposases and their only main two members are detailed in biochemically and structurally in the literature (Garcillán-Barcia et al., 2009). MOB_P is the largest relaxase family that contains many plasmids that highly promiscuous or being recognized by their ability to disseminate antibiotic resistance (Garcillán-Barcia et al., 2009). Also, the IncP incompatibility group plasmids belong to a subgroup of this relaxase family (Garcillán-Barcia et al., 2009). Relaxase is crucial for the transfer of plasmids during bacterial conjugation. It is the key protein that initiates and terminates conjugative DNA transfer by catalyzing cleavage at the origin of transfer (oriT) site (Garcillán-Barcia et al., 2009). Relaxase typing is used for classifying conjugative plasmids based on the sequence and properties of their relaxase proteins (Garcillán-Barcia et al., 2009). Relaxases are classified into 6

classes as MOB_F, MOB_P, MOB_H, MOB_Q, MOB_C, and MOB_V (Garcillán-Barcia et al., 2023). Although relaxase typing shows whether a plasmid conjugative or not, generally the T4CP sequence adjacent to relaxase is analyzed for confirmation of a functional conjugative system (Garcillán-Barcia et al., 2009). The differences in relaxase families may suggest variations in the transfer mechanism and host interaction, however, it is unknown the mechanisms causing the difference between these families (Garcillán-Barcia et al., 2009).

p9751 and pRK24 share a mate-pair formation type classified as MPF_T, which is typical for conjugative plasmids (Coluzzi et al., 2022). MPF typing is based on the classification of the *VirB* genes in the T4SS gene cluster of plasmids in proteobacteria (Smillie et al., 2010). There are four MPF classes based on archetypes as; plasmid F (MPF_F), plasmid Ti (MPF_T), plasmid R64 (MPF_I), and the genomic loci of ICEHin1056 (MPF_G). The class of the focused plasmids in this study, MPF_T, is the most abundant type which indicates its transfer success; however, this type of plasmids' conjugation rate is quite low in liquid media. On the other hand, the origin of transfer for p9751 is unspecified, while pRK24 is noted as MOB_unknown. Depending on the mentioned properties, these plasmids were predicted to be conjugative, meaning they can transfer genetic material between bacteria through direct contact.

The closest database matches for these plasmids indicate a strong association with *Pseudomonas* aeruginosa, a bacterium known for its role in various infections and its capacity for antibiotic resistance (Ramos et al., 2020). The accession number for p9751 is associated with an unnamed plasmid (CP027168), while pRK24 matches the Birmingham IncP alpha-plasmid (L27758). The mash distances from the query to the match are relatively small, indicating close genetic relationships (Ondov et al., 2016).

The host range for p9751 is observed as the genus level corresponding to *Pseudomonas*, while the host range of pRK24 is at the multi-phyla level as Actinomycetota and Pseudomonadota. However, pRK24 is a broad-host-range plasmid with various hosts, from E. coli to cyanobacteria (Gale et al., 2019; Ma et al., 2014).

In summary, the p9751 and pRK24 plasmids are conjugative and exhibit high GC content, with distinct incompatibility and relaxase types. Their close association with *Pseudomonas* aeruginosa emphasizes their potential significance in microbial ecology and the study of antibiotic resistance. Further research could provide deeper insights into their specific roles within their host organisms and their implications for genetic transfer and adaptation.

Table 4.1. MOB-suite plasmid classification analysis results.

Property	p9751	pRK24
Number of contigs	1	1
Size (bp)	50534	65630
GC (%)	59.98	60.86
Replicon type(s)	IncQ	IncP
Relaxase type(s)	MOB_F	MOB_P
Mate-Pair formation type	MPF_T	MPF_T
Origin of transfer type	-	MOB_unknown
Mobility prediction for the plasmid (Conjugative, Mobilizable, Non-mobilizable)	conjugative	conjugative
Accession of the closest plasmid database match	unnamed1 (CP027168)	Birmingham IncP alpha-plasmid (L27758)
Mash distance from query to match	0.0466675	0.00299754
Host taxonomy of the plasmid database match	*Pseudomonas* aeruginosa	*Pseudomonas* aeruginosa
Taxon rank and name of convergence between observed and reported host ranges	genus (*Pseudomonas*)	multi-phyla (Actinomycetota, Pseudomonadota)
Taxon rank and name of convergence of literature reported host ranges	-	phylum (Pseudomonadota)

After classification, the plasmid maps were generated by annotation with PGAP (Tatusova et al., 2013) and oriTfinder (X. Li et al., 2018). Since these maps focused more on conjugative and vital properties of plasmids, other genes were not included, and the maps were kept simple. The genes closely located and working for a common purpose were shown under a gene cluster array, such as the T4SS gene cluster.

The plasmid map of p9751 is given in Figure 4.1 The plasmid p9751 contains the main conjugative regions to be a self-transmissible plasmid, which is the origin of transfer (oriT), a relaxase gene, type IV coupling protein (T4CP), and the gene cluster of type IV secretion system (T4SS) (Li et al., 2018). The type of oriT couldn't be defined by either PGAP, oriTfinder, or MOB-suite. Moreover, the genes annotated as TrfB-related DNA-binding protein and TrbM/KikA/MpfK family conjugal transfer protein by PGAP are related to the conjugative feature of the plasmid. Both PGAP annotation and MOB-suite analysis classified the relaxase as MOB_F family relaxase, which was only mentioned as relaxase in Figure 4.1 for simplification. The T4SS gene cluster is divided into two parts by a Tn3 family transposon. The T4SS gene cluster can be incorporated into transposons and conjugation function may not be affected (Wallden et al., 2010). However, this transposon insertion can disrupt the conjugation function of the plasmid since it is inserted within the T4SS gene cluster.

In addition to the Tn3 family transposon, plasmid p9751 harbors two IS1474s from the IS21 family, resulting in three transposable elements.

Plasmid inheritance and regulative genes were StbB family protein gene, plasmid stabilization protein StbC gene, and type II toxin-antitoxin system VapB family antitoxin. The replication initiation gene of p9751 is *repA*, which encodes the RepA protein. Typically, IncQ incompatibility group plasmids harbor *repA*, *repB*, and *repC* replication genes that make the plasmid fully independent from the host (Jain & Srivastava, 2013). In general, IncQ plasmids share a common core that is simply composed of three *mob* genes (*mobA*, *mobB*, and *mobC*) and three *rep* genes (mentioned above) (Meyer, 2009). However, p9751 carries only *mobF* (not shown in Figure 4.1) and *repA*. With respect to both the MOB-suite analysis and PGAP annotation, p9751 contains fewer sophisticated genes that other IncQ family plasmids do.

On the other hand, the plasmid pRK24 is larger and more complex than p9751. The plasmid map of pRK24 is given in Figure 4.2. The plasmid pRK24 contains the main conjugative regions for self-transmissibility as an oriT, a relaxase gene, T4CP, and the gene cluster of T4SS (X. Li et al., 2018). The type of oriT was defined as MOB_unkonwn by MOB-suite analysis, however, the properties of the oriT could not be completely determined. Moreover, an Mpf gene cluster consisting of *traM*, *traL*, and *traK* genes was determined. These genes are generally found in IncP-type plasmids (Murata et al., 2024). The genes annotated as *traM*, *traF*, *traD*, *traB*, *traA*, *traR/dksA* are related to the conjugative feature of the plasmid but could not be included in any gene cluster.

The relaxase type of pRK24 classified as MOB_P family by MOB-suite analysis and the PGAP annotation determined it as TraI/MobA(P) family conjugative relaxase. These two nomenclatures are the same, therefore, the relaxase of pRK24 was classified as MOB_P. In order to simplify the plasmid maps, the relaxase types were not mentioned in the figure 4.2. The plasmid pRK24 is a broad-host-range plasmid (Ma et al., 2014) with more diverse conjugation-related genes than p9751. This diversity of the conjugative elements reinforces its broad-host-range feature. With its strong conjugative properties, pRK24 has also two transposable elements: an IS21 family IS and a Tn3 transposon.

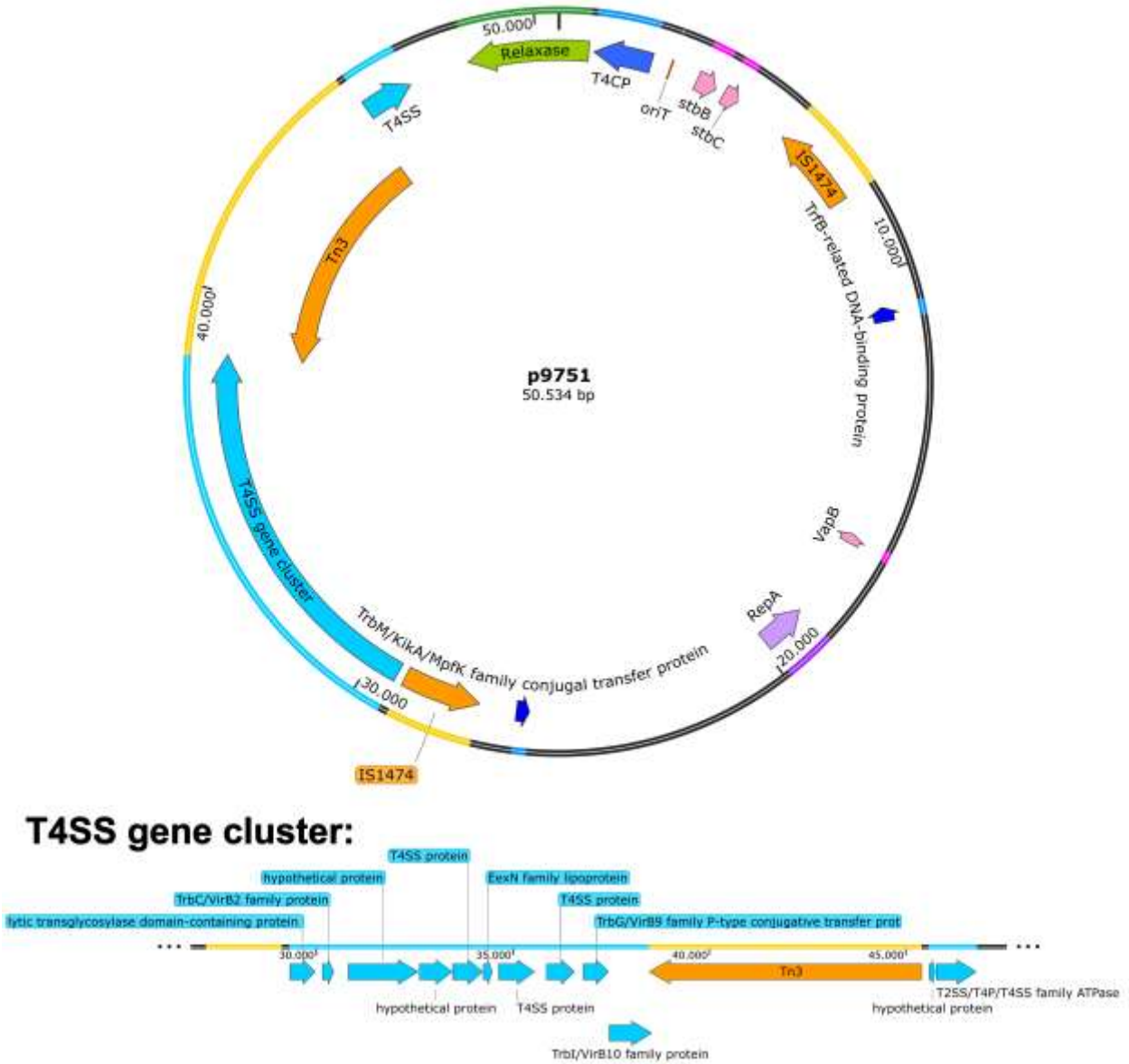

Figure 4.1. Plasmid map of the native plasmid of *P. saponiphila* DSM 9751, p9751, and its T4SS gene cluster members. p9751 has a 50534 bp length. It has conjugative genes labeled as oriT, TrfB-related DNA-binding protein, TrbM/KikA/MpfK family conjugal transfer protein, T4SS gene clusters, relaxase, and a T4CP. The T4SS gene cluster members are shown at the bottom of the figure in detail. The conjugative-related genes were labeled different shades of blue, and oriT was labeled brown. It has a Tn3 family transposon and two IS21 family IS1474 and these mobile genes were labeled orange. Moreover, it contains three regulatory genes: stbB, stbC, and VapB, as well as a RepB. The regulatory genes were labeled pink. Also, the replication initiator RepA is labeled purple.

In terms of antimicrobial resistance, pRK24 has various resistance genes such as tellurium resistance, APH(3’) (APH(3') family aminoglycoside O-phosphotransferase), tetracycline resistance, and blaTEM with an AmpR promoter. Tellurium resistance of pRK24 is provided by multiple genes such as toxic anion resistance protein, tellurium resistance system protein *klaB*, and tellurium resistance system protein *klaC* determined by PGAP. APH(3’) gene confers antibiotic resistance by modifying aminoglycoside antibiotics such as kanamycin and neomycin (Zeng & Jin, 2003). The TetR gene provides the plasmid's most common tetracycline resistance property (Cuthbertson & Nodwell, 2013). The other resistance gene that contributes to the pRK24 profile, the *blaTEM* gene with the strong promoter AmpR, contributes to the ampicillin resistance. However, it also provides resistance to other penicillins and cephalosporins (Jafari-Sales et al., 2023).

Plasmid inheritance and regulative genes were found as two parts of IncP-1 partitioning systems containing *korC*, *kleA*, *kleE*, *korA*, and *parA* genes, *kfrB* (IncP plasmid survival protein KfrB), *traJ* (oriT-recognizing protein), P-loop NTPase fold protein, type II toxin-antitoxin system (RelE/ParE family toxin, antitoxin ParD), two recombinases, and *trfA* (trans-acting replication protein that binds to and activates oriV). The toxin-antitoxin system is a useful module for plasmid stability that either inhibits cell growth or causes cell death of plasmid-free cells to prevent the proliferation of plasmid-free cells (Yano et al., 2019).

In conclusion, the plasmids p9751 and pRK24 analysis reveal significant insights into their structural and functional characteristics, highlighting their roles in microbial ecology and antibiotic resistance. Both plasmids exhibit high GC content and distinct incompatibility and relaxase types, indicating their evolutionary adaptations and potential interactions within bacterial hosts. The classification of p9751 as an IncQ group plasmid and pRK24 as an IncP group plasmid emphasizes their differing capacities for coexistence in the same bacterial environment. The plasmid classification into Inc groups is based on the plasmid incompatibility of the same group to be present in the same host because of the similar partitioning and replication systems (Suzuki et al., 2010). Additionally, the presence of various genes related to conjugation in both plasmids and antimicrobial resistance in pRK24 emphasizes its broad-host-range capabilities, which may facilitate the spread of resistance traits among diverse bacterial populations. The generated plasmid maps, focusing on crucial conjugative features, provide a clearer understanding of their genetic architecture.

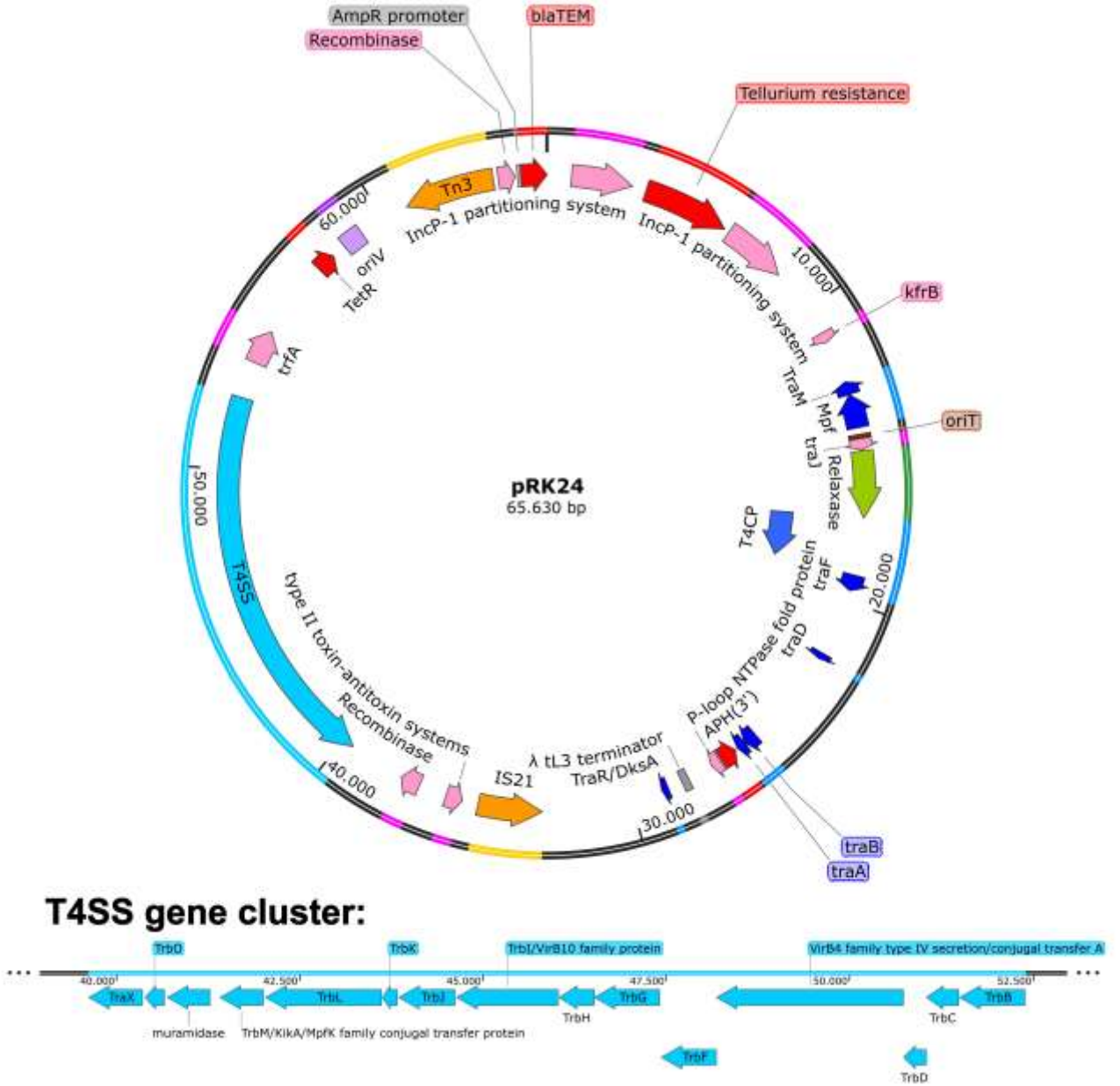

Figure 4.2. Plasmid map of the commercial conjugative plasmid, pRK24, and its T4SS gene cluster members. pRK24 has a 65630 bp length. It has conjugative genes labeled as oriT, relaxase, T4CP, traF, traD,traB, traA, TraR/DksA, T4SS gene cluster, TrabM, and Mpf. The T4SS gene cluster members are shown at the bottom of the figure in detail. The conjugative-related genes were labeled with shades of blue, and oriT was labeled brown. It has a Tn3 family transposon and an IS21 family IS and these mobile genes were labeled orange. pRK24 contains antimicrobial resistance genes: tellurium resistance genes, APH(3'), tetracycline resistance (TcR and TetR), and blaTEM with an AmpR promoter. The antimicrobial resistance genes were labeled red. Moreover, the regulatory genes of pRK24 are two IncP-1 partitioning system protein gene groups, kfrB, traJ, P-loop NTPase fold protein, type II toxin-antitoxin systems, two recombinases, and trfA. The regulatory genes were labeled with pink. Also, the replication initiator oriV is labeled with purple

4.2. TEs on *P. saponiphila* DSM 9751 and *P. sessilinigenes* BIOMIG1 Genome

Transposable elements (TEs) are genetic sequences that can move around within genomes, contributing to genetic diversity (Lima-Mendez et al., 2020). The transposition mechanisms of TEs and their effects on prokaryotic genomes have been a subject of interest after their discovery (Lima-Mendez et al., 2020). Therefore, defining the TE profile of the studied species is essential.

In this study, to obtain TE profiles of *P. saponiphila* DSM 9751 and *P. sessilinigenes* BIOMIG1, the genomic DNA FASTA files were obtained from the NCBI database. Since *P. saponiphila* DSM 9751's genome is at the contig level, the NCBI Assembly database (Sayers et al., 2022) was used, and the FASTA file of the genome was obtained through Whole Genome Shotgun (WGS) project number FNTJ01 as four contigs. Also, *P. sessilinigenes* BIOMIG1's genome was obtained by the NCBI Taxonomy database (Schoch et al., 2020) with GenBank ID CP049045. ISEScan analysis was done to search insertion sequences (ISs) and transposons (Tns) (Xie & Tang, 2017), and further analysis of the transposable elements was done by ISfinder database (Siguier et al., 2015).

Table 4.2 focuses on the ISs and Tns found in the genome of *P. saponiphila* DSM 9751. It includes various families of insertion sequences, each with specific features such as their names, copy numbers, transposition mechanisms, and associated genes. The table reveals various insertion sequences, with notable families. The genome of DSM 9751 harbors eight families of TEs: IS21, IS3, IS1380, IS5, Tn3, IS481, IS4, and IS630. The copy numbers of ISs in these families vary significantly, with the IS21 family having the highest count at 108 ISs, where 105 were determined as a DDE-type transposase containing IS1474. Two of the IS21 family ISs are ISPst3, and the last one of the IS21 family ISs is ISSsp5. These two types of ISs are also DDE transposase-containing ISs. The family following the highest number of ISs is the IS1380 family, which has nine DDE transposase-containing ISs: seven are ISPa33, and two are ISAzs25. IS4, IS5, and IS630 families have the same amount of ISs. The IS4 family has two ISPa1635 DDE transposase-containing ISs with a cut-and-paste transposition mechanism. IS5 family has ISPst5 and ISPst12 DDE transposase-containing ISs.

The IS630 family has two ISPpu1 DDE transposase-containing ISs with a cut-and-paste transposition mechanism. Also, IS3 and Tn3 family ISs only have one DDE transposase-containing ISs. ISPmo5, as an IS3 IS, has a copy-paste mechanism for transposition, whereas ISThsps9 has a co-integrate mechanism for transposition and a Tn3 resolvase accessory gene. The Tn3 family of transposons is the most prevalent transposon group, especially in bacteria (Lima-Mendez et al., 2020). These transposons shape their host genomes through a co-integrate mechanism that copies and pastes

the TE, employing a DDE transposase enzyme to create a cointegrate structure during transposition (Lima-Mendez et al., 2020). In addition to the genes required for transposition, members of Tn3 family often carry extra genes that benefit their host bacteria, such as resistance to antibiotics or heavy metals or increased virulence (Lima-Mendez et al., 2020). These genes are called passenger genes (Lima-Mendez et al., 2020). However, ISThsps9 found in *P. saponiphila* DSM 9751 does not carry a passenger gene.

The TEs found in *P. saponiphila* DSM 9751 constitute 4.55% of the entire genome. This variation in transposable elements may indicate differing roles in genomic stability and adapt for these sequences. This suggests that some may be more crucial for the organism's survival or evolution. The transposition mechanisms identified are primarily of the DDE type, which includes various transposition methods shown in Figure 2.3 This reliance on DDE mechanisms suggests that these transposable elements play a significant role in genomic rearrangements, potentially influencing gene expression and the organism's evolutionary trajectory (Siguier et al., 2015). Moreover, as shown in Figure 4.1 the two of IS1474 from IS21 family and ISThsps9 from Tn3 family are found on the native plasmid of DSM 9751.

Table 4.3 provides insights into the ISs and Tns present in the genome of *P. sessilinigenes* BIOMIG1. This table includes vital details such as the family of each insertion sequence, its specific name, the number of copies found in the genome, the type of transposition chemistry, the mechanism involved and associated accessory and passenger genes.

Table 4.2. The IS/Tn list of *P. saponiphila* DSM 9751 and their properties.

Family	Name	Copy number	Chemistry	Mechanism	Accessory genes	Identity (%)	Reference
IS1380	ISPa33	7	DDE			99	Raymond et al., 2002; Siguier et al., 2015; Szuplewska et al., 2014
	ISAzs25	2	DDE			83	Kaneko et al., 2010; Siguier et al., 2015
	IS1474	105	DDE		istB: helper of transposition	98	Yeo & Poh, 1997
IS21	ISPst3	2	DDE			87	Maeda et al., 2003
	ISSsp5	1	DDE			100	Habe et al., 2002; Inoue et al., 2005; Urata et al., 2006
IS3	ISPmo5	1	DDE	copy-paste mechanism		80	NR[a]
IS4	ISPa1635	2	DDE	cut-and-paste mechanism		99	De Palmenaer et al., 2008; Wolter et al., 2004
IS5	ISPst5	1	DDE			99	NR
	ISPst12	1	DDE			96	Siguier et al., 2015; Yan et al., 2008
IS630	ISPpu1	2	DDE	cut-and-paste mechanism		80-85	Van Beilen et al., 2001
Tn3	ISThsp9	1	DDE	co-integrate mechanism	Tn3 resolvase	79	NR[a]

[a] Not reported

The genome of *P. sessilinigenes* BIOMIG1 harbors ten families of TEs: IS1182, IS21, IS256, IS3, IS30, IS5, IS630, IS66, IS91, and Tn3. Among these, IS5 stands out with the highest IS number of 35. The IS5 family ISs found in BIOMIG1 include 30 ISs of ISPre2 and one IS of each ISPa96, ISPre1, ISPsfu1, ISPst5, and ISThi1. The family following the highest number of ISs is the IS30 family. Members of this family are ISPsp8, ISPsp7, and ISShes10, which have 14, 2, and 1 ISs in the BIOMIG1 genome, respectively. All IS5 family ISs have a copy-and-paste mechanism for transposition. IS630 family found in the BIOMIG1 genome with 11 ISs of ISPa47 that have a cut-and-paste transposition mechanism.

IS21 family ISs were detected as nine ISs of ISPpu27 that carry an IS21 helper accessory gene. IS3 family ISs were detected as two ISPen2 and two ISPa121.Tn3 family Tns were detected as three ISPa40 and an ISThsp9. These transposons are known for their ability to carry passenger genes. ISPa40 can carry chromate resistance protein, manganese, iron superoxide dismutase, and iron superoxide dismutase as passenger genes, while ISThsp9 is mainly known for its ability to carry mercuric resistance *merPTR* operon (Siguier et al., 2015). In *P. sessilinigenes* BIOMIG1's genome, ISThsp9 has a role as a mercury resistance transposon since it harbors the *merPTR* operon. Tn3 family transposons have a co-integrate transposition mechanism and carry Tn3 resolvase accessory genes (Siguier et al., 2015). Also, IS66 family two ISs were detected as ISPsy43. This IS type can harbor the IS66 TnpB accessory gene. The remaining IS1182, IS256, and IS91 families were detected as single ISs ISPa94, ISPa103, and IS1071, respectively. ISPa103 has the copy-and-paste transposition mechanism, while IS1071 has the rolling circle transposition mechanism and lacks the resolvase gene. All ISs in this dataset utilize the DDE transposition mechanism, like TEs in *P. saponiphila* DSM 9751 genome.

Table 4.3. The IS/Tn list of *P. sessilinigenes* BIOMIG1 and their properties. ND means "Not Determined".

Family	Name	Copy number	Chemistry	Mechanism	Accessory genes	Identity (%)	Reference
IS1182	ISPa94	1	DDE			80	NR[a]
IS21	ISPpu27	9	DDE		IS21 helper	99	Cury et al., 2016; Molina et al., 2013
IS256	ISPa103	1	DDE	copy-paste mechanism		83	D. Shen et al., 2019

[a] Not reported

Table 4.3. Cont.

Family	Name	Copy number	Chemistry	Mechanism	Accessory genes	Identity (%)	Reference
IS3	ISPen2	1	DDE		Two parts of transposase	100	Szuplewska et al., 2014; Vodovar et al., 2006
	ISPa121	2	DDE		Two parts of transposase	100	Shankar Chilambi et al., n.d.
IS30	ISPsp8	14	DDE	copy-paste mechanism		85-99	Szuplewska et al., 2014
	ISPsp7	2	DDE	copy and paste mechanism		85-99	Szuplewska et al., 2014
	ISShes10	1	DDE	copy and paste mechanism		85	Fredrickson et al., 2008
IS5	ISPre2	30	DDE			100	Maeda et al., 2003; Szuplewska et al., 2014; Urata et al., 2004
	ISPa96	1	DDE			81	Setubal et al., 2018; Snesrud et al., 2018
	ISPre1	1	DDE			88	Maeda et al., 2003; Szuplewska et al., 2014; Urata et al., 2004
	ISPsfu1	1	DDE			83	Dueholm et al., 2014; Yamaguchi-Kabata et al., 2018
	ISPst5	1	DDE			87	NR[a]
	ISThi1	1	DDE			99	Copeland et al., 2009; Siguier et al., 2015
IS630	ISPa47	11	DDE	cut-and-paste mechanism		99	González-Domínguez et al., 2012
IS66	ISPsy43	2	DDE		IS66 TnpB	97	Butler et al., 2013

[a] Not reported

Table 4.3. Cont.

Family	Name	Copy number	Chemistry	Mechanism	Accessory genes	Identity (%)	Reference
IS91	IS1071	1	DDE	rolling circle mechanism		99	Di Gioia et al., 1998; Nakatsu et al., 1991; Poh et al., 2002
Tn3	ISPa40	3	DDE	co-integrate mechanism	Tn3 resolvase	84	Siguier et al., 2015; L. Yang et al., 2011
	ISThsp9	1	DDE		Tn3 resolvase	100	NR[a]

[a] Not reported

The TEs in BIOMIG1 constitute 1.82% of the entire genome. Since BIOMIG1 and DSM 9751's genome sizes are close, respectively as 7.6 Mbp and 7.3 Mbp, it can be said that DSM 9751 has more transposable elements than BIOMIG1. However, the diversity of TEs in BIOMIG1 is greater than that in DSM 9751.

Overall, the data provides valuable insights into the genomic structure of DSM 9751 and BIOMIG1, highlighting the complexity and diversity of their transposable elements. Understanding these elements can offer deeper insights into the organism's adaptability, evolution, and potential applications in biotechnology and environmental science.

The inverted repeats (IRs) and direct repeats (DRs) of *P. saponiphila* DSM 9751 and *P. sessilinigenes* BIOMIG1 were listed with respect to their ISs and Tns in Table A.1.

4.3. Transposition Events Targeting Conjugative Plasmids During BAC Biodegradation

After classification of the plasmids and TE analysis of the species, transposition experiments were conducted under three conditions according to the carbon source: 1000 mg/L acetate, 500 mg/L acetate + 200 mg/L BACs, and 200 mg/L BACs. *P. saponiphila* DSM 9751 and *P. sessilinigenes* BIOMIG1+pRK24 were incubated as triplicate under these conditions for 48 hours at 28°C with shaking at 110 RPM. Samples were taken at 0^{th}, 24^{th} and 48^{th} hours of incubation to monitor the growth by spot-plating (spotting) and turbidity measurement. Also, the C-source consumptions were measured by HPLC.

In order to monitor the growth of the cultures, spot-plating was performed. The agar media used in spotting for *P.saponiphila* DSM 9751 were LB and M63B1*BAC* to measure the total cell density and the number of BAC degraders in the culture. DSM 9751's daily spotting are shown in Figure 4.3 and CFU/mL results are shown in Figure 4.4 (B), Figure 4.5 (B), and Figure 4.6 (C). It is clear that the growth under 500 mg/L Acetate + 200 mg/L BACs and 200 mg/L BACs conditions increased until 24th hours and reached its maximum at 48th hours of the experiment. The growth for 500 mg/L Acetate + 200 mg/L BACs condition was 2.33 x 10^8 CFU/mL and 1 x 10^8 CFU/mL for LB and M63B1*BAC*, respectively. The growth for the 200 mg/L BACs condition was 1.66 x 10^8 CFU/mL and 1 x 10^8 CFU/mL for LB and M63B1*BAC*, respectively. On the other hand, the growth under 1000 mg/L Acetate condition reached its maximum on 24th hours and started to decrease after 48 hours. After 24 hours, the growth on LB was 5 x 10^8 CFU/mL, and on M63B1*BAC* was 1.6 x 10^8 CFU/mL. On 48th hours, the growth on LB was 7 x 10^8 CFU/mL, and on M63B1*BAC* was 2 x 10^7 CFU/mL. All conditions showed a higher growth for total cells when compared to the BAC degraders.

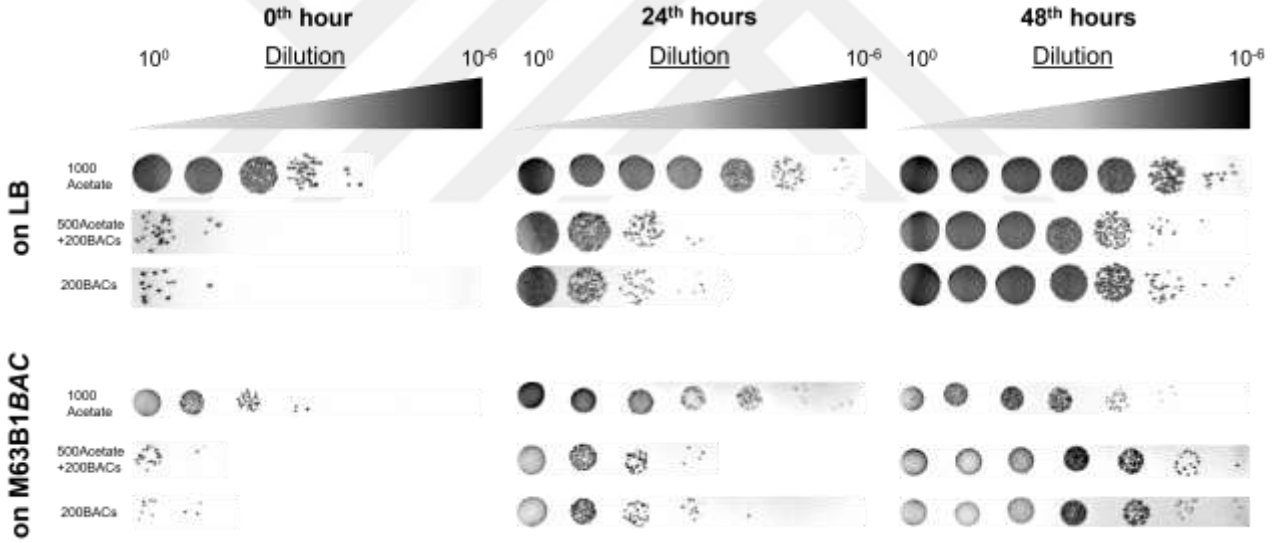

Figure 4.3. Images of spots inoculated with *P. saponiphila* DSM 9751 growing in 1000 mg/L acetate, 500 mg/L acetate + 200 mg/L BACs and only 200 mg/L BACs on LB or M63B1*BAC* agar during 48 hours of incubation.

The agar media used in spotting for *P. sessilinigenes* BIOMIG1+pRK24 were LB*Tet* and M63B1*BACTet* to measure the total cell density and the number of BAC degraders in the culture. Since pRK24 has tetracycline resistance, tetracycline was included in every medium used to incubate the strain. *P. sessilinigenes* BIOMIG1+pRK24's daily spotting results are shown in Figure 4.7 and CFU/mL results are shown in Figure 4.8 (B), Figure 4.9 (B), and Figure 4.10 (C). It is clear that for 500 mg/L acetate + 200 mg/L BACs condition, the growth increased until the 48th hours and reached

its maximum. The growths were 2 x 10^9 CFU/mL and 1.66 x 10^9 CFU/mL on LB*Tet* and M63B1*BACTet* agar media, respectively.

On the other hand, the growth under 1000 mg/L acetate and 200 mg/L BACs conditions reached their maximum growth rate at 24th hours and started to decrease afterwards. The decrease on 48th hours was higher for the 1000 mg/L acetate group. At 24th hours, the growth on LB*Tet* was 2.62 x 10^9 CFU/mL, and M63B1*BACTet* was 1.66 x 10^9 CFU/mL. At 48th hours, the growth on LB*Tet* was 1.66 x 10^9 CFU/mL, and M63B1*BACTet* was 5 x 10^8 CFU/mL. For 200 mg/L BACs condition, the growths at 24th hours were 2.09 x 10^9 CFU/mL for both cultivations. However, the growth after 48 hours decreased to 2 x 10^9 CFU/mL and 1.66 10^9 CFU/mL, respectively, on LB*Tet* and M63B1*BACTet* agar media.

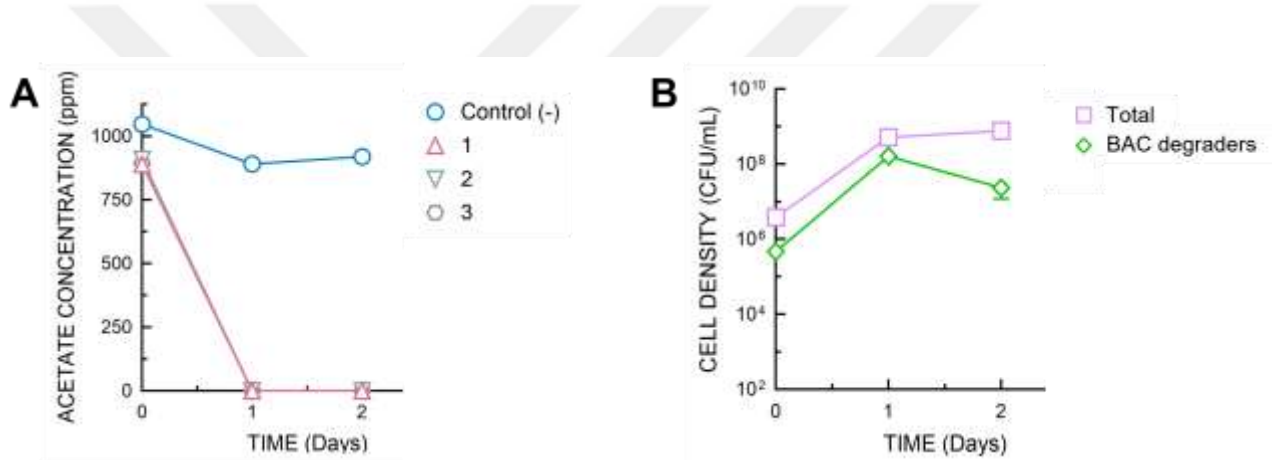

Figure 4.4. Profiles of (A) acetate utilization and (B) cell growth in the flasks inoculated with *P. saponiphila* DSM 9751 in Control (1000 mg/L acetate) condition in the course of 48 hours (*n*= 3). The carbon source utilizations were shown as the control (-) (without inoculation) and the triplicate samples. The cell growths were shown as total cell density and the BAC degraders.

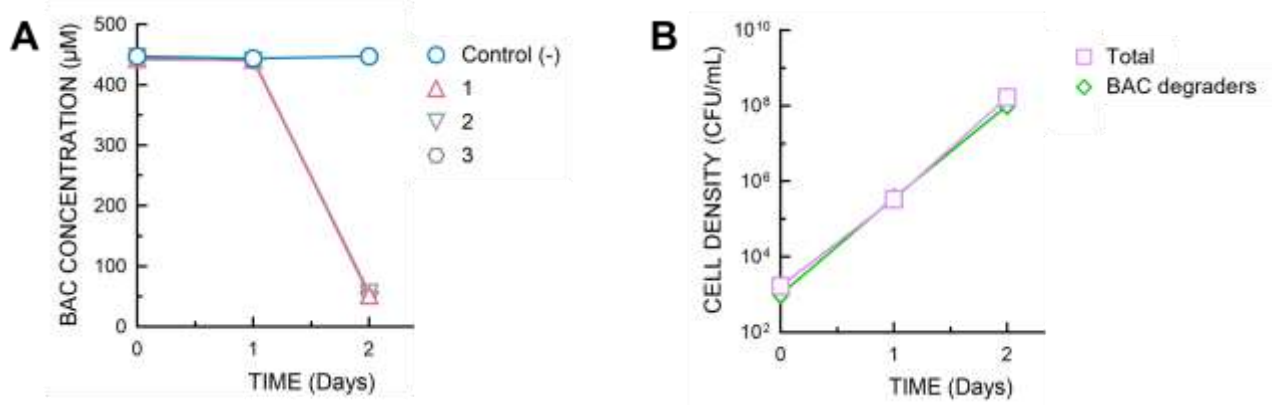

Figure 4.5. Profiles of (A) BACs utilization and (B) cell growth in the flasks inoculated with *P. saponiphila* DSM 9751 in BACs (200 mg/L BACs) condition in the course of 48 hours (n= 3). The carbon source utilizations were shown as the control (-) (without inoculation) and the triplicate samples. The cell growths were shown as total cell density and the BAC degraders.

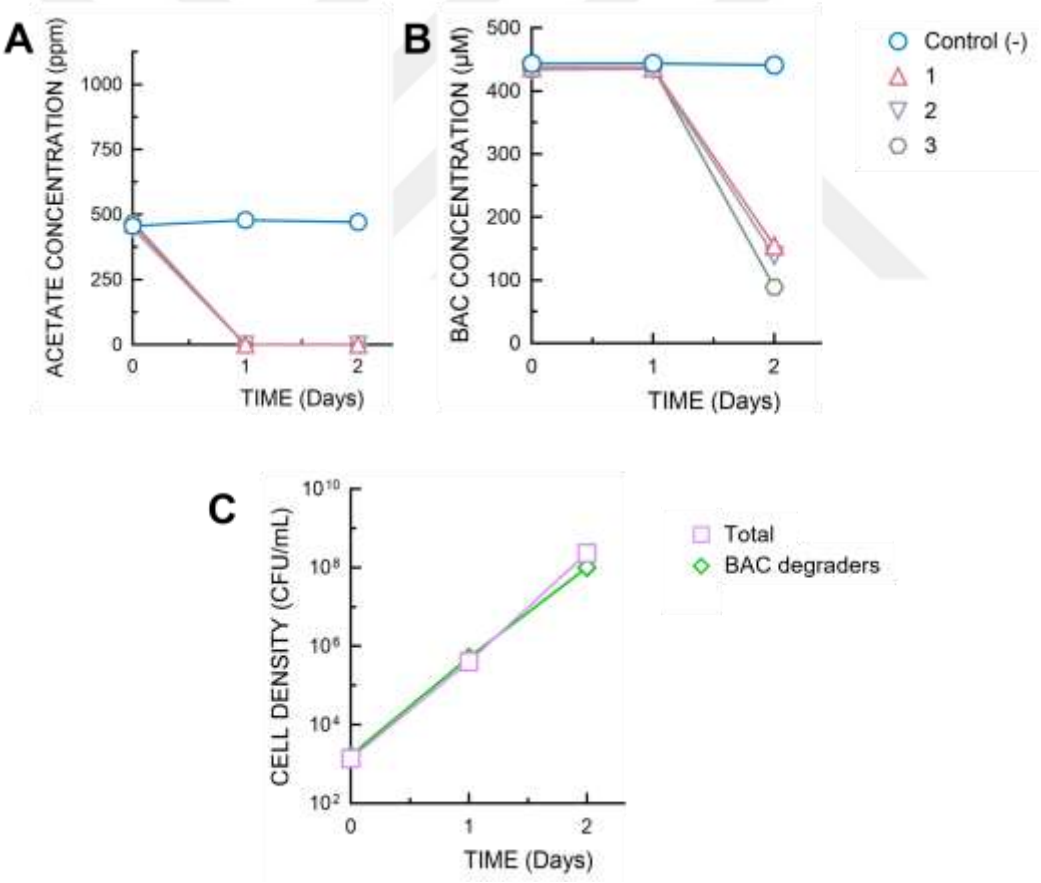

Figure 4.6. Profiles of (A) acetate utilization, (B) BACs utilization, and (C) cell growth in the flasks inoculated with *P. saponiphila* DSM 9751 in Acetate + BACs (500 mg/L acetate and 200 mg/L BACs) condition in the course of 48 hours (n= 3). The carbon source utilizations were shown as the control (-) (without inoculation) and the triplicate samples. The cell growths were shown as total cell density and the BAC degraders.

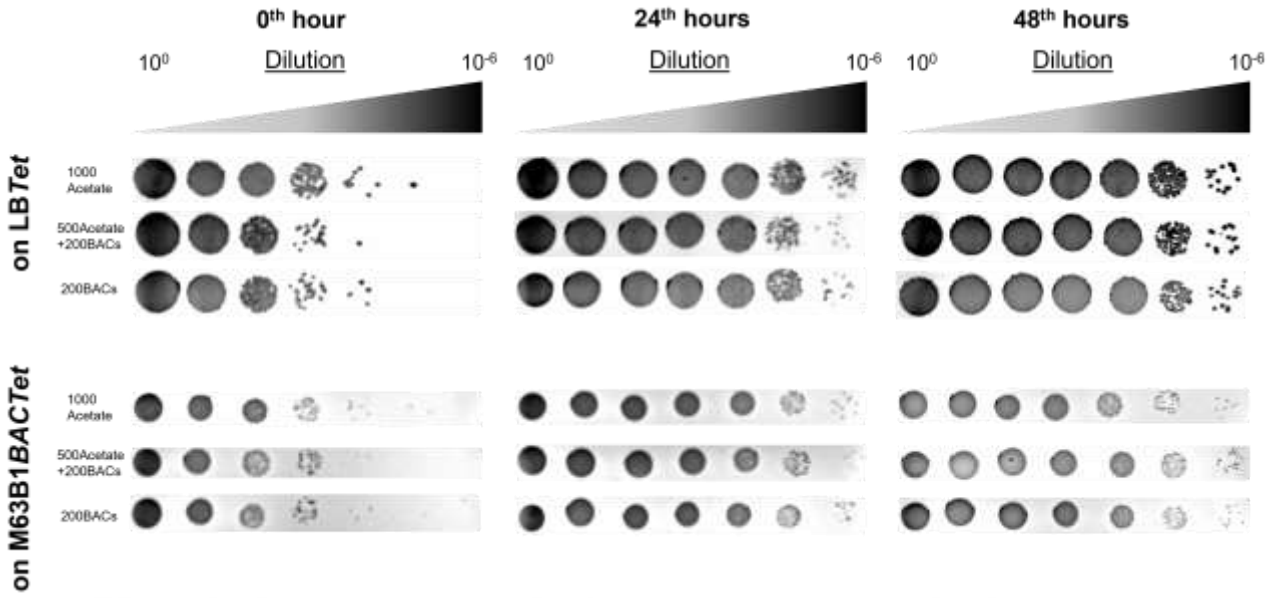

Figure 4.7. Images of spots inoculated with *P. sessilinigenes* BIOMIG1+pRK24 growing in 1000 mg/L acetate, 500 mg/L acetate + 200 mg/L BACs and only 200 mg/L BACs on LB or M63B1*BAC* agar during 48 hours of incubation.

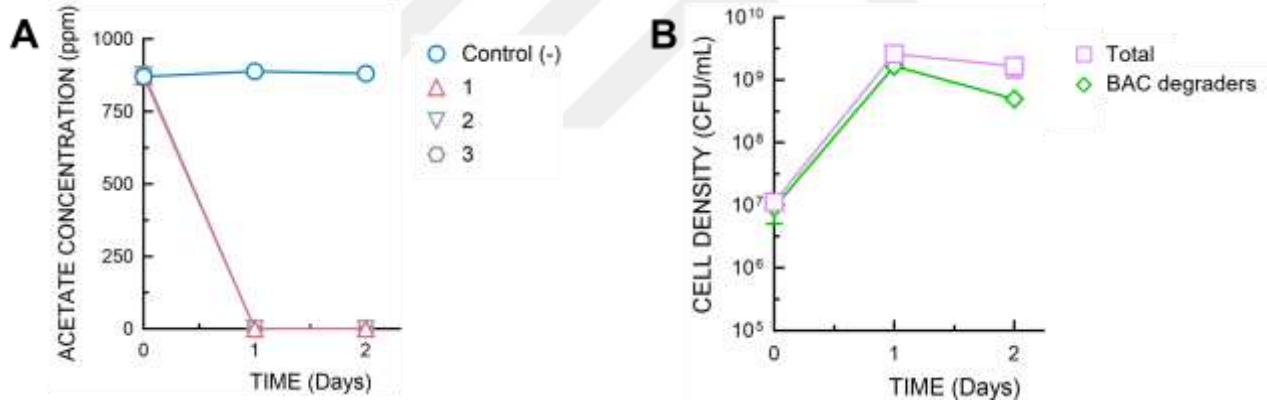

Figure 4.8. Profiles of (A) acetate utilization and (B) cell growth in the flasks inoculated with *P. sessilinigenes* BIOMIG1+pRK24 in Control (1000 mg/L acetate) condition in the course of 48 hours (n= 3). The carbon source utilizations were shown as the control (-) (without inoculation) and the triplicate samples. The cell growths were shown as total cell density and the BAC degraders.

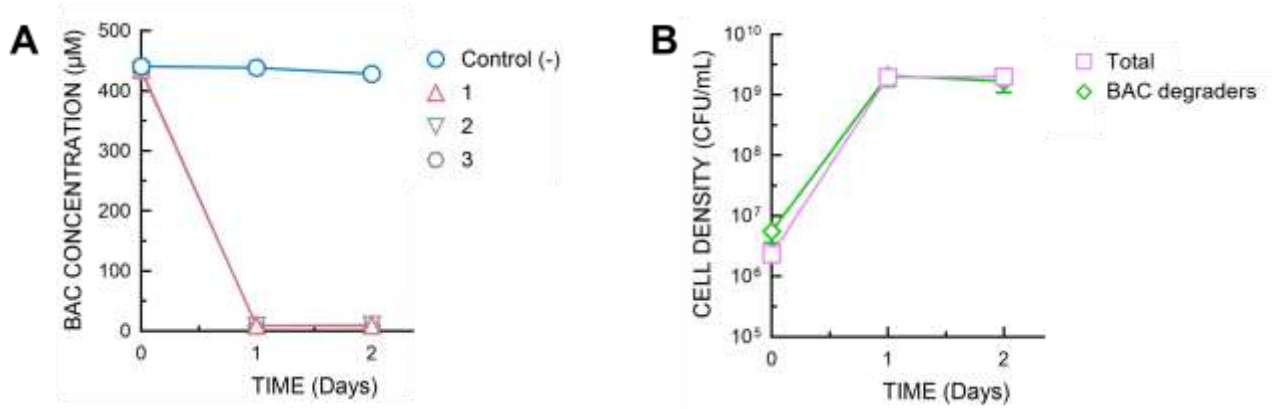

Figure 4.9. Profiles of (A) BACs utilization and (B) cell growth in the flasks inoculated with *P. sessilinigenes* BIOMIG1+pRK24 in BACs (200 mg/L BACs) condition in the course of 48 hours (n= 3). The carbon source utilizations were shown as the control (-) (without inoculation) and the triplicate samples. The cell growths were shown as total cell density and the BAC degraders.

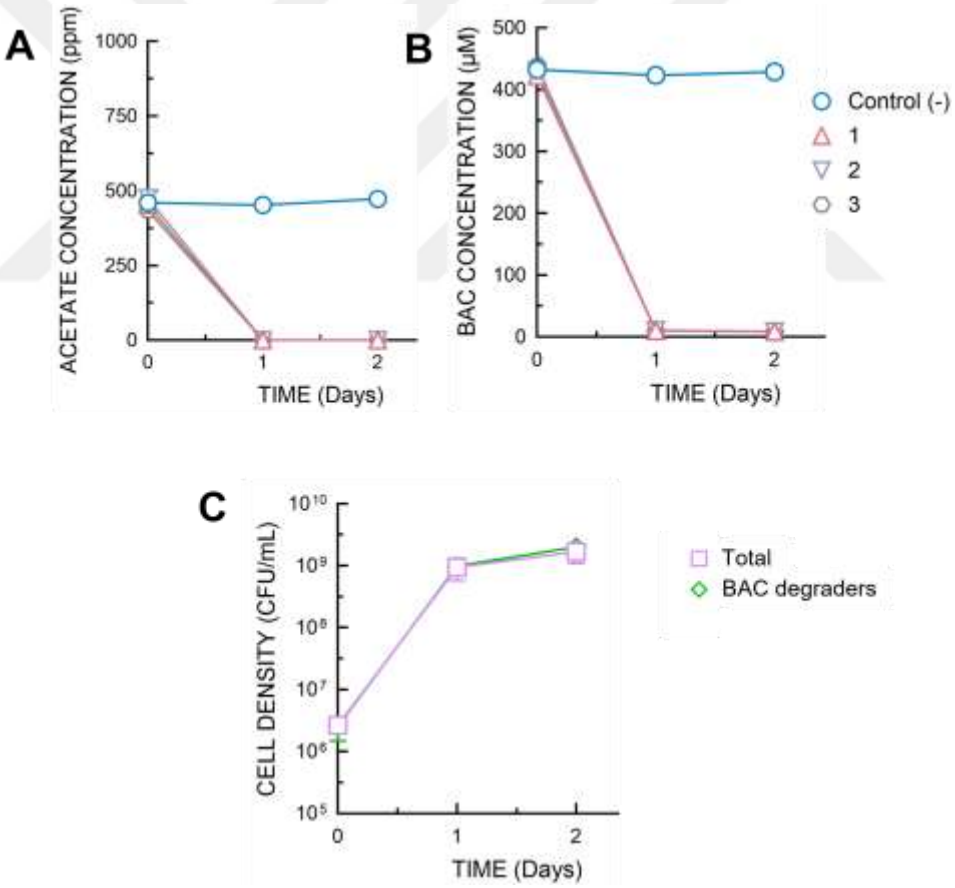

Figure 4.10. Profiles of (A) acetate utilization, (B) BACs utilization, and (C) cell growth in the flasks inoculated with *P. sessilinigenes* BIOMIG1+pRK24 in Acetate + BACs (500 mg/L acetate and 200 mg/L BACs) condition in the course of 48 hours (n= 3). The carbon source utilizations were shown as the control (-) (without inoculation) and the triplicate samples. The cell growths were shown as total cell density and the BAC degraders.

According to spot-plating results, the growth in only acetate-containing medium is higher than in the other media since the pathway for assimilating acetate as a carbon source is notably straightforward (Gong et al., 2022). Also, acetate is highly soluble and completely ionized in the surrounding medium (Gong et al., 2022). Its small molecular size facilitates its passage across the cell membrane through simple diffusion, which promotes efficient transport into the cytoplasm (Gong et al., 2022). That is why the growth reached the maximum at 24th hours for both BIOMIG1 and DSM 9751, then started to decrease. On the other hand, for complex carbon sources, such as BACs, the assimilation is more challenging than ready-to-use carbon sources and takes longer. This slows down the growth rate of the cultures which can be seen the growth of DSM 9751 under only BACs condition. This effect can also be seen in the 500 mg/L Acetate + 200 mg/L BACs condition. Even though there was acetate as a carbon source, the presence of BAC slowed down the growth. DSM 9751 cannot mineralize BAC like BIOMIG1; it can only degrade BAC into BDMA. Since BAC assimilation is less efficient for DSM 9751, the growth rates were lower than BIOMIG1's. The BACs mineralization ability of BIOMIG1 makes BACs a carbon source as efficient as a ready-to-use carbon source. These can be seen by comparing the HPLC results of acetate in Figure 4.4 (A), Figure 4.6 (A), Figure 4.8 (A), and Figure 4.10 (A), and the HPLC results of BACs in Figure 4.5 (A), Figure 4.6 (B), Figure 4.9 (A), and Figure 4.10 (B).

C-source consumption monitoring was separately performed for acetate and BACs. HPLC measurements for acetate were performed for the experiment groups 1000 mg/L acetate and 500 mg/L acetate + 200 mg/L BACs since their acetate content. HPLC measurements for BACs were performed for the experiment groups 500 mg/L acetate + 200 mg/L BACs and 200 mg/L BACs since their BAC content. The results of the HPLC analysis are shown in Figure 4.4 (A), Figure 4.5 (A), and Figure 4.6 (A and B) for DSM 9751 and Figure 4.8 (A), Figure 4.9 (A), and Figure 4.10 (A and B) for BIOMIG1. The acetate was consumed at first 24 hours for all of the experimental groups (Figure 4.4 (A), Figure 4.6 (A), Figure 4.8 (A), and Figure 4.10 (A)). The interesting part was the BAC consumption. As mentioned, BAC assimilation is more complex for DSM 9751 than BIOMIG1, and HPLC results support this. When comparing Figure 4.5 (A) and Figure 4.6 (B) with Figure 4.9 (A) and Figure 4.10 (B), it is evident that BIOMIG1 assimilated BAC more rapidly than DSM 9751. Additionally, at 48th hours, BACs were still present in the media of the DSM 9751 experimental groups.

After the transposition experiment, the plasmids were isolated by ThermoScientific GeneJET Plasmid Miniprep Kit (Vilnius, Lithuania). The extracted plasmids were controlled by running 0.7% agarose gel electrophoresis for 55 minutes and 70 V. The results are shown in Figure 4.11 for both strains. The ThermoScientificTM GeneRuler 1 kb DNA ladder (Vilnius, Lithuania) ranges between

20 kb and 75 bp was used. In the figure, each conditions' triplicates were shown separately. Since p9751 is 50534 bp (~50 kb) and pRK24 is 65.630 bp (~65 kb), they were out of the DNA ladder's range. Nevertheless, we can see the position difference between the gel images. The plasmids show distinct bands that are pointed by a row. Also, the bands at 20 kb show the fragmented chromosomal DNA, which should be cleaned for further steps.

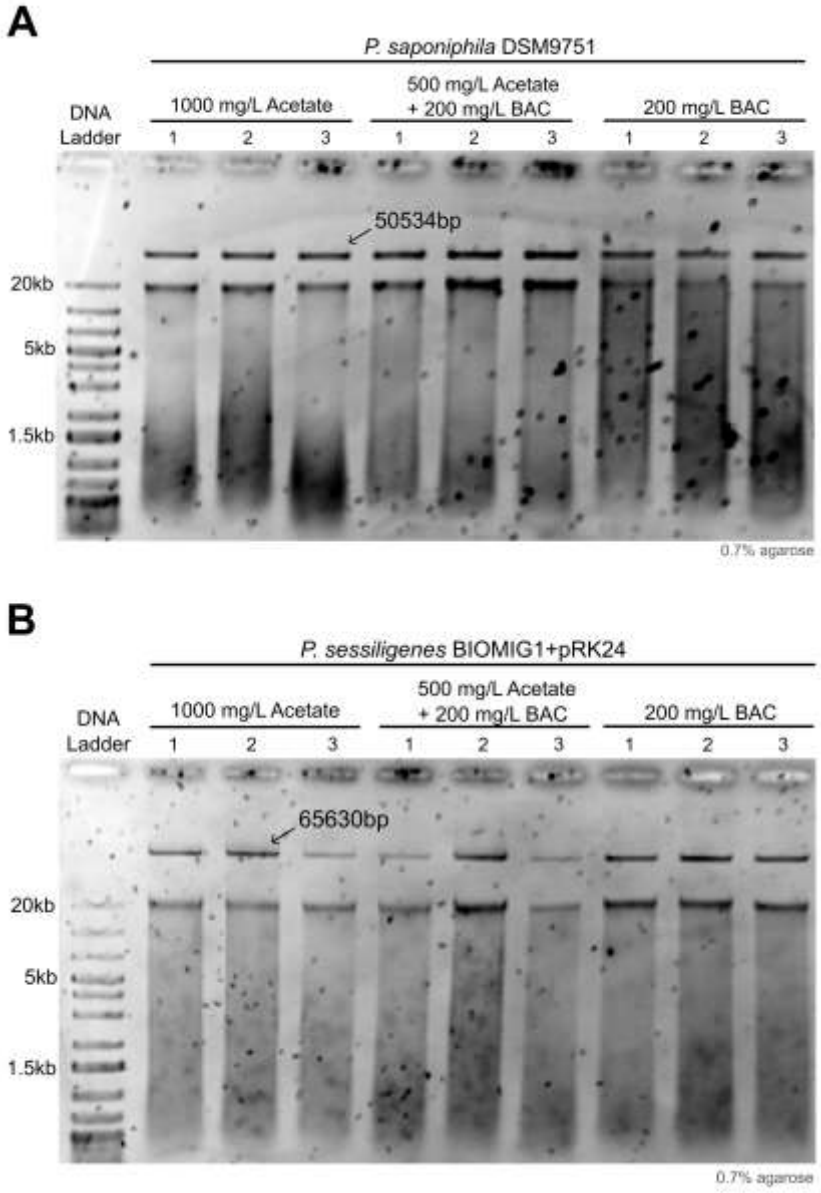

Figure 4.11. Plasmid isolation results of (A) p9751 from *P. saponiphila* DSM 9751 and (B) pRK24 from *P. sesslinigenes* BIOMIG1+pRK24. The DNA ladder is on the first column, with a maximum range of 20 kb. The following columns were grouped as three columns to show the triplicates of each condition. The 0.7% agarose gel was run for 55 minutes and 70 V.

The extracted triplicate plasmids for each condition were combined before the further purification step. Plasmid purification was done using the PlasmidSafe™ ATP-Dependent DNase (Epicentre, Illumina, Madison, WI, USA) kit. After purifying the plasmids, they were linearized by HpaI enzyme digestion. HpaI cuts from the GTTAAC site (5' to 3'). HpaI double cuts p9751 and pRK24, as shown in Figure 4.12 It cuts from 12320 bp and 12633 bp sites of p9751 and releases a 313 bp gene fragment with a linearized p9751. HpaI releases a larger region of pRK24 than p9751. It cuts from 30299 bp and 34561 bp sites of pRK24 and releases a 4262 bp gene fragment with a linearized pRK24.

After endonuclease digestion, the linearized plasmids were purified by MagBead DNA purification kit (MobiomX; Massive Bioinformatics, İstanbul, Türkiye). The purified linear plasmids were controlled by running 0.7% agarose gel electrophoresis for 55 minutes and 70 V. The results are shown in Figure 4.13 for both plasmids. The same DNA ladder was used. The plasmids were detected at 20 kb since linearized plasmids can travel further on agarose gel. In the gel of pRK24, the bands between 5 kb and 4 kb show the released DNA fragment of pRK24 after digestion. The small DNA fragment released from p9751's digestion was not observed since the run time of the gel limits the travel of the DNA in agarose gel making it impossible to see the ladder's lower ranges on these agarose gel results.

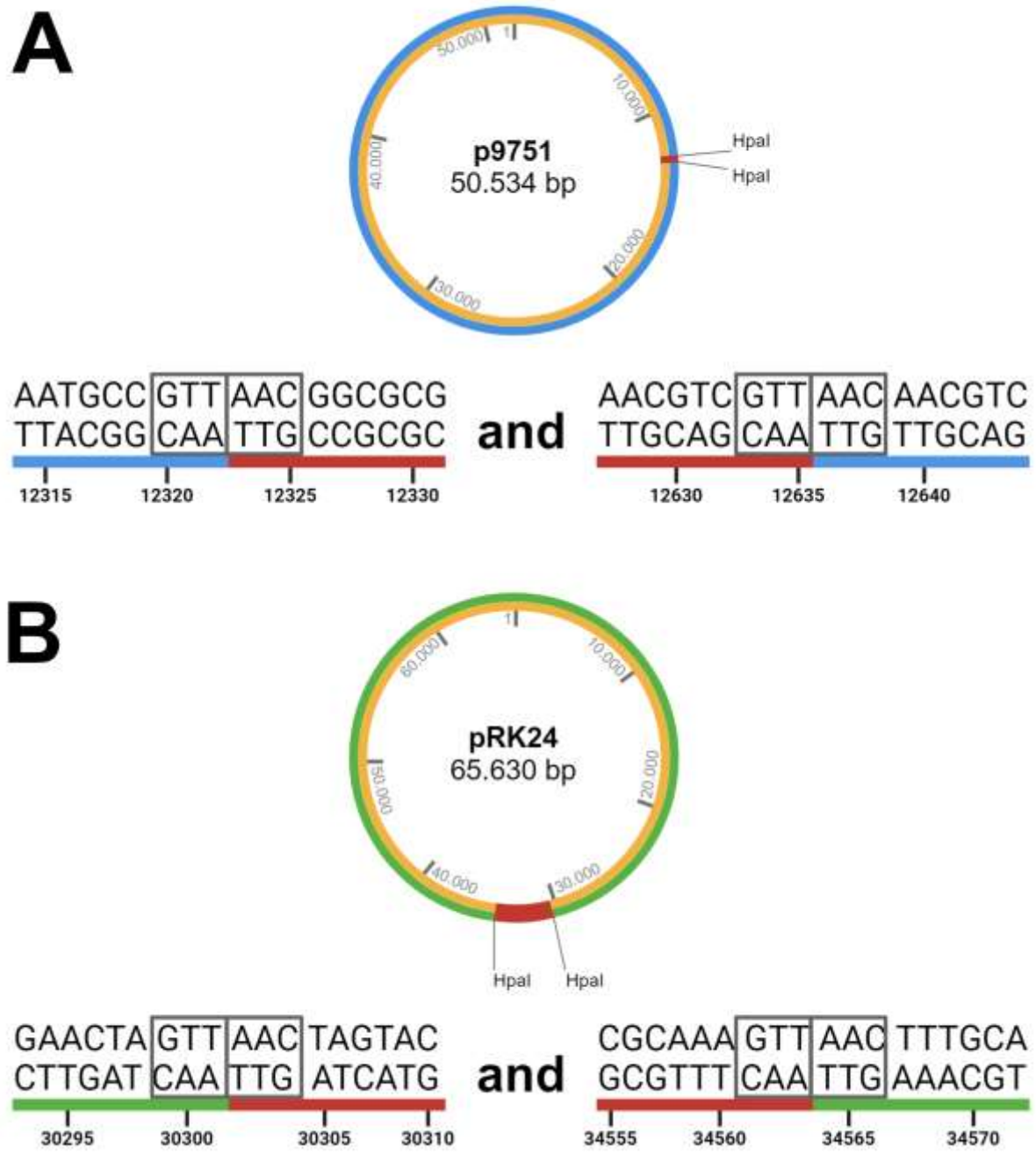

Figure 4.12. HpaI enzyme restriction sites maps of p9751 and pRK24. The HpaI cutting site is GTTAAC region from 5' to 3' of the DNA. HpaI endonuclease double cuts p9751 and pRK24. The cutting sites of p9751 are 12320 bp and 12633 bp. The cutting sites of pRK24 are 30299 bp and 34561 bp.

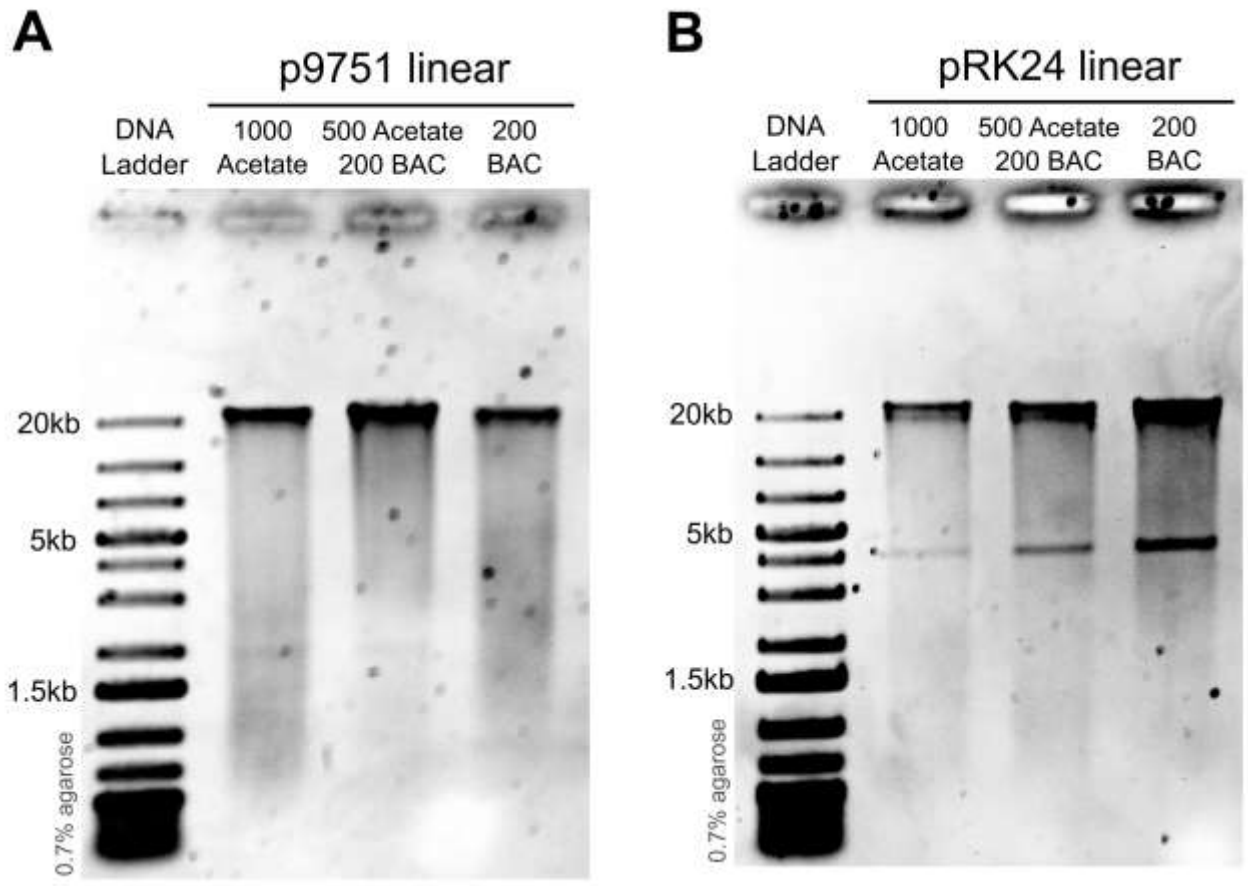

Figure 4.13. Linear and pure (A) p9751 and (B) pRK24 agarose gel electrophoresis results after PlasmidSafe application, HpaI digestion and magnetic bead purification. The DNA ladders are on the first columns, with a maximum range of 20 kb. The 0.7% agarose gel was run for 55 minutes and 70 V.

The pure and linearized plasmids were investigated by sequencing to see transpositional events. For this purpose, plasmids were prepared for sequencing with respect to the sequencing kit (SQK-NBD114.24; Oxford Nanopore Technologies, Oxford, United Kingdom), and the sequence libraries were prepared. At the end of the library preparation, the samples were pooled into a single tube. Since each plasmid was chemically tagged with a specific predefined barcode provided by the kit, they were safely separated during sequencing. After sequencing with 87 active pores for 24 hours, the high-quality sequences were taken by basecalling and trimming using the ONT's software MinKNOW. The FASTQ files were investigated using NanoPlot (v1.42.0) (De Coster & Rademakers, 2023). For this purpose, all FASTQ files of each plasmid were pooled into a single FASTQ file. The results of the Nanoplot are given in Figure 4.14. The graph shows the obtained sequence data is at high quality and has high read lengths. Considering keeping the majority of the high-quality and high-length data, the low quality (<Q8) and short length (<1000bp) reads were filtered for each barcode separately by Chopper (v0.8.0) (De Coster & Rademakers, 2023).

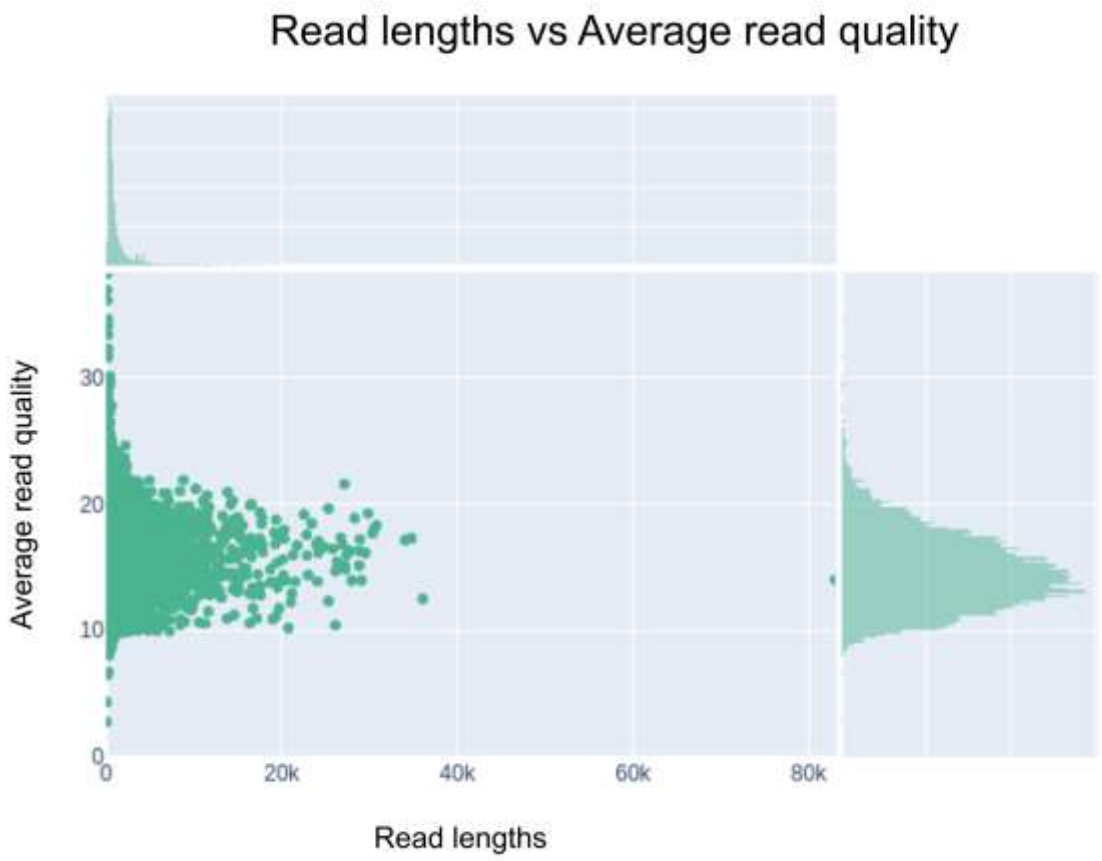

Figure 4.14. The quality and length analysis graphs of all sequence reads are done by NanoPlot. The y-axis shows the quality of the reads while the x-axis shows the length of the reads.

In order to identify the transposition events, gene annotation is essential. Each barcode file was mapped to its reference plasmid using minimap2 (v2.28) (H. Li, 2018) to determine the regions corresponding to the reference sequence, and the resulting FASTQ files were converted to FASTA format. These mapped sequences were then blasted by Blast+ (v2.15.0) (Camacho et al., 2009) to generate a database from the sequence reads, which was subsequently aligned to identify unaligned regions, likely indicative of transposition events. Any reads that lacked unaligned regions were filtered using SeqKit (v2.8.2) (W. Shen et al., 2024) for further analysis. This process was repeated for each barcode, including the large unclassified file (357 MB, three times larger than other barcodes' file size), which was also mapped to p9751 and pRK24 for further analysis. After filtering all unaligned sequences with SeqKit (v2.8.2) (W. Shen et al., 2024) to ensure a minimum length of 200 bp, these sequences were annotated using PGAP (v6.7) (Tatusova et al., 2013). The annotations were done by focusing on the reference genomes of *P. saponiphila* DSM 9751 for p9751 and *P. sessilinigenes* BIOMIG1 for pRK24. PGAP is a straightforward NCBI program with a single-line code (Tatusova et al., 2013). The annotation results were investigated using Geneious Prime (v2024.0.2).

Following these pre-processing and annotation steps, it was necessary to align the pooled sequence files of p9751 and pRK24 with the genomic DNA of their host strains and the plasmid sequences. Figures 4.11 and 4.12 present the results of these alignments and previous annotations.

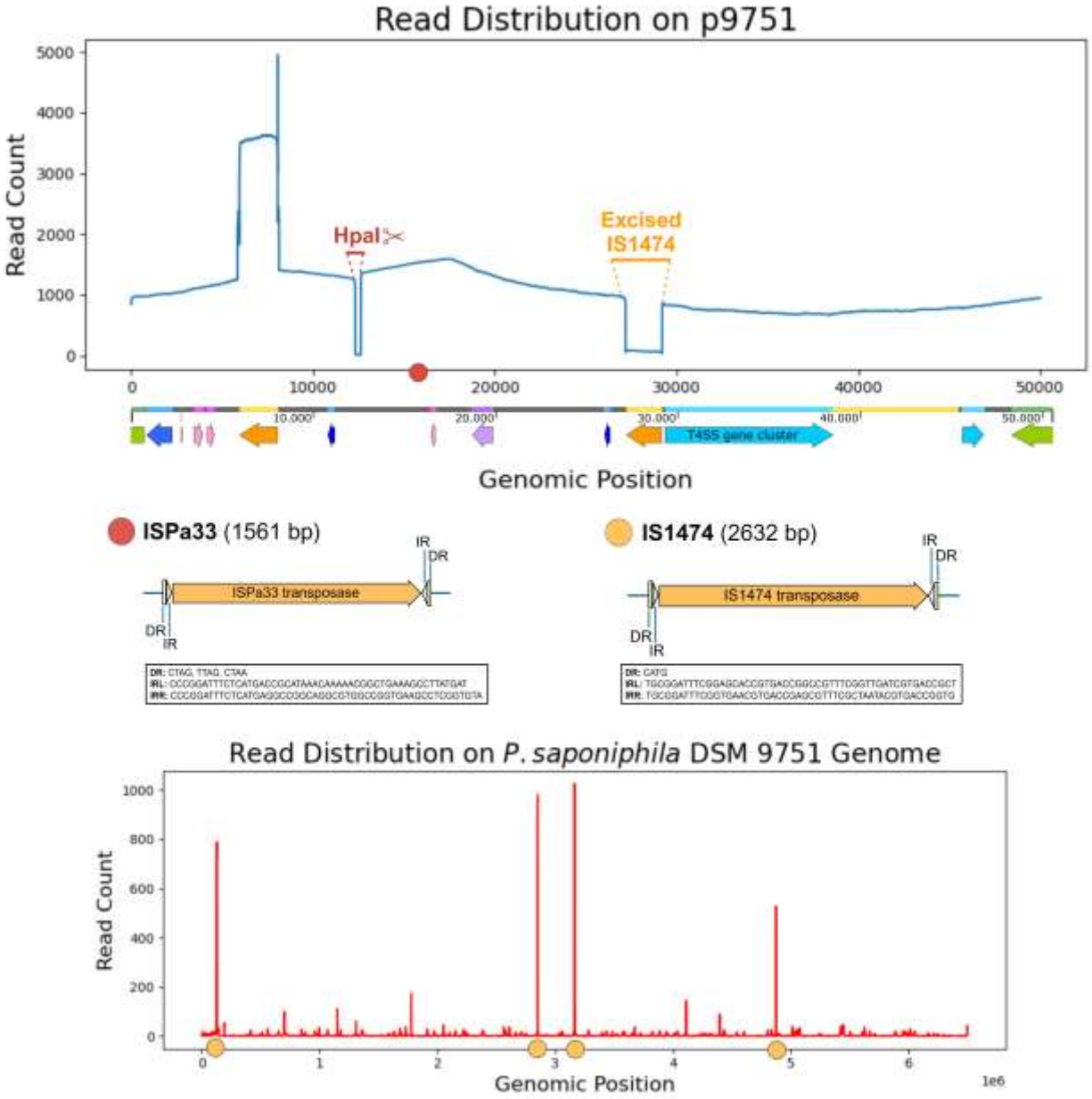

Figure 4.15. The alignment of pooled p9751 sequence reads to p9751 reference sequence (top graph) and the genomic DNA of *P. saponiphila* DSM 9751 (bottom graph) is presented. In the top graph the x-axis represents the plasmid map of p9751. The ISPa33 insertion point on the plasmid is indicated with a red circle (16120 bp). The excised IS1474 IS of p9751 (located between 27194 bp and 29110 bp) and the HpaI restriction sites (restriction from 12320 bp and 12633 bp) are highlighted. The IS informations are given under the top graph. In the bottom graph, four matching IS1474s between the plasmid and the genomic DNA of *P. saponiphila* DSM 9751 are marked with yellow circles.

The alignment of p9751 sequence data to the p9751 plasmid sequence reveals the number of reads that align with the plasmid (Figure 4.15 top graph). Notably, two regions exhibited either low or no read coverage. The first region is between 12320 bp and 12633 bp, corresponding to the HpaI restriction sites shown in Figure 4.12 with no read coverage. Since the restriction sites are closely located the gene fragment released by HpaI digestion is approximately 313 bp, and its small size relative to the plasmid, it may have been lost during purification. The second region between 27194 bp and 29110 bp showed a low read coverage. This region corresponds to one of the IS1474 ISs on the plasmid, suggesting that this IS was excised. Besides, the alignment analysis showed four distinct peaks in the bottom graph of Figure 4.15 correspond to IS1474 ISs on p9751, which are homologous to the ISs found on the genome of *P. saponiphila* DSM 9751.

Furthermore, the unaligned regions of the p9751 sequence data were primarily composed of short gene fragments that could not be annotated. Among the longer unaligned regions, fewer were successfully annotated. Notably, only one transposition was detected under the 200 mg/L BACs condition, identified as an IS1380 family transposase. This IS's entry point into p9751 was at 16120 bp, where the PIN domain-containing protein is located, as shown in the top graph of Figure 4.15 Database searches identified this IS as ISPa33, which contains a DDE-type transposase (Siguier et al., 2006). Previous studies have discovered variants of ISPa33 in other *Pseudomonas* strains, such as *P. mendocina* LM7, where it transposed into the entrapment vector pMAT1's sacB cassette (Szuplewska et al., 2014). However, the transposition mechanism of this IS family remains unknown (Siguier et al., 2015). Also, the direct relationship between this IS with AMGs is unknown.

While only one transposition was detected in the unaligned regions of the p9751 sequence data, numerous insertions originated from the *P. saponiphila* DSM 9751 genome were found. Table 4.4 lists the gene arrays inserted into p9751, along with their source locations on the *P. saponiphila* DSM 9751 genome and their size in base pairs. Some gene groups were incomplete in the unaligned region data and were therefore excluded from the table. Since the genome of *P. saponiphila* DSM 9751 is available only at the contig level, the source WGS project numbers were indicated in Table 4.4.

Table 4.4. The list of inserted gene arrays to p9751 with their locations on *P. saponiphila* DSM 9751's genome and size in base pair (bp).

Medium	Genome location	Size (bp)	Inserted Genes
1000 mg/L Acetate	FNTJ01000002.1 1816459 bp - 1821983 bp	6221	Cysteine synthase A, hypothetical protein, putative lipoprotein, NAD(P)-dependent dehydrogenase, short-chain alcohol dehydrogenase family, transcriptional regulator (LysR family), putative oxidoreductase, Putative DNA-binding domain-containing protein, hypothetical protein
	FNTJ01000002.1 1863253 bp - 1865142 bp	1915	3-carboxy-cis,cis-muconate cycloisomerase, 3-oxoadipate enol-lactonase, 4-carboxymuconolactone decarboxylase, OprD family membrane porin
500 mg/L Acetate + 200 mg/L BACs	FNTJ01000001.1 4379333 bp - 4393259 bp	13754	Aconitase, hypothetical protein, methyl-accepting chemotaxis sensory transducer with Pas/Pac sensor, hypothetical protein, cytochrome c oxidase cbb3-type subunit 1, cytochrome c oxidase cbb3-type subunit 2, cytochrome c oxidase cbb3-type subunit 4, cytochrome c oxidase cbb3-type subunit 3, cytochrome c oxidase cbb3-type subunit 1, cytochrome c oxidase cbb3-type subunit 2, cytochrome c oxidase cbb3-type subunit 4, cytochrome c oxidase cbb3-type subunit 3, cytochrome c oxidase accessory protein FixG
	FNTJ01000001.1 3898459 bp - 3900806 bp	2304	Putrescine transport system permease protein, putrescine transport system substrate-binding protein
	FNTJ01000001.1 315189 bp - 316102 bp	917	Uncharacterized conserved protein, winged helix family two component transcriptional regulator

The absence of clear evidence for a transposition event in the sequences listed in Table 4.4 complicates the determination of whether the mobilization was caused by transposable elements (Muszewska et al., 2019). For these reasons, alternative scenarios should be considered such as homologous recombination.

Bacterial evolution employs various mechanisms to relocate genes, including homologous recombination (legitimate recombination) (Gogarten et al., 2002; Iranzo et al., 2019) and non-homologous recombination (illegitimate recombination) (Gogarten et al., 2002; Vos, 2009). Homologous recombination is an evolutionarily significant mechanism facilitates gene exchange between DNA molecules, affecting both essential and accessory genes (Vos, 2009). This process

requires sequence homology and primarily functions to repair damaged DNA by stressors such as oxidative stress (Holmes & Jobling, 1996; Vos, 2009). In contrast, non-homologous recombination, associated with lateral gene transfer, does not require homology and typically involves accessory genes (Vos, 2009).

Table 4.4. Cont.

Medium	Genome location	Size (bp)	Inserted Genes
200 mg/L BACs	FNTJ01000001.1 3648004 bp - 3652989 bp	4970	AAA domain-containing protein, Transposase DDE domain group 1, DNA repair protein RadC
	FNTJ01000002.1 1126225 bp - 1127767 bp	1545	YigZ family uncharacterized protein, transcriptional regulator, TetR family, xanthine permease XanP
	FNTJ01000001.1 2061171 bp - 2062400 bp	1239	Beta-lactamase class C, LysR family transcriptional regulator, regulator of gene expression of beta-lactamase, YXWGXW repeat-containing protein
	FNTJ01000001.1 1374278 bp - 1375900 bp	1626	Protein of unknown function, Flp pilus assembly protein TadD (contains TPR repeats), pilus assembly protein CpaC

Although recombination processes generally involve gene exchange between genomic DNA and extra-chromosomal DNA, the reverse is not impossible. Recombination events may contribute to the creation of new plasmid families, particularly in conjugative plasmids (Norberg et al., 2011). When p9751 was aligned to the DSM 9751 genome, it covered an average of 9.4% of the genome, suggesting that the insertions listed in Table 4.4 may have resulted from homologous recombination. However, given the limited number of insertions among the 18003 sequences, homologous recombination seems less likely as a consistent gene exchange mechanism. Instead, non-homologous recombination, characterized by its random nature, appears to be a more plausible mechanism for such stochastic transitions. Nevertheless, this interpretation remains speculative. To accurately determine the mechanism responsible for the small amount of gene entries into p9751 in this study. Therefore, further analysis using sophisticated methods like the phi (Φ) test for recombination detection are needed (Bruen et al., 2006).

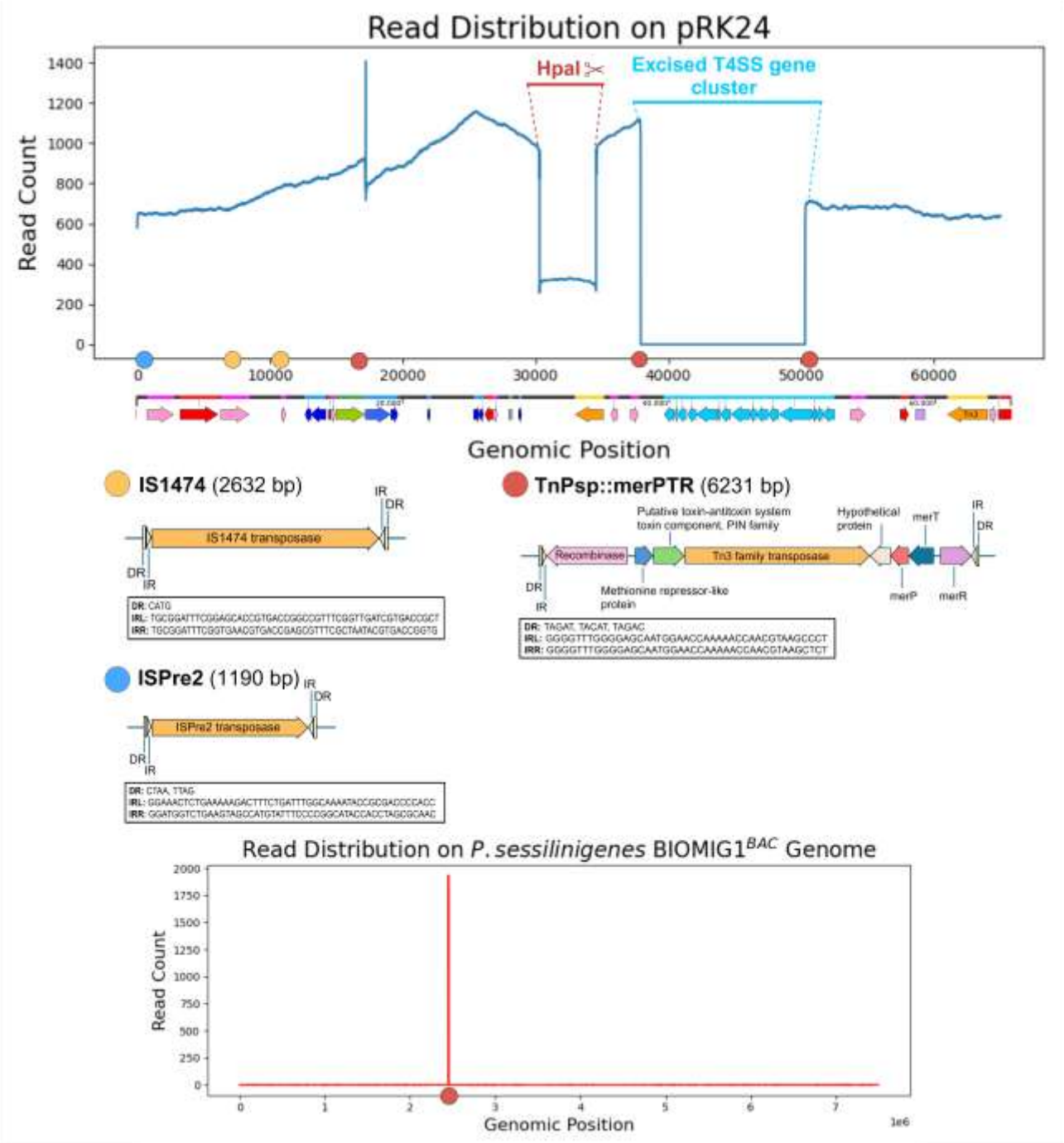

Figure 4.16. The alignment of pooled pRK24 sequence reads with both the pRK24 reference sequence (top graph) and the genomic DNA of *P. sessilinigenes* BIOMIG1 (bottom graph) is presented. In the top graph, the x-axis represents the plasmid map of pRK24. Key features highlighted include the ISPre2 insertion at 52 bp (blue circle), the IS1471 insertions at 7238 bp and 10335 bp (yellow circle), and three TnPsp::merPTR insertions at 17221 bp, 37918 bp, and 50300 bp (red circles). The HpaI restriction sites (restriction from 30299 bp and 34561 bp) and the excised T4SS gene cluster of pRK24 (between 37918 bp and 50300 bp) are highlighted. The IS and Tn information are given under the top graph. In the bottom graph, a single matching TnPsp::merPTR transposon between the sequence reads and the genomic DNA of *P. sessilinigenes* BIOMIG1 is indicated by a red circle.

The alignment of pRK24 sequence data to the pRK24 plasmid sequence reveals regions with either low or no read coverage (Figure 4.16, top graph). The region between 30299 bp and 34561 bp, corresponding to the HpaI restriction site shown in Figure 4.12, displayed low read coverage. Given that the gene fragment released by HpaI digestion was approximately 4.2 kb, a low frequency of reads from this region was observed.

The sequence data from 500 mg/L acetate + 200 mg/L BACs and 200 mg/L BACs conditions revealed various insertions. Specifically, two ISPre2 insertions (Figure 4.16, blue circle), containing IS5 family transposase, to 52 bp region of pRK24 and an IS1474 insertion (Figure 4.16, yellow circle), containing IS21 family transposase, to 7238 bp region of pRK24 were found in the sequence data of 500 mg/L acetate + 200 mg/L BACs and 200 mg/L BACs conditions, respectively. Also, an IS1474 insertion was found at 10335 bp region of pRK24 in the unclassified sequence data containing (Figure 4.16, yellow circle). The transposition rates were calculated respectively as 1.39×10^{-3}, 2.15×10^{-4}, and 1.71×10^{-4} for ISPre2 (500 mg/L acetate + 200 mg/L BACs), IS1474 (200 mg/L BACs), and IS1474 (unclassified sequence data). These listed insertions contain DDE-type transposase (Siguier et al., 2015). None of the ISs transposed a gene with them. Only the IS1474 from unclassified read data was observed with genes surrounding the IS; however, no matching region was found when it was blasted against BIOMIG1's genome. Therefore, it seems to be an overestimated annotation of PGAP.

The other IS21 family, ISPre2s, were blasted by the ISfinder database (Siguier et al., 2015). They do not have accessory genes, only harbor a DDE-type transposase, and have a 99% similarity with IS1384 (Siguier et al., 2015). The IS5 family IS1474 was blasted by ISfinder, too, and it was found that this IS harbors a DDE transposase with an *istB* helper gene for transposition, and its transposition is at a low frequency (Siguier et al., 2015). The transposition mechanisms of these ISs remain undetermined. Also, the direct relationship between these ISs with AMGs is unknown.

Moreover, the alignment results reveal a specific region within the genomic DNA of *P. sessilinigenes* BIOMIG1 that was frequently detected in the sequence data, with approximately 2000 reads. This region corresponds to a Tn3 family transposase-containing composite transposon: the mercury resistance transposon (TnPsp::merPTR) showed in Figure 4.16 as indicated by red circle. It is located between 2448219 bp and 2454120 bp in *P. sessilinigenes* BIOMIG1 shown in Figure 4.16 bottom graph. The transposition rate of TnPsp::merPTR varied under different conditions: the highest rate observed in the 1000 mg/L acetate condition as 1.62×10^{-2}, followed by the 200 mg/L BACs condition as 9.66×10^{-3}, and the lowest was in the 500 mg/L acetate + 200 mg/L BACs condition as

7.67×10^{-3}. Additionally, the transposition rate of the same composite transposon was calculated for the unclassified pRK24 sequence data as 9.74×10^{-3}.

The TnPsp::merPTR transposon, measuring 6.2 kb, harbors several critical genes, including a recombinase, a methionine repressor-like protein, a putative toxin-antitoxin system toxin component (PIN family), a Tn3 family transposase (ISThsp9), a hypothetical protein, a mercury resistance periplasmic binding protein (*merP*), mercury transporter (*merT*), Hg(II)-responsive transcriptional regulator (*merR*). ISThsp9 transposon is a member of Tn3 family transposons and contains a DDE-type transposase and a Tn3 resolvase, which facilitate the replicative transposition and dissemination of catabolic genes between bacteria (Siguier et al., 2015). According to the ISfinder database, the *merPTR* operons found in TnPsp::merPTR transposon enables the expression of mercury resistance genes (Siguier et al., 2015). All mercury resistance transposons harbor four core operons: a regulatory gene *merR*, mercury transport genes *merT* and *merP*, and a mercury reductase gene *merA* (Matsui & Endo, 2018). The transposon identified in this study contains nearly all the core operons, *merP*, *merT*, and *merR*, at the end of the transposon. Despite the variation of the transposase types and the operon content, mercury resistance transposons are widespread. *Bacilli*, a Gram-positive bacterium identified as the primary distributor of mercury resistance transposons (specifically the TnMERI1 transposon, a Tn3-family replicative transposon), shares similarities with the mercury resistance transposons found in Gram-negative bacteria. In this study, the mercury resistance transposon was derived from *P. sessilinigenes* BIOMIG1, a Gram-negative strain.

The recombinase enzyme in TnPsp::merPTR plays a key role in resolving cointegrates, intermediate structures formed during transposition, and may assist in moving transposons to other replicons within the cell (Matsui & Endo, 2018). Adjacent to this, the methionine repressor-like protein regulates methionine biosynthesis and transport based on the cell's methionine levels (Augustus et al., 2010). Additionally, the PIN family toxin-antitoxin system within TnPsp::merPTR enhances bacterial survival under stress by promoting plasmid maintenance and biofilm formation (Jurėnas et al., 2022; Q. E. Yang & Walsh, 2017).

Mercury-resistance transposons are well-characterized in both Gram-positive and Gram-negative bacteria across diverse environments, including clinical samples (Matsui & Endo, 2018). These transposons, associated with Tn21, Tn501, Tn5053, and Tn3 families, vary in the operons they carry (Matsui & Endo, 2018). While the molecular mechanisms of Tn3-family transposons are understood, the factors triggering or suppressing their transposition remain unclear. Although

environmental stress is often linked to transposition events, recent studies suggest that horizontal gene transfer (HGT) can occur even without selective pressure.

Mercury resistance has been found in Bacilli from non-contaminated areas, indicating that its spread is not solely dependent on mercury exposure (Matsui & Endo, 2018). This can explain why the TnPsp::merPTR transposon's rate was highest for the 1000 mg/L acetate condition. Conversely, a higher transposition rate was observed under the 200 mg/L BACs condition compared to the 500 mg/L acetate + 200 mg/L BACs condition remains unexplained.

The initial analysis of the pRK24 plasmid sequence alignment to the pRK24 plasmid reference sequence revealed a missing region (Figure 4.16, top graph). This region is in between 37917 bp and 50300 bp which encompasses the T4SS gene cluster, lacked read coverage entirely.

4.4. Structural Modifications on pRK24 due to Transposition of TnPsp::merPTR

The sequencing results of pRK24 didn't give a complete sequence of pRK24 plasmid. After the alignment of the sequence reads to the reference sequence of pRK24, a missing region from T4SS gene cluster was observed. In order to obtain further insights from this loss, the annotated reads surrounding this region were compared with the reference plasmid map in the Figure 4.17. The used reads in Figure 4.17, contains all TnPsp::merPTR insertion regions. The homologous regions were shown in different color rectangles and the ends of the homologous regions were labelled with letters from A to H. Interestingly, the gene order of pRK24 plasmid varied in Read 1, where the T4CP-containing region (indicated by a purple rectangle in Figure 4.17) was relocated to another part of the plasmid. Alignment data similar to the Read 1 consistently points to entries in pRK24 at positions 17221 bp and 50300 bp. The 17221 bp region corresponds to the terminal sequences of pRK24 relaxase gene, while the 50300 bp region corresponds to VirB4 family type IV secretion/conjugal transfer A in the T4SS gene cluster of pRK24.

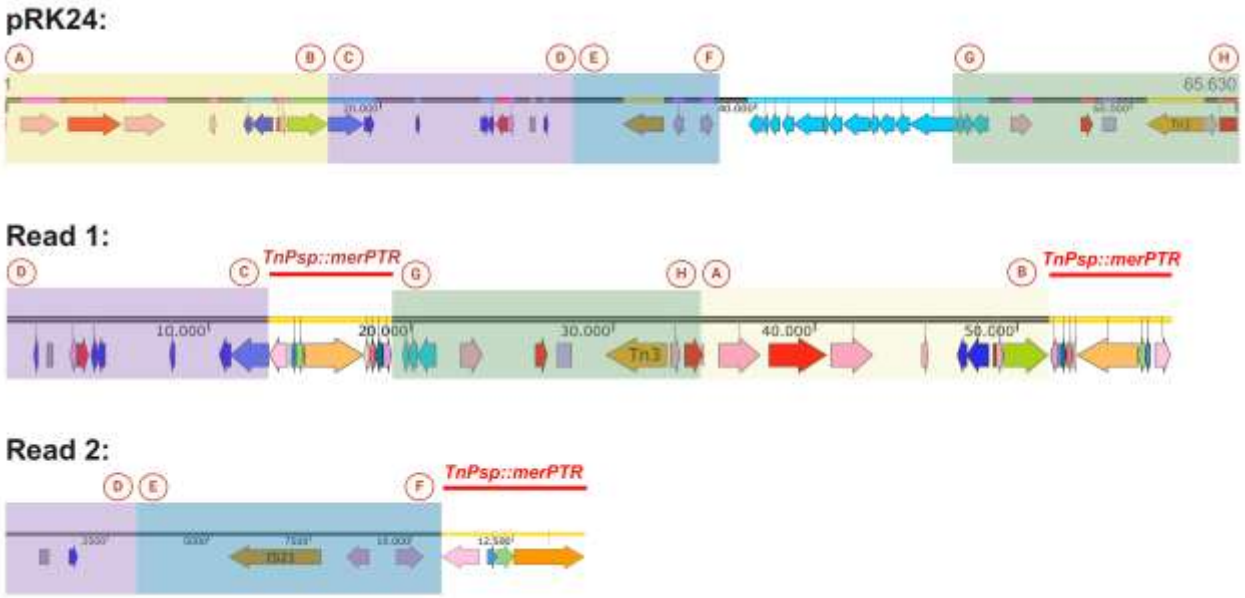

Figure 4.17. The comparison of the annotated reference pRK24 plasmid with two sequence reads that surrounds the excised T4SS gene cluster and harbors the TnPsp::merPTR insertions. The yellow, purple, blue and green rectangles showing the homologous regions with the reads and the pRK24 reference plasmid. The ends of the homologous regions were labelled with letters from A to H. TnPsp::merPTR insertions are shown as two insertions in Read 1 (17221 bp and 50300 bp) and one insertion in Read 2 (37918 bp).

On the other hand, Read 2 alignment data indicates an entry into pRK24 at 37918 bp, which aligns with a hypothetical protein in pRK24. Both the annotated (Figure 4.17) and alignment data (Figure 4.16, top graph) reveal that the region between 37917 bp and 50300 bp which encompasses the T4SS gene cluster, lacked read coverage entirely. The complete absence of the read is surprising. Analyzing the apparent entries and the lack of T4SS gene cluster sequence data leads us to propose a mechanism, illustrated in Figure 4.18. We hypothesize that the relocated parts in the read in Figure 4.17 (Read 1) and the excised T4SS gene cluster (Figure 4.16, top graph) are due to multiple insertions of TnPsp::merPTR transposon into pRK24. After the alignment of these three homologous transposons with respect to their directions, three loops were formed which subsequently split into two distinct plasmid fragments. One fragment, labeled as 1, obtained from the sequence data of this study, is similar in size to pRK24 due to double transposon insertions. The other fragment, labeled as 2, has a size of 18650 bp that carries the T4SS gene cluster and a TnPsp::merPTR transposon. Since the hypothetically obtained fragment lacks an HpaI restriction site, this region wasn't obtained during sequencing. Plasmids must be linearized to be sequenced. The outcomes of this proposed mechanism are depicted in Figure 4.19.

The T4SS gene cluster is crucial for successful conjugation, as it is involved in the formation of conjugative pili (Costa et al., 2024). The near-complete absence of this gene cluster in the pRK24 plasmid is significant. While literature does not document the total loss of T4SS, partial reductions have been observed (Gillespie et al., 2009) , and artificial inactivation by mutation has been studied (Juhas et al., 2008). Mutants with T4SS mutations were unable to generate pili and showed conjugation frequency reduction by up to 100,000 times compared to the parental strain (Juhas et al., 2008). Since the T4SS gene cluster harbors many of the essential genes for conjugation, its absence makes the conjugation impossible. The reason for T4SS excision can be due to the act of transposable elements by their ability to excision genes (Darmon & Leach, 2014).

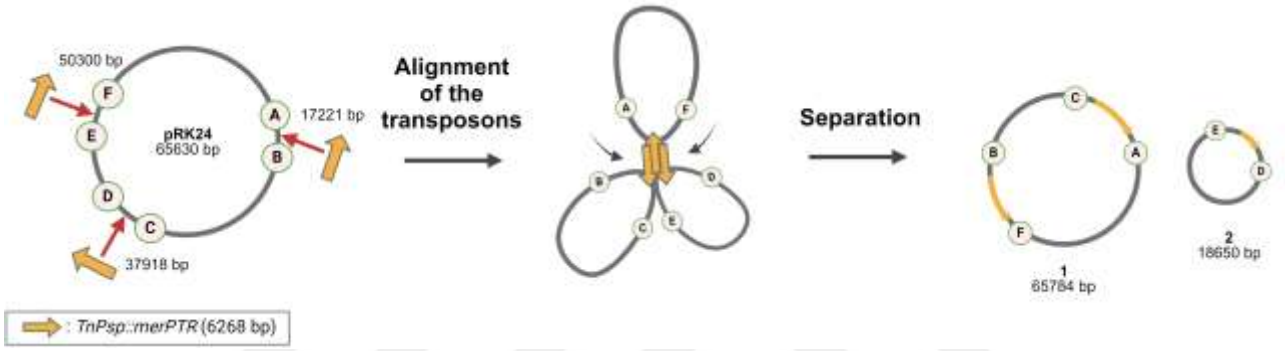

Figure 4.18. Proposed mechanism of pRK24's structural modification by TnPsp::merPTR transposition. The TnPsp::merPTR composite transposon is shown as an orange arrow and the three insertion regions to pRK24 are pointed with red arrows. The regions A, B, C, D, E, and F are labelled to show how the insertions affect the plasmid. The three homologous composite transposons are aligned with respect to their directions and create three loops resulting in two separated plasmid pieces: a plasmid labelled as 1 with a size 65784 bp and a small plasmid piece labelled as 2 with a size 18650 bp.

The pRK24 plasmid was successfully transferred to *P. sessilinigenes* BIOMIG1 through pair-mating conjugation from the ECNR2+pRK24 strain. The protocol was further validated by performing pair-mating conjugation to *E.coli* DH5α+pMAT1 with the same donor, yielding a conjugation rate of 7.55 x 10^{-1} after 3 hours of incubation, which is within the typical bacterial conjugation rate range of 10^{-8} and 10^{-1} (Shafieifini et al., 2022). However, conjugation to *P. sessilinigenes* BIOMIG1 was more challenging, as only a single colony was successfully transformed. Subsequent attempts to conjugate from *P. sessilinigenes* BIOMIG1+pRK24 to four different recipient species were unsuccessful. Therefore, the proposed mechanism described in Figure 4.18, resulting the proposed maps in Figure 4.19, likely to have contributed to the loss of conjugative function in pRK24.

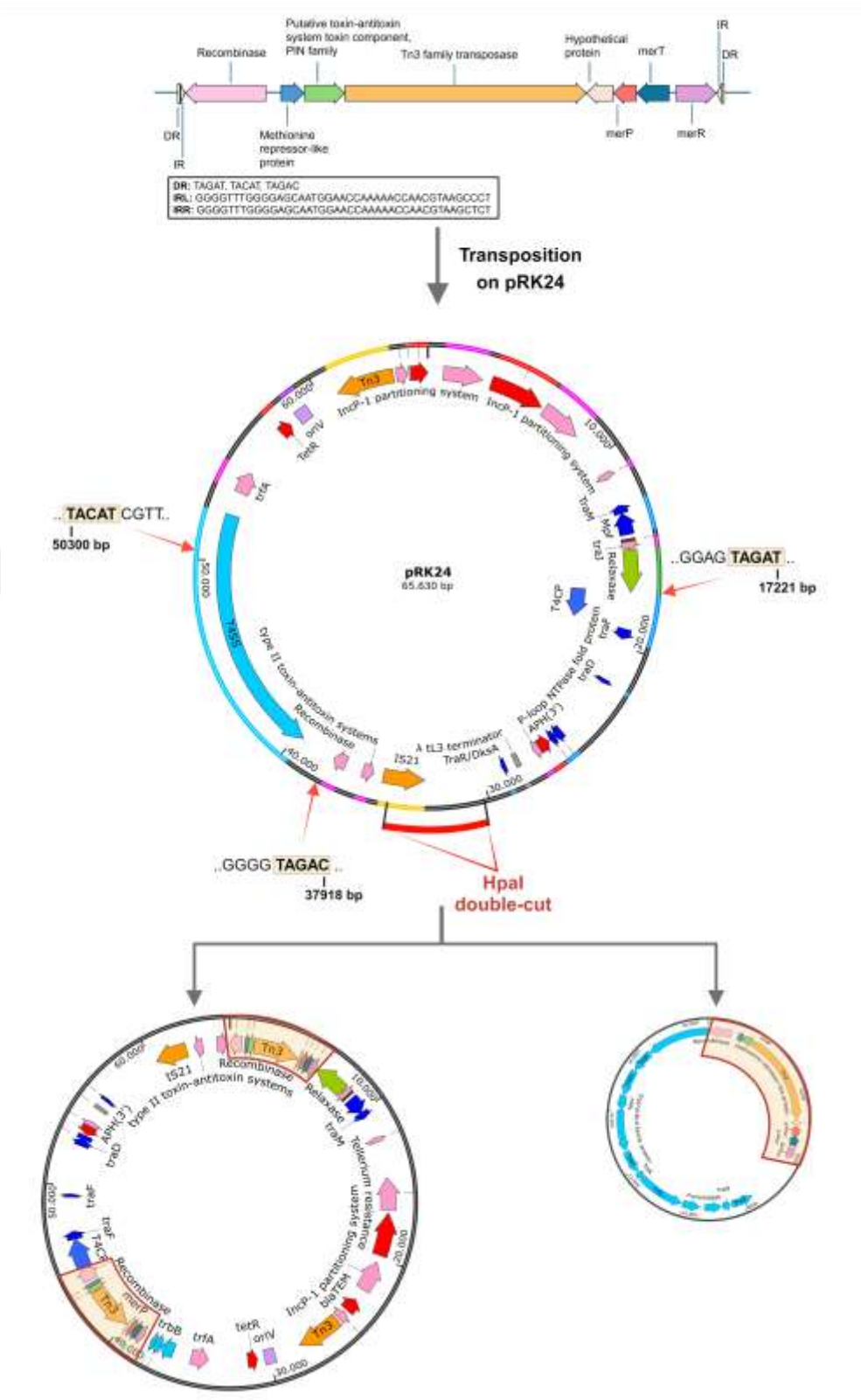

Figure 4.19. Proposed maps of circular extrachromosomal DNA fragments generated after TnPsp::merPTR insertions. The TnPsp::merPTR composite transposon is given in detail with its DR and IR lists. The entry regions of this transposon to pRK24 are shown with red arrows and their DR matching entry sequences. The separated plasmids are shown as annotated maps and the inserted TnPsp::merPTR composite transposons that they harbor are framed with yellow slices.

5. CONCLUSIONS

The primary aimed to investigate the transposition properties of *Pseudomonas sessilinigenes* BIOMIG1 and *Pseudomonas saponiphila* DSM 9751 strains, known for their highly plastic genomes and ability to degrade BAC, under quaternary ammonium disinfectants (QACs) exposure. To achieve this, *P. sessilinigenes* BIOMIG1 was initially transformed with the pRK24 plasmid utilizing the pair-mating method. Since *P. saponiphila* DSM 9751 already had a native plasmid, no additional transformation was performed. The conjugative properties of both plasmids were elucidated by classifying them and generating their maps. The broad-host-range pRK24 is a commercially utilized IncP plasmid. In contrast, the native p9751 plasmid remains uncharacterized mainly, with scant literature available. This study established that p9751 is an IncQ-type plasmid with a host range at the genus level compared to pRK24. Although it is classified as a conjugative plasmid and harbors numerous essential genes for this function, the influence of the Tn3 family transposon, located within the T4SS gene cluster, on its conjugative properties remains a critical issue that requires further investigation.

The IS/Tn analysis of the genomes of *P. sessilinigenes* BIOMIG1 and *P. saponiphila* DSM 9751 revealed that both strains possess highly plastic genomes, with transposable element percentages of 1.82% and 4.55%, respectively.

BAC and acetate served as carbon sources in the transposition experiments to evaluate the impact of BAC stress on transposition events. The results of these experiments indicated various transpositions. The analysis of the p9751 plasmid sequence revealed a singular insertion of an IS1380 family IS, ISPa33, into p9751 under only BAC conditions. Additionally, one of the IS1474 on the p9751 plasmid appears to have undergone translocation. In contrast, various insertions were identified in the absence of detectable transposable elements. The mechanisms underlying these insertions may involve homologous or non-homologous recombination; however, additional investigations are required to elucidate this.

The results also reveals that the transposition activity within *P. sessilinigenes* BIOMIG1 primarily involves a mercury resistance composite transposon (TnPsp::merPTR), particularly under acetate and BAC conditions. This insertion originated from the genome of BIOMIG1, specifically within the region spanning from 2,447,959 bp to 2,454,211 bp. The highest transposition rate was observed in the 1000 mg/L acetate conditions. In the presence of only 200 mg/L BACs, the

transposition rate was 1.67 times lower than that observed in the acetate-only condition. Furthermore, in the combined condition of 500 mg/L acetate and 200 mg/L BACs, the transposition rate was 2.1 times lower than in the acetate-only condition. With the frequent TnPsp::merPTR transpositions, a notable absence of the T4SS gene cluster in the pRK24 plasmid was revealed. T4SS gene cluster is crucial for successful conjugation. This absence likely resulted from multiple insertions of the same transposon, leading to the proposed structural modification mechanism. Despite successful initial conjugation, subsequent attempts with other recipients failed, suggesting that the loss of the T4SS cluster compromised conjugative functionality. Additional insertions of ISs were detected in other conditions, though these did not carry genes, and their transposition mechanisms remain undetermined.

Considering these findings, it was evident that the transposition experiments did not yield a significant increase in transposition events in *P. saponiphila* DSM 9751. Additionally, the mercury resistance transposon in *P. sessilinigenes* BIOMIG1 exhibited a decreased transposition rate under BAC stress compared to the stress-free condition.

The findings provide valuable insights into the characteristics of *P. saponiphila* DSM 9751 and its native plasmid p9751, as well as the transposition activity of *P. sessilinigenes* BIOMIG1. Transposition events and conjugative plasmids are critical components of bacterial evolution, and it is well-established that their activation is enhanced under various environmental stress conditions. Numerous uncertainties remain regarding these phenomena. Future research is essential to determine the potential of these two species, characterized by their TE-rich genomes, to transfer significant genes related to QAC degradation and various other resistance to other conjugative plasmids and, thereby, to other bacteria. Identifying the conditions that facilitate the transfer of these genes via transposition and conjugation is of great importance in addressing various environmental challenges. Moreover, different analytical methods can be used to obtain further insights into the structural modification of pRK24 and identify the T4SS gene cluster.

REFERENCES

Altinbag, R. C., Ertekin, E., & Tezel, U. (2020). Complete Genome Sequence of Pseudomonas sp. Strain BIOMIG1 BAC , Which Mineralizes Benzalkonium Chloride Disinfectants . *Microbiology Resource Announcements*, *9*(20). https://doi.org/10.1128/mra.00309-20

Amirfard, K. D., Moriyama, M., Suzuki, S., & Sano, D. (2024). Effect of environmental factors on conjugative transfer of antibiotic resistance genes in aquatic settings. *Journal of Applied Microbiology*, *135*(6). https://doi.org/10.1093/jambio/lxae129

Arnold, W. A., Blum, A., Branyan, J., Bruton, T. A., Carignan, C. C., Cortopassi, G., Datta, S., Dewitt, J., Doherty, A. C., Halden, R. U., Harari, H., Hartmann, E. M., Hrubec, T. C., Iyer, S., Kwiatkowski, C. F., Lapier, J., Li, D., Li, L., Muñiz Ortiz, J. G., … Zheng, G. (2023). Quaternary Ammonium Compounds: A Chemical Class of Emerging Concern. *Environmental Science and Technology*, *57*(20), 7645–7665. https://doi.org/10.1021/acs.est.2c08244

Augustus, A. M., Sage, H., & Spicer, L. D. (2010). Binding of metJ repressor to specific and nonspecific DNA and effect of S -adenosylmethionine on these interactions. *Biochemistry*, *49*(15), 3289–3295. https://doi.org/10.1021/bi902011f

Biémont, C., & Vieira, C. (2006). Junk DNA as an evolutionary force. *Nature*, *443*, 552–524. https://doi.org/https://doi.org/10.1038/443521a

Brambilla, E., & Sclavi, B. (2015). Gene regulation by H-NS as a function of growth conditions depends on chromosomal position in Escherichia coli. *G3: Genes, Genomes, Genetics*, *5*(4), 605–614. https://doi.org/10.1534/g3.114.016139

Bruen, T. C., Philippe, H., & Bryant, D. (2006). A simple and robust statistical test for detecting the presence of recombination. *Genetics*, *172*(4), 2665–2681. https://doi.org/10.1534/genetics.105.048975

Butler, M. I., Stockwell, P. A., Black, M. A., Day, R. C., Lamont, I. L., & Poulter, R. T. M. (2013). Pseudomonas syringae pv. actinidiae from Recent Outbreaks of Kiwifruit Bacterial Canker

Belong to Different Clones That Originated in China. *PLoS ONE*, *8*(2). https://doi.org/10.1371/journal.pone.0057464

Camacho, C., Coulouris, G., Avagyan, V., Ma, N., Papadopoulos, J., Bealer, K., & Madden, T. L. (2009). BLAST+: Architecture and applications. *BMC Bioinformatics*, *10*. https://doi.org/10.1186/1471-2105-10-421

Campbell Wyndham, R., & NG, J. (1993). IS1071-mediated recombinational equilibrium in Alcaligenes sp. BR60 carrying the 3-chlorobenzoate catabolic transposon Tn5271. *Canadian Journal of Microbiology*, *39*(1), 92–100. https://doi.org/https://doi.org/10.1139/m93-013

Casacuberta, E., & González, J. (2013). The impact of transposable elements in environmental adaptation. In *Molecular Ecology* (Vol. 22, Issue 6, pp. 1503–1517). https://doi.org/10.1111/mec.12170

Cecchetelli, A., Cortez, C., Cronin, H., Dotson, H., Fan, M., Ferenc, M., Fors, T. J., Gearing, M., Giquel, B., Haliw, L., Hazen, A., Hannon, J., Juchheim, A. M., Kenkel, B., LaManna, C., Leimieux, M. G., Leeson, R., Markham, E., Monroe, M. R., … Welch, J. (2023). *Plasmids 101* (4th ed.). Addgene's eBook Collection.

Changey, F., Devers-Lamrani, M., Rouard, N., & Martin-Laurent, F. (2011). In vitro evolution of an atrazine-degrading population under cyanuric acid selection pressure: Evidence for the selective loss of a 47kb region on the plasmid ADP1 containing the atzA, B and C genes. *Gene*, *490*(1–2), 18–25. https://doi.org/10.1016/j.gene.2011.09.005

Che, Y., Yang, Y., Xu, X., Rinda, K. B., Polz, M. F., Hanage, W. P., & Zhang, T. (2021). Conjugative plasmids interact with insertion sequences to shape the horizontal transfer of antimicrobial resistance genes. *Proceedings of the National Academy of Sciences of the United States of America*, *118*(6). https://doi.org/10.1073/pnas.2008731118

Chen, S., Larsson, M., Robinson, R. C., & Chen, S. L. (2017). Direct and convenient measurement of plasmid stability in lab and clinical isolates of E. coli. *Scientific Reports*, *7*(1). https://doi.org/10.1038/s41598-017-05219-x

Clark, I. C., Melnyk, R. A., Engelbrektson, A., & Coates, J. D. (2013). Structure and evolution of chlorate reduction composite transposons. *MBio*, *4*(4). https://doi.org/10.1128/mBio.00379-13

Coluzzi, C., Garcillán-Barcia, M. P., De La Cruz, F., & Rocha, E. P. C. (2022Evolution of Plasmid Mobility: Origin and Fate of Conjugative and Nonconjugative Plasmids, *Molecular Biology and Evolution*, *39*(6). https://doi.org/10.1093/molbev/msac115ï

Copeland, A., Lapidus, A., del Rio, T. G., Nolan, M., Lucas, S., Chen, F., Tice, H., Cheng, J. F., Bruce, D., Goodwin, L., Pitluck, S., Mikhailova, N., Pati, A., Ivanova, N., Mavromatis, K., Chen, A., Palaniappan, K., Chain, P., Land, M., … Klenk, H. P. (2009). Complete genome sequence of Catenulispora acidiphila type strain (ID 139908T). *Standards in Genomic Sciences*, *1*(2), 119–125. https://doi.org/10.4056/sigs.17259

Costa, T. R. D., Patkowski, J. B., Macé, K., Christie, P. J., & Waksman, G. (2024). Structural and functional diversity of type IV secretion systems. *Nature Reviews Microbiology*, *22*(3), 170–185. https://doi.org/10.1038/s41579-023-00974-3

Cury, J., Jové, T., Touchon, M., Néron, B., & Rocha, E. P. (2016). Identification and analysis of integrons and cassette arrays in bacterial genomes. *Nucleic Acids Research*, *44*(10), 4539–4550. https://doi.org/10.1093/nar/gkw319

Cuthbertson, L., & Nodwell, J. R. (2013). The TetR Family of Regulators. *Microbiology and Molecular Biology Reviews*, *77*(3), 440–475. https://doi.org/10.1128/mmbr.00018-13

Darmon, E., & Leach, D. R. F. (2014). Bacterial Genome Instability. *Microbiology and Molecular Biology Reviews*, *78*(1), 1–39. https://doi.org/10.1128/mmbr.00035-13

De Coster, W., & Rademakers, R. (2023). NanoPack2: population-scale evaluation of long-read sequencing data. *Bioinformatics*, *39*(5). https://doi.org/10.1093/bioinformatics/btad311

De Palmenaer, D., Siguier, P., & Mahillon, J. (2008). IS4 family goes genomic. *BMC Evolutionary Biology*, *8*(1). https://doi.org/10.1186/1471-2148-8-18

Dewey, H. M., Jones, J. M., Keating, M. R., & Budhathoki-Uprety, J. (2022). Increased Use of Disinfectants During the COVID-19 Pandemic and Its Potential Impacts on Health and Safety. *ACS Chemical Health & Safety*, *29*(1), 27–38. https://doi.org/10.1021/acs.chas.1c00026

Di Gioia, D., Peel, M., Fava, F., & Campbell Wyndham, A. R. (1998). Structures of Homologous Composite Transposons Carrying cbaABC Genes from Europe and North America. *APPLIED AND ENVIRONMENTAL MICROBIOLOGY*, *64*(5), 1940–1946. https://journals.asm.org/journal/aem

Didelot, X., Walker, A. S., Peto, T. E., Crook, D. W., & Wilson, D. J. (2016). Within-host evolution of bacterial pathogens. *Nature Reviews Microbiology*, *14*(3), 150–162. https://doi.org/10.1038/nrmicro.2015.13

Dionisio, F., Conceição, I. C., Marques, A. C. R., Fernandes, L., & Gordo, I. (2005). The evolution of a conjugative plasmid and its ability to increase bacterial fitness. *Biology Letters*, *1*(2), 250–252. https://doi.org/10.1098/rsbl.2004.0275

Dueholm, M. S., Danielsen, H. N., & Nielsen, P. H. (2014). Complete genome sequence of Pseudomonas sp. UK4, a model organism for studies of functional amyloids in Pseudomonas. *Genome Announcements*, *2*(5). https://doi.org/10.1128/genomeA.00898-14

Dunon, V., Bers, K., Lavigne, R., Top, E. M., & Springael, D. (2018). Targeted metagenomics demonstrates the ecological role of IS1071 in bacterial community adaptation to pesticide degradation. *Environmental Microbiology*, *20*(11), 4091–4111. https://doi.org/10.1111/1462-2920.14404

Ertekin, E., Hatt, J. K., Konstantinidis, K. T., & Tezel, U. (2016). Similar Microbial Consortia and Genes Are Involved in the Biodegradation of Benzalkonium Chlorides in Different Environments. *Environmental Science and Technology*, *50*(8), 4304–4313. https://doi.org/10.1021/acs.est.5b05959

Fan, C., Wu, Y. H., Decker, C. M., Rohani, R., Gesell Salazar, M., Ye, H., Cui, Z., Schmidt, F., & Huang, W. E. (2019). Defensive Function of Transposable Elements in Bacteria. *ACS Synthetic Biology*, *8*(9), 2141–2151. https://doi.org/10.1021/acssynbio.9b00218

Fraikin, N., Couturier, A., & Lesterlin, C. (2024). The winding journey of conjugative plasmids toward a novel host cell. *Current Opinion in Microbiology*, *78*. https://doi.org/10.1016/j.mib.2024.102449

Fredrickson, J. K., Romine, M. F., Beliaev, A. S., Auchtung, J. M., Driscoll, M. E., Gardner, T. S., Nealson, K. H., Osterman, A. L., Pinchuk, G., Reed, J. L., Rodionov, D. A., Rodrigues, J. L. M., Saffarini, D. A., Serres, M. H., Spormann, A. M., Zhulin, I. B., & Tiedje, J. M. (2008). Towards environmental systems biology of Shewanella. In *Nature Reviews Microbiology* (Vol. 6, Issue 8, pp. 592–603). https://doi.org/10.1038/nrmicro1947

Fulthorpe, R. R., & Campbell Wyndham, R. (1992). Involvement of a Chlorobenzoate-Catabolic Transposon, Tn5271, in Community Adaptation to Chlorobiphenyl, Chloroaniline, and 2,4-Dichlorophenoxyacetic Acid in a Freshwater Ecosystem. *APPLIED AND ENVIRONMENTAL MICROBIOLOGY*, *58*(1), 314–325.

Gale, G. A. R., Schiavon Osorio, A. A., Puzorjov, A., Wang, B., & McCormick, A. J. (2019). Genetic modification of cyanobacteria by conjugation using the cyanogate modular cloning toolkit. *Journal of Visualized Experiments*, *2019*(152). https://doi.org/10.3791/60451

Garcillán-Barcia, M. P., Francia, M. V., & De La Cruz, F. (2009). The diversity of conjugative relaxases and its application in plasmid classification. *FEMS Microbiology Reviews*, *33*(3), 657–687. https://doi.org/10.1111/j.1574-6976.2009.00168.x

Garcillán-Barcia, M. P., Redondo-Salvo, S., & de la Cruz, F. (2023). Plasmid classifications. *Plasmid*, *126*. https://doi.org/10.1016/j.plasmid.2023.102684

Gillespie, J. J., Ammerman, N. C., Dreher-Lesnick, S. M., Rahman, M. S., Worley, M. J., Setubal, J. C., Sobral, B. S., & Azad, A. F. (2009). An anomalous type IV secretion system in Rickettsia is evolutionarily conserved. *PLoS ONE*, *4*(3). https://doi.org/10.1371/journal.pone.0004833

Gogarten, J. P., Ford Doolittle, W., & Lawrence, J. G. (2002). Prokaryotic Evolution in Light of Gene Transfer. *Mol. Biol. Evol*, *19*(12), 2226–2238. https://academic.oup.com/mbe/article/19/12/2226/997576

Gomila, M., Peña, A., Mulet, M., Lalucat, J., & García-Valdés, E. (2015). Phylogenomics and systematics in Pseudomonas. *Frontiers in Microbiology*, *6*(MAR). https://doi.org/10.3389/fmicb.2015.00214

Gong, G., Wu, B., Liu, L., Li, J., Zhu, Q., He, M., & Hu, G. (2022). Metabolic engineering using acetate as a promising building block for the production of bio- based chemicals. *Engineering Microbiology*, *2*(4). https://doi.org/10.1016/j.engmic.2022.100036

González-Domínguez, M., Seral, C., Sáenz, Y., Salvo, S., Gude, M. J., Porres-Osante, N., Torres, C., & Castillo, F. J. (2012). Epidemiological features, resistance genes, and clones among community-onset methicillin-resistant Staphylococcus aureus (CO-MRSA) isolates detected in northern Spain. *International Journal of Medical Microbiology*, *302*(7–8), 320–326. https://doi.org/10.1016/j.ijmm.2012.10.003

Habe, H., Ashikawa, Y., Saiki, Y., Yoshida, T., Nojiri, H., & Omori, T. (2002). Sphingomonas sp. strain KA1, carrying a carbazole dioxygenase gene homologue, degrades chlorinated dibenzo-p -dioxins in soil . *FEMS Microbiology Letters*, *211*(1), 43–49. https://doi.org/10.1111/j.1574-6968.2002.tb11201.x

Hesse, C., Schulz, F., Bull, C. T., Shaffer, B. T., Yan, Q., Shapiro, N., Hassan, K. A., Varghese, N., Elbourne, L. D. H., Paulsen, I. T., Kyrpides, N., Woyke, T., & Loper, J. E. (2018). Genome-based evolutionary history of Pseudomonas spp. *Environmental Microbiology*, *20*(6), 2142–2159. https://doi.org/10.1111/1462-2920.14130

Holmes, R. K., & Jobling, M. G. (1996). Genetics. In S. Baron (Ed.), *Medical Microbiology* (4th ed.). University of Texas Medical Branch at Galveston. https://www.ncbi.nlm.nih.gov/books/NBK7908/

Hora, P. I., Pati, S. G., McNamara, P. J., & Arnold, W. A. (2020). Increased Use of Quaternary Ammonium Compounds during the SARS-CoV-2 Pandemic and Beyond: Consideration of Environmental Implications. In *Environmental Science and Technology Letters* (Vol. 7, Issue 9, pp. 622–631). American Chemical Society. https://doi.org/10.1021/acs.estlett.0c00437

Hu, Q., Zhang, L., Yang, R., Tang, J., & Dong, G. (2024). Quaternary ammonium biocides promote conjugative transfer of antibiotic resistance gene in structure- and species-dependent manner. *Environment International*, *189*. https://doi.org/10.1016/j.envint.2024.108812

Hunter, J. D. (2007). Matplotlib: A 2D Graphics Environment. *Computing in Science & Engineering* , *9*(3), 90–95. https://doi.org/10.1109/MCSE.2007.55

Inoue, K., Habe, H., Yamane, H., Omori, T., & Nojiri, H. (2005). Diversity of carbazole-degrading bacteria having the car gene cluster: Isolation of a novel gram-positive carbazole-degrading bacterium. *FEMS Microbiology Letters*, *245*(1), 145–153. https://doi.org/10.1016/j.femsle.2005.03.009

Iranzo, J., Wolf, Y. I., Koonin, E. V., & Sela, I. (2019). Gene gain and loss push prokaryotes beyond the homologous recombination barrier and accelerate genome sequence divergence. *Nature Communications*, *10*(1). https://doi.org/10.1038/s41467-019-13429-2

Jafari-Sales, A., Emrahimzadeh, M., Mehdizadeh, F., Pourbeiragh, G., & Pashazadeh, M. (2023). Examining the frequency of blaCTX-M, blaTEM, and blaSHV genes in Escherichia coli isolates from patients in Tabriz hospitals, Iran. *J Exp Clin Med*, *40*(4), 734–739. https://doi.org/10.52142/omujecm.40.4.14

Jain, A., & Srivastava, P. (2013). Broad host range plasmids. *FEMS Microbiology Letters*, *348*(2), 87–96. https://doi.org/10.1111/1574-6968.12241

Juhas, M., Crook, D. W., & Hood, D. W. (2008). Type IV secretion systems: Tools of bacterial horizontal gene transfer and virulence. *Cellular Microbiology*, *10*(12), 2377–2386. https://doi.org/10.1111/j.1462-5822.2008.01187.x

Jurėnas, D., Fraikin, N., Goormaghtigh, F., & Van Melderen, L. (2022). Biology and evolution of bacterial toxin–antitoxin systems. *Nature Reviews Microbiology*, *20*(6), 335–350. https://doi.org/10.1038/s41579-021-00661-1

Kaneko, T., Minamisawa, K., Isawa, T., Nakatsukasa, H., Mitsui, H., Kawaharada, Y., Nakamura, Y., Watanabe, A., Kawashima, K., Ono, A., Shimizu, Y., Takahashi, C., Minami, C., Fujishiro,

T., Kohara, M., Katoh, M., Nakazaki, N., Nakayama, S., Yamada, M., … Sato, S. (2010). Complete genomic structure of the cultivated rice endophyte azospirillum sp. B510. *DNA Research*, *17*(1), 37–50. https://doi.org/10.1093/dnares/dsp026

Kim, M., Weigand, M. R., Oh, S., Hatt, J. K., Krishnan, R., Tezel, U., Pavlostathis, S. G., & Konstantinidis, K. T. (2018). *Widely Used Benzalkonium Chloride Disinfectants Can Promote Antibiotic Resistance*. https://journals.asm.org/journal/aem

Kleckner, N. (1990). Regulation of Transposition in Bacteria. *Annual Review of Cell and Developmental Biology*, *6*, 297–327. https://doi.org/https://doi.org/10.1146/annurev.cb.06.110190.001501

Król, J. E., Penrod, J. T., McCaslin, H., Rogers, L. M., Yano, H., Stancik, A. D., Dejonghe, W., Brown, C. J., Parales, R. E., Wuertz, S., & Top, E. M. (2012). Role of IncP-1β plasmids pWDL7::rfp and pNB8c in chloroaniline catabolism as determined by genomic and functional analyses. *Applied and Environmental Microbiology*, *78*(3), 828–838. https://doi.org/10.1128/AEM.07480-11

Lang, E., Burghartz, M., Spring, S., Swiderski, J., & Spröer, C. (2010). Pseudomonas benzenivorans sp. nov. and Pseudomonas saponiphila sp. nov., represented by xenobiotics degrading type strains. *Current Microbiology*, *60*(2), 85–91. https://doi.org/10.1007/s00284-009-9507-7

Lederberg, J., Cavalli, L. L., & Lederberg, E. M. (1952). SEX COMPATIBILITY IN ESCHERICHIA COLI. *Genetics*, *37*(6), 720–730. https://doi.org/10.1093/genetics/37.6.720

Li, H. (2018). Minimap2: Pairwise alignment for nucleotide sequences. *Bioinformatics*, *34*(18), 3094–3100. https://doi.org/10.1093/bioinformatics/bty191

Li, X., Xie, Y., Liu, M., Tai, C., Sun, J., Deng, Z., & Ou, H. Y. (2018). OriTfinder: A web-based tool for the identification of origin of transfers in DNA sequences of bacterial mobile genetic elements. *Nucleic Acids Research*, *46*(W1), W229–W234. https://doi.org/10.1093/nar/gky352

Lima-Mendez, G., Alvarenga, D. O., Ross, K., Hallet, B., Van Melderen, L., Varani, A. M., & Chandler, M. (2020). Toxin-antitoxin gene pairs found in Tn3 family transposons appear to be

an integral part of the transposition module. *MBio*, *11*(2). https://doi.org/10.1128/mBio.00452-20

Lipszyc, A., Szuplewska, M., & Bartosik, D. (2022). How Do Transposable Elements Activate Expression of Transcriptionally Silent Antibiotic Resistance Genes? *International Journal of Molecular Sciences*, *23*(15). https://doi.org/10.3390/ijms23158063

Lu, H., Giordano, F., & Ning, Z. (2016). Oxford Nanopore MinION Sequencing and Genome Assembly. *Genomics, Proteomics and Bioinformatics*, *14*(5), 265–279. https://doi.org/10.1016/j.gpb.2016.05.004

Ma, N. J., Moonan, D. W., & Isaacs, F. J. (2014). Precise manipulation of bacterial chromosomes by conjugative assembly genome engineering. *Nature Protocols*, *9*(10), 2285–2300. https://doi.org/10.1038/nprot.2014.081

Maeda, K., Nojiri, H., Shintani, M., Yoshida, T., Habe, H., & Omori, T. (2003). Complete nucleotide sequence of carbazole/dioxin-degrading plasmid pCAR1 in Pseudomonas resinovorans strain CA10 indicates its mosaicity and the presence of large catabolic transposon Tn4676. *Journal of Molecular Biology*, *326*(1), 21–33. https://doi.org/10.1016/S0022-2836(02)01400-6

Martinez, B., Tomkins, J., Wackett, L. P., Wing, R., & Sadowsky, M. J. (2001). Complete nucleotide sequence and organization of the atrazine catabolic plasmid pADP-1 from Pseudomonas sp. strain ADP. *Journal of Bacteriology*, *183*(19), 5684–5697. https://doi.org/10.1128/JB.183.19.5684-5697.2001

Matsui, K., & Endo, G. (2018). Mercury bioremediation by mercury resistance transposon-mediated in situ molecular breeding. In *Applied Microbiology and Biotechnology* (Vol. 102, Issue 7, pp. 3037–3048). Springer Verlag. https://doi.org/10.1007/s00253-018-8847-2

McKinney, W. (2010). *Data Structures for Statistical Computing in Python*. 56–61.

Meyer, R. (2009). Replication and conjugative mobilization of broad host-range IncQ plasmids. *Plasmid*, *62*(2), 57–70. https://doi.org/10.1016/j.plasmid.2009.05.001

Molina, L., Bernal, P., Udaondo, Z., Segura, A., & Ramos, J. L. (2013). Complete genome sequence of a Pseudomonas putida clinical isolate, strain H8234. *Genome Announcements*, *1*(4). https://doi.org/10.1128/genomeA.00496-13

Murata, T., Gotoh, Y., & Hayashi, T. (2024). A comprehensive list of genes required for the efficient conjugation of plasmid Rts1 was determined by systematic deletion analysis. *DNA Research*, *31*(1). https://doi.org/10.1093/dnares/dsae002

Muszewska, A., Steczkiewicz, K., Stepniewska-Dziubinska, M., & Ginalski, K. (2019). Transposable elements contribute to fungal genes and impact fungal lifestyle. *Scientific Reports*, *9*(1). https://doi.org/10.1038/s41598-019-40965-0

Nakatsu, C., Ng, J., Singhtf, R., Straust, N., & Wyndham, C. (1991). Chlorobenzoate catabolic transposon Tn5271 is a composite class I element with flanking class II insertion sequences (trposase/Tn3 famfly/evolton). *Microbiology*, *88*, 8312–8316. https://www.pnas.org

Nojiri, H., Shintani, M., & Omori, T. (2004). Divergence of mobile genetic elements involved in the distribution of xenobiotic-catabolic capacity. *Applied Microbiology and Biotechnology*, *64*(2), 154–174. https://doi.org/10.1007/s00253-003-1509-y

Norberg, P., Bergström, M., Jethava, V., Dubhashi, D., & Hermansson, M. (2011). The IncP-1 plasmid backbone adapts to different host bacterial species and evolves through homologous recombination. *Nature Communications*, *2*(1). https://doi.org/10.1038/ncomms1267

Ogawa, N., & Miyashita, K. (1999). The Chlorocatechol-Catabolic Transposon Tn5707 of Alcaligenes eutrophus NH9, Carrying a Gene Cluster Highly Homologous to That in the 1,2,4-Trichlorobenzene-Degrading Bacterium Pseudomonas sp. Strain P51, Confers the Ability To Grow on 3-Chlorobenzoate. *APPLIED AND ENVIRONMENTAL MICROBIOLOGY*, *65*(2), 724–731.

Ondov, B. D., Treangen, T. J., Melsted, P., Mallonee, A. B., Bergman, N. H., Koren, S., & Phillippy, A. M. (2016). Mash: Fast genome and metagenome distance estimation using MinHash. *Genome Biology*, *17*(1). https://doi.org/10.1186/s13059-016-0997-x

Özen, A. I., & Ussery, D. W. (2012). Defining the Pseudomonas Genus: Where Do We Draw the Line with Azotobacter? *Microbial Ecology*, *63*(2), 239–248. https://doi.org/10.1007/s00248-011-9914-8

Palm, M., Fransson, A., Hultén, J., Búcaro Stenman, K., Allouche, A., Chiang, O. E., Constandse, M. L., van Dijk, K. J., Icli, S., Klimesova, B., Korhonen, E., Martínez-Crespo, G., Meggers, D., Naydenova, M., Polychronopoulou, M. A., Schuntermann, D. B., Unal, H., Wasylkowska, A., & Farewell, A. (2022). The Effect of Heavy Metals on Conjugation Efficiency of an F-Plasmid in Escherichia coli. *Antibiotics*, *11*(8). https://doi.org/10.3390/antibiotics11081123

Partridge, S. R., Kwong, S. M., Firth, N., & Jensen, S. O. (2018). Mobile Genetic Elements Associated with Antimicrobial Resistance. *Clinical Microbiology Reviews*, *31*(4). https://doi.org/10.1128/CMR.00088-17

Peix, A., Ramírez-Bahena, M. H., & Velázquez, E. (2009). Historical evolution and current status of the taxonomy of genus Pseudomonas. *Infection, Genetics and Evolution*, *9*(6), 1132–1147. https://doi.org/10.1016/j.meegid.2009.08.001

Poh, P.-C., Smith, A. R. W., & Bruce, I. J. (2002). Complete characterisation of Tn5530 from Burkholderia cepacia strain 2a (pIJB1) and studies of 2,4-dichlorophenoxyacetate uptake by the organism. *Plasmid*, *48*(1), 1–12. www.academicpress.com

Rajabal, V., Taner, F., Sanlidag, T., Suer, K., Guler, E., Sayan, M., & Petrovski, S. (2021). Genetic characterisation of antibiotic resistance transposons Tn6608 and Tn6609 isolated from clinical Pseudomonas strains in Cyprus. *Journal of Global Antimicrobial Resistance*, *26*, 330–334. https://doi.org/10.1016/j.jgar.2021.07.016

Ramos, M. S., Furlan, J. P. R., Gallo, I. F. L., dos Santos, L. D. R., de Campos, T. A., Savazzi, E. A., & Stehling, E. G. (2020). High Level of Resistance to Antimicrobials and Heavy Metals in Multidrug-Resistant Pseudomonas sp. Isolated from Water Sources. *Current Microbiology*, *77*(10), 2694–2701. https://doi.org/10.1007/s00284-020-02052-w

Raymond, C. K., Sims, E. H., Kas, A., Spencer, D. H., Kutyavin, T. V., Ivey, R. G., Zhou, Y., Kaul, R., Clendenning, J. B., & Olson, M. V. (2002). Genetic variation at the O-antigen biosynthetic

locus in Pseudomonas aeruginosa. *Journal of Bacteriology*, *184*(13), 3614–3622. https://doi.org/10.1128/JB.184.13.3614-3622.2002

Rizzo, L., Manaia, C., Merlin, C., Schwartz, T., Dagot, C., Ploy, M. C., Michael, I., & Fatta-Kassinos, D. (2013). Urban wastewater treatment plants as hotspots for antibiotic resistant bacteria and genes spread into the environment: A review. In *Science of the Total Environment* (Vol. 447, pp. 345–360). https://doi.org/10.1016/j.scitotenv.2013.01.032

Robertson, J., & Nash, J. H. E. (2018). MOB-suite: software tools for clustering, reconstruction and typing of plasmids from draft assemblies. *Microbial Genomics*, *4*(8). https://doi.org/10.6084/m9.figshare.6177188

Rumbaugh, K. P. (2014). Genomic complexity and plasticity ensure Pseudomonas success. *FEMS Microbiology Letters*, *356*(2), 141–143. https://doi.org/10.1111/1574-6968.12517

Sakarya, F. K., Haznedaroglu, B. Z., & Tezel, U. (2021). Biological removal of benzalkonium chlorides from wastewater by immobilized cells of Pseudomonas sp. BIOMIG1 in an up-flow packed bed reactor. *Journal of Hazardous Materials*, *418*. https://doi.org/10.1016/j.jhazmat.2021.126210

Sayers, E. W., Bolton, E. E., Brister, J. R., Canese, K., Chan, J., Comeau, D. C., Connor, R., Funk, K., Kelly, C., Kim, S., Madej, T., Marchler-Bauer, A., Lanczycki, C., Lathrop, S., Lu, Z., Thibaud-Nissen, F., Murphy, T., Phan, L., Skripchenko, Y., … Sherry, S. T. (2022). Database resources of the national center for biotechnology information. *Nucleic Acids Research*, *50*(D1), D20–D26. https://doi.org/10.1093/nar/gkab1112

Schoch, C. L., Ciufo, S., Domrachev, M., Hotton, C. L., Kannan, S., Khovanskaya, R., Leipe, D., McVeigh, R., O'Neill, K., Robbertse, B., Sharma, S., Soussov, V., Sullivan, J. P., Sun, L., Turner, S., & Karsch-Mizrachi, I. (2020). NCBI Taxonomy: A comprehensive update on curation, resources and tools. *Database*, *2020*. https://doi.org/10.1093/database/baaa062

Schröder, G., & Lanka, E. (2005). The mating pair formation system of conjugative plasmids - A versatile secretion machinery for transfer of proteins and DNA. *Plasmid*, *54*(1), 1–25. https://doi.org/10.1016/j.plasmid.2005.02.001

Setubal, J. C., Stoye, J., & Stadler Editors, P. F. (2018). *Comparative Genomics Methods and Protocols (Methods in Molecular Biology 1704)*. Springer Nature. http://www.springer.com/series/7651

Shafieifini, M., Sun, Y., Staley, Z. R., Riethoven, J. J., & Li, X. (2022). Effects of Nutrient Level and Growth Rate on the Conjugation Process That Transfers Mobile Antibiotic Resistance Genes in Continuous Cultures. *Applied and Environmental Microbiology*, *88*(19). https://doi.org/10.1128/aem.01121-22

Shankar Chilambi, G., Nordstrom, H. R., Evans, D. R., Ferrolino, J. A., Hayden, R. T., Marón, G. M., Vo, A. N., Gilmore, M. S., Wolf, J., Rosch, J. W., & Van Tyne, D. (n.d.). *Evolution of vancomycin-resistant Enterococcus faecium during colonization and infection in immunocompromised pediatric patients*. https://doi.org/10.1073/pnas.1917130117/-/DCSupplemental

Shen, D., Ma, G., Li, C., Jia, X., Qin, C., Yang, T., Wang, L., Jiang, X., Ding, N., Zhang, X., Yue, L., Yin, Z., Zeng, L., Zhao, Y., Zhou, D., & Chen, F. (2019). Emergence of a Multidrug-Resistant Hypervirulent Klebsiella pneumoniae Sequence Type 23 Strain with a Rare bla CTX-M-24-Harboring Virulence Plasmid. *Antimicrobial Agents and Chemotherapy*, *63*(3). https://journals.asm.org/journal/aac

Shen, W., Sipos, B., & Zhao, L. (2024). SeqKit2: A Swiss army knife for sequence and alignment processing. *IMeta*, *3*(3). https://doi.org/10.1002/imt2.191

Shi, Q., Chen, C., Zhang, W., Wu, P., Sun, M., Wu, H., Wu, H., Fu, P., & Fan, J. (2021). Transgenic eukaryotic microalgae as green factories: providing new ideas for the production of biologically active substances. *Journal of Applied Phycology*, *33*(2), 705–728. https://doi.org/10.1007/s10811-020-02350-7

Siguier, P., Gourbeyre, E., Varani, A., Ton-Hoang, B., & Chandler, M. (2015). Everyman's Guide to Bacterial Insertion Sequences. *Microbiology Spectrum*, *3*(2). https://doi.org/10.1128/microbiolspec.mdna3-0030-2014

Siguier, P., Perochon, J., Lestrade, L., Mahillon, J., & Chandler, M. (2006). ISfinder: the reference centre for bacterial insertion sequences. *Nucleic Acids Research*, *34*(Database issue). https://doi.org/10.1093/nar/gkj014

Smillie, C., Garcillán-Barcia, M. P., Francia, M. V., Rocha, E. P. C., & de la Cruz, F. (2010). Mobility of Plasmids. *Microbiology and Molecular Biology Reviews*, *74*(3), 434–452. https://doi.org/10.1128/mmbr.00020-10

Snesrud, E., Maybank, R., Kwak, Y. I., Jones, A. R., Hinkle, M. K., & McGann, P. (2018). Chromosomally encoded mcr-5 in colistin-nonsusceptible pseudomonas aeruginosa. *Antimicrobial Agents and Chemotherapy*, *62*(8). https://doi.org/10.1128/AAC.00679-18

Snyder, L., Peters, J. E., Henkin, T. M., Champness, W., Silhavy, T. J., Parke-Davis Professor, W.-L., & Peters Henkin Champness, S. (2013). *Molecular Genetics of Bacteria* (4th ed.). ASM press.

Sousa, A., Bourgard, C., Wahl, L. M., & Gordo, I. (2013). Rates of transposition in Escherichia coli. *Biology Letters*, *9*(6). https://doi.org/10.1098/rsbl.2013.0838

Suzuki, H., Yano, H., Brown, C. J., & Top, E. M. (2010). Predicting plasmid promiscuity based on genomic signature. *Journal of Bacteriology*, *192*(22), 6045–6055. https://doi.org/10.1128/JB.00277-10

Szuplewska, M., Ludwiczak, M., Lyzwa, K., Czarnecki, J., & Bartosik, D. (2014). Mobility and generation of mosaic non-autonomous transposons by Tn3-Derived Inverted-repeat Miniature Elements (TIMEs). *PLoS ONE*, *9*(8). https://doi.org/10.1371/journal.pone.0105010

Tatusova, T., Dicuccio, M., Badretdin, A., Chetvernin, V., Ciufo, S., & Li, W. (2013). Prokaryotic Genome Annotation Pipeline. In *The NCBI Handbook [Internet]* (2nd ed.). National Center for Biotechnology Information (US). https://www.ncbi.nlm.nih.gov/books/

Tezel, U., & Pavlostathis, S. G. (2009). Fate and effect of quaternary ammonium compounds in biological systems. In *ProQuest Dissertations and Theses*.

https://www.proquest.com/dissertations-theses/fate-effect-quaternary-ammonium-compounds/docview/304891552/se-2?accountid=9645

Tezel, U., & Pavlostathis, S. G. (2011). Role of Quaternary Ammonium Compounds Antimicrobial Resistance in the Environment, https://doi.org/10.1002/9781118156247.ch20

Urata, M., Miyakoshi, M., Kai, S., Maeda, K., Habe, H., Omori, T., Yamane, H., & Nojiri, H. (2004). Transcriptional regulation of the ant operon, encoding two-component anthranilate 1,2-dioxygenase, on the carbazole-degradative plasmid pCAR1 of Pseudomonas resinovorans strain CA10. *Journal of Bacteriology*, *186*(20), 6815–6823. https://doi.org/10.1128/JB.186.20.6815-6823.2004

Urata, M., Uchimura, H., Noguchi, H., Sakaguchi, T., Takemura, T., Eto, K., Habe, H., Omori, T., Yamane, H., & Nojiri, H. (2006). Plasmid pCAR3 contains multiple gene sets involved in the conversion of carbazole to anthranilate. *Applied and Environmental Microbiology*, *72*(5), 3198–3205. https://doi.org/10.1128/AEM.72.5.3198-3205.2006

Van Beilen, J. B., Panke, S., Lucchini, S., Franchini, A. G., Ro $ Thlisberger, M., & Witholt, B. (2001). Analysis of Pseudomonas putida alkane-degradation gene clusters and flanking insertion sequences : evolution and regulation of the alk genes. In *Microbiology* (Vol. 147).

Vigil-Stenman, T., Ininbergs, K., Bergman, B., & Ekman, M. (2017). High abundance and expression of transposases in bacteria from the Baltic Sea. *ISME Journal*, *11*(11), 2611–2623. https://doi.org/10.1038/ismej.2017.114

Virolle, C., Goldlust, K., Djermoun, S., Bigot, S., & Lesterlin, C. (2020a). Plasmid transfer by conjugation in gram-negative bacteria: From the cellular to the community level. In *Genes* (Vol. 11, Issue 11, pp. 1–33). MDPI AG. https://doi.org/10.3390/genes11111239

Virolle, C., Goldlust, K., Djermoun, S., Bigot, S., & Lesterlin, C. (2020b). Plasmid transfer by conjugation in gram-negative bacteria: From the cellular to the community level. *Genes*, *11*(11), 1–33. https://doi.org/10.3390/genes11111239

Vodovar, N., Vallenet, D., Cruveiller, S., Rouy, Z., Barbe, V., Acosta, C., Cattolico, L., Jubin, C., Lajus, A., Segurens, B., Vacherie, B., Wincker, P., Weissenbach, J., Lemaitre, B., Médigue, C., & Boccard, F. (2006). Complete genome sequence of the entomopathogenic and metabolically versatile soil bacterium Pseudomonas entomophila. *Nature Biotechnology*, *24*(6), 673–679. https://doi.org/10.1038/nbt1212

Vos, M. (2009). Why do bacteria engage in homologous recombination? *Trends in Microbiology*, *17*(6), 226–232. https://doi.org/10.1016/j.tim.2009.03.001

Wallden, K., Rivera-Calzada, A., & Waksman, G. (2010). Type IV secretion systems: Versatility and diversity in function. In *Cellular Microbiology* (Vol. 12, Issue 9, pp. 1203–1212). https://doi.org/10.1111/j.1462-5822.2010.01499.x

Wang, S., Dai, E., Jiang, X., Zeng, L., Cheng, Q., Jing, Y., Hu, L., Yin, Z., Gao, B., Wang, J., Duan, G., Cai, X., & Zhou, D. (2019). Characterization of the plasmid of incompatibility groups IncFIIpkf727591 and IncpKPHS1 from enterobacteriaceae species. *Infection and Drug Resistance*, *12*, 2789–2797. https://doi.org/10.2147/IDR.S212321

Wei, M., Zhang, J. J., Liu, H., Wang, S. J., Fu, H., & Zhou, N. Y. (2009). A transposable class I composite transposon carrying mph (methyl parathion hydrolase) from Pseudomonas sp. strain WBC-3. *FEMS Microbiology Letters*, *292*(1), 85–91. https://doi.org/10.1111/j.1574-6968.2008.01468.x

Wick, R. R., Judd, L. M., & Holt, K. E. (2019). Performance of neural network basecalling tools for Oxford Nanopore sequencing. *Genome Biology*, *20*(1). https://doi.org/10.1186/s13059-019-1727-y

Wolter, D. J., Hanson, N. D., & Lister, P. D. (2004). Insertional inactivation of oprD in clinical isolates of Pseudomonas aeruginosa leading to carbapenem resistance. *FEMS Microbiology Letters*, *236*(1), 137–143. https://doi.org/10.1016/j.femsle.2004.05.039

Wu, L., Shang, H., Wang, Q., Gu, H., Liu, G., & Yang, S. (2016). Isolation and characterization of antagonistic endophytes from Dendrobium candidum Wall ex Lindl., and the biofertilizing

potential of a novel Pseudomonas saponiphila strain. *Applied Soil Ecology*, *105*, 101–108. https://doi.org/10.1016/j.apsoil.2016.04.008

Xie, Z., & Tang, H. (2017). ISEScan: automated identification of insertion sequence elements in prokaryotic genomes. *Bioinformatics (Oxford, England)*, *33*(21), 3340–3347. https://doi.org/10.1093/bioinformatics/btx433

Yamaguchi-Kabata, Y., Yasuda, J., Tanabe, O., Suzuki, Y., Kawame, H., Fuse, N., Nagasaki, M., Kawai, Y., Kojima, K., Katsuoka, F., Saito, S., Danjoh, I., Motoike, I. N., Yamashita, R., Koshiba, S., Saigusa, D., Tamiya, G., Kure, S., Yaegashi, N., … Yamamoto, M. (2018). Evaluation of reported pathogenic variants and their frequencies in a Japanese population based on a whole-genome reference panel of 2049 individuals article. *Journal of Human Genetics*, *63*(2), 213–230. https://doi.org/10.1038/s10038-017-0347-1

Yan, Y., Yang, J., Dou, Y., Chen, M., Ping, S., Peng, J., Lu, W., Zhang, W., Yao, Z., Li, H., Liu, W., He, S., Geng, L., Zhang, X., Yang, F., Yu, H., Zhan, Y., Li, D., Lin, Z., … Jin, Q. (2008). Nitrogen fixation island and rhizosphere competence traits in the genome of root-associated Pseudomonas stutzeri A1501. *PNAS*, *105*(21). https://doi.org//doi/10.1073/pnas.0801093105

Yang, K., Chen, M. L., & Zhu, D. (2023). Exposure to benzalkonium chloride disinfectants promotes antibiotic resistance in sewage sludge microbiomes. *Science of the Total Environment*, *867*. https://doi.org/10.1016/j.scitotenv.2023.161527

Yang, L., Jelsbak, L., Marvig, R. L., Damkiær, S., Workman, C. T., Rau, M. H., Hansen, S. K., Folkesson, A., Johansen, H. K., Ciofu, O., Høiby, N., Sommer, M. O. A., & Molin, S. (2011). Evolutionary dynamics of bacteria in a human host environment. *Proceedings of the National Academy of Sciences of the United States of America*, *108*(18), 7481–7486. https://doi.org/10.1073/pnas.1018249108

Yang, Q. E., & Walsh, T. R. (2017). Toxin-antitoxin systems and their role in disseminating and maintaining antimicrobial resistance. In *FEMS Microbiology Reviews* (Vol. 41, Issue 3, pp. 343–353). Oxford University Press. https://doi.org/10.1093/femsre/fux006

Yano, H., Shintani, M., Tomita, M., Suzuki, H., & Oshima, T. (2019). Reconsidering plasmid maintenance factors for computational plasmid design. In *Computational and Structural Biotechnology Journal* (Vol. 17, pp. 70–81). Elsevier B.V. https://doi.org/10.1016/j.csbj.2018.12.001

Yao, Y., Maddamsetti, R., Weiss, A., Ha, Y., Wang, T., Wang, S., & You, L. (2022). Intra- and interpopulation transposition of mobile genetic elements driven by antibiotic selection. *Nature Ecology and Evolution*, *6*(5), 555–564. https://doi.org/10.1038/s41559-022-01705-2

Yeo, C. C., & Poh, C. L. (1997). Characterization of IS1474, an insertion sequence of the IS21 family isolated from Pseudomonas alcaligenes NCIB 9867. *FEMS Microbiology Letters*, *149*, 257–263. https://doi.org/doi.org/10.1016/S0378-1097(97)00085-2

Zeng, L., & Jin, S. (2003). aph(3′)-IIb, a Gene Encoding an Aminoglycoside-Modifying Enzyme, Is under the Positive Control of Surrogate Regulator HpaA. *Antimicrobial Agents and Chemotherapy*, *47*(12), 3867–3876. https://doi.org/10.1128/AAC.47.12.3867-3876.2003

Zhang, C., Cui, F., Zeng, G. ming, Jiang, M., Yang, Z. zhu, Yu, Z. gang, Zhu, M. ying, & Shen, L. qing. (2015). Quaternary ammonium compounds (QACs): A review on occurrence, fate and toxicity in the environment. *Science of the Total Environment*, *518–519*, 352–362. https://doi.org/10.1016/j.scitotenv.2015.03.007

Zheng, G., Schreder, E., Sathyanarayana, S., & Salamova, A. (2022). The first detection of quaternary ammonium compounds in breast milk: Implications for early-life exposure. *Journal of Exposure Science and Environmental Epidemiology*, *32*(5), 682–688. https://doi.org/10.1038/s41370-022-00439-4

Zhou, H., Lu, Z., Liu, X., Bie, X., Xue, F., Tang, S., Feng, Q., Cheng, Y., & Yang, J. (2024). Environmentally Relevant Concentrations of Tetracycline Promote Horizontal Transfer of Antimicrobial Resistance Genes via Plasmid-Mediated Conjugation. *Foods*, *13*(11). https://doi.org/10.3390/foods13111787

APPENDIX A: *P. saponiphila* DSM 9751 AND *P. sessilinigenes* BIOMIG1 ISs AND TNs DETAILS

Table A.1. The sequences of inverted repeats (IRs) and direct repeats (DRs) of *P. saponiphila* DSM 9751's ISs and Tns.

P. saponiphila DSM 9751				
Family	Name	IRL	IRR	DR
IS1380	ISPa33	CTAGCCCGGATTTCTCATGA	CTAGCCCGGATTTCTCATGA	CTAG, TTAG, CTAA
	ISAzs25	GGAAATGGTTGAGGGCTTTGAC	GGACATTTTTGAGGTTTTTGAC	-
IS21	IS1474	TGCGGATTTCGGAGCACCGTGACCGGCCGTTTCGGTTGATCGTGACCGGT	TGCGGATTTCGGTG-AACGTGACCGAGCGTTTCGCTAATACGTGACCGGT	CATG
	ISPst3	CTGCCGATCGAAAACTGACCCAGG	CTGCCGATTGAAATTTGACCCAGG	CAGTCATGG
IS21	ISSsp5	AACGGCGGAGCAAAAGTCGGCCATGC-GGCGGCG	AACGGCGGAGCAATATTCGGCCACGCTAGCGGCG	-
IS3	ISPmo5	CTGAAGTACCTG	CTGAAGAACCTG	GTC
IS4	ISPa1635	CCCAATGTCATCAAC	CCCAATGTCATCAAC	GGCGGTCGGT

Table A.1. Cont.

P. saponiphila DSM 9751				
Family	Name	IRL	IRR	DR
IS5	ISPst5	TGACTTCAGCC	TGACTCCAGCC	CTAG, TCCTTAGG
	ISPst12	TAGCAGGCCGTTGAAAAA	TACCAGGCCGTTGAAAAA	CTAG, GTAG, CTAG
IS630	ISPpu1	TTGCTGGGCACCTAGTGTCTTGTCTCAAAAATAA	TTGCTCGTACACTAGTGTCCTGTTTCATATAAAA	CTAA
Tn3	ISThsp9	TTGGCCGCTATGTTGATTCGCCCAGCCG	TTGCCCGCGCTGCGGCTTCGCCAAGCCG	AAAGA

Table A.2. The sequences of inverted repeats (IRs) and direct repeats (DRs) of *P. sessilinigenes* BIOMIG1's ISs and Tns.

P. sessilinigenes BIOMIG1				
Family	Name	IRL	IRR	DR
IS1182	ISPa94	GGCCGGTTCTGTTGAAAAAGT	GGCCGATTCTGTTGAAAAAGT	CTAA, TTAG
IS21	ISPpu27	CTGCCGATTGAAAATTGACCCAGG	CTGCCGACTGAAAACTGACCCAGG	CGAT
IS256	ISPa103	AGATATGTGCTGGCGC	AGAAAGGTGCAGGCGC	TCCCGGTGG
IS3	ISPen2	GACTGAATCGCCCCTGGTTTTCTAGACACTCTCCAAGCTCAGAAAATG	GAGTGAATCGCCCCGGATTTCGTAGACAC-CTCCATGC-CTTAAAATG	
	ISPa121	TGGTCTGTCCCGG-GCTGAGTGGACACTGACTTAAG	TGGTCTGTCCCGGAGCTG-GTGGACAGGTAGTTAAG	

Table A.2. Cont.

P. sessilinigenes BIOMIG1				
Family	Name	IRL	IRR	DR
IS30	ISPsp8	GGCGGCGGCAAAAACTGAGTGCAACAC	GGCGGTTGCAGGAGCTGAGTGCAACAC	CAG
	ISPsp7	GGCGGTTGCAGGAGCTGAGTGCAACAC	GGCGGCGGCAAAAACTGAGTGCAACAC	AGAAG, GCG
	ISShes10	GGCGGTTGCAGGATCTGAGTGCAACAC	GGCGGCCGCAAAAACTGAGTGCAACAC	-
IS5	ISPre2	TAAGGATGGTCTGAA	TAGGGAAACTCTGAA	CTAA, TTAG
	ISPa96	TTAAGGAACATCTGCATAAATCGTGCCCCGATGTGCTAAT	TTAAGGAAGGTCTGCTTTAAGCACTTTGCGATGTGCTAAT	-
	ISPre1	TCTGAAGAAG	TCTGAAGTAG	CTAG, TTAA
	ISPsfu1	AGCCCAATAACTATGCTTGCCGGGTACTCGGGTA	AGACCAAGGCCAATGCTTCCCGTGACGTTGGGTA	CTAA, CTAA
	ISPst5	GAAAACGCAAACAG	GACAACGCAAACAG	CTAG, TCCTTAGG
	ISThi1	-	-	CTAG
IS630	ISPa47	TATTAACCCGGCAATCAAATA	TATTAACCTGGCAAATAAATA	TA
IS66	ISPsy43	TGATCCAGCGCGTCGAGAC	TGATCCAGTGCGGCTTGAC	GCTCTTCG

Table A.2. Cont.

P. sessilinigenes BIOMIG1				
Family	Name	IRL	IRR	DR
IS91	IS 1071	CGGGGTCTC CTCGTTTTCA GTGCAATAA GTGACGGTA CGAAAAGCT AGCACTGGC GCGGAGGTG GTGTTGGTA GATCGTTGA TTTCATTGAC TTTCCTGTTC ACTTTCAAA TCTGCGATTC GTGGCGTC	CGGGGTCTCCTCG TTTTCAGTGCAAT AAGTGACGGTAC GCAAAGCTAGCA CTGGCGCGGGGG TGGTCTGGGTAG ACCGTTGATTTCA TTGACTTTCCTGT TCGCTTTGTAAAC - GGGTATGGTGGC CTC	-
Tn3	ISPa40	-	-	-
	ISThsp9	TTGGCCGCT ATGTTGATTC GCCCAGCCG	TTGCCCGCGCTGC GGCTTCGCCAAG CCG	AAAGA